Characterization of the Role of CSA1 in Maintaining Homeostasis of BAK1-BIR3 Complexes and Triggering Autoimmune Cell Death

Dissertation

der Mathematisch-Naturwissenschaftlichen Fakultät

der Eberhard Karls Universität Tübingen

zur Erlangung des Grades lines

Doktors der Naturwissenschaften

(Dr. rer. nat.)

vorgelegt von

M. Sc. Liping Yu

aus Shandong, China

Tübingen

2023

Tag der mündlichen Qualifikation:	09.02.2024
Dekan:	Prof. Dr. Thilo Stehle
1. Berichterstatter:	PD Dr. Birgit Kemmerling
2. Berichterstatter:	Prof. Dr. Rosa Lozano-Durán

Table of Contents

List of abbreviations

°C	Degree Celsius
µ	Micro (10^{-6})
%	Percent sign
35S	Promotor of cauliflower mosaic virus
aa	Amino acid
A. brassicicola	*Alternaria brassicicola*
A. thaliana	*Arabidopsis thaliana*
Ade	Adenine
ADP	Adenosine diphosphate
ATP	Adenosine triphosphate
AtPep1	Arabidopsis thaliana peptide 1
A. tumefaciens	*Agrobacterium tumefaciens*
Avr	Avirulence
AvrB	Avirulence protein B from *P. syringae* pv*. glycinea*
AvrRpm1	Avirulence protein 1 from *P. syringae* pv. *maculicola*
AvrRpt2	Avirulence protein 2 from *P*. syringae pv. *tomato*
AvrPphB	Avirulence protein from *P. syringae* pv*. phaseolicola*
AvrPto	Avirulence protein from *P. syringae* pv*. tomato*
AvrPtoB	Avirulence protein from *P. syringae* pv*. tomato*
BAK1	BRI1-associated kinase
BIR	BAK1-interacting RLK
BKK1	BAK1-like 1
BL	Brassinolide
bp	Base pair
BR	Brassinosteroid
BRI1	Brassinosteroid-insensitive 1
Ca^{2+}	Calcium ion

CC	Coiled-coil
cDNA	complementary DNA
CHS3	Chilling sensitive 3
Cl^-	Chloride ion
CLV	Clavata
CNL	CC-NBS-LRR
CoIP	Coimmunoprecipitation
Col-0	Columbia-0
CSA1	CONSTITUTIVE SHADE AVOIDANCE 1
CSM	Complete synthetic medium
DAMP	Danger-associated molecular pattern
ddH_2O	double-distilled water
DMSO	Dimethyl sulfoxide
DN	Dominant negative
DNA	Desoxyribonucleic acid
DND1	Defense no death 1
dNTPs	Deoxyribonucleotide triphosphate
dpi	Days post inoculation
EDS	Enhanced disease susceptibility
EFR	EF-TU receptor
e.g.	for example
ETI	Effector-triggered immunity
EtOH	Ethanol
flg22	a 22-amino-acid peptide derived from flagellin
FLS2	Flagellin-sensing 2
fwd	Forward
g	Gram
GFP	Green fluorescent protein

hr	Hour
His	Histidine
HopB1	HRP (hypersensitive response and pathogenicity) outer protein B1
HR	Hypersensitive response
HRP	Horseradish peroxidase
IP	Immunoprecipitation
JA	Jasmonic acid
K+	Potassium ion
kb	Kilo base pair
kDa	Kilo Dalton
KD	Kinase domain
KO	Knock-out
L	Liter
LB	Lysogeny broth
LC-MS/MS	Liquid chromatography-mass spectrometry/mass spectrometry
Leu	Leucine
LRR	Leucine-rich repeat
M	Molar
m	Milli (10^{-3})
MAMP	Microbe-associated molecular pattern
MAPK	Mitogen-activated protein kinase
MEKK	MAPK / ERK (extracellular signal-regulated kinase) kinase kinase
Met	Methionine
min	Minute
MKK	Mitogen activated protein (MAP) kinase kinase
MPK	MAP kinase
MS	Murashige and Skoog
MS	Mass spectrometry

n	nano (10^{-9})
N. benthamiana	*Nicotiana benthamiana*
NB-LRR	Nucleotide-binding leucine-rich repeat
NDR1	Non-race specific disease resistance 1
NLR / NB-LRR	Nucleotide-binding leucine-rich repeat
NLP	Ethylene-inducing peptide 1 (Nep1)-like protein
PAMP	Pathogen-associated molecular pattern
PCR	Polymerase chain reaction
PEPR1	Pep1 receptor 1
PP2A	Protein phosphatase 2A
PRR	Pattern recognition receptor
P. syringae	*Pseudomonas syringae*
PSKR	Phytosulfokine (PSK) receptor
PSY1	Plant peptide containing sulfated tyrosine 1
PSY1R	PSY1 receptor
PTI	PAMP or pattern triggered immunity
Pto	*Pseudomonas. syringae pv. tomato*
R gene	Resistance gene
RK	Receptor kinase
R protein	Resistance protein
rev	Reverse
RIN4	RPM1-interacting protein 4
RLCK	Receptor-like cytoplasmic kinase
RLK	Receptor-like kinase
RLP	Receptor-like protein
RLU	Relative light units
RNA	Ribonucleic acid
ROS	Reactive-oxygen species

RPM1	Resistance to *P. syringae* pv. *maculicola* protein 1
RPS2	Resistance to *P. syringae* protein 2
RPW8	Resistance to Powdery Mildew 8
RNLs	RPW8-NLRs
RT	Reverse transcription
s	Second
SA	Salicylic acid
SAG101	Senescence associated gene 101
SDS	Sodium dodecyl sulfate
SERK	Somatic embryogenesis receptor kinase
SNC1	Suppressor of *npr1-1* constitutive 1
SOBIR1	Suppressor of bir1
T-DNA	Transfer DNA
T3SE	Type III secretion effector
Ta	Annealing temperature
TIR	Toll-Interleukin 1 (IL-1) receptor
Tm	Melting temperature
TMV	Tobacco mosaic virus
TNL	TIR-NBS-LRR
Trp	Tryptophan
Ura	Uracil
v/v	Volume per volume
w/v	Weight per volume
WB	Western blot
WRKY	Tryptophane, arginine, lysine, tyrosine containing transcription factor
WT	Wild-type
Y2H	Yeast-two-hybrid
YPD	Yeast extract peptone dextrose

List of figures

List of tables

1. Introduction

To survive in nature, plants must respond to many kinds of environmental factors, which include both microbial signals and abiotic factors. Although some plants are observed to be sick in the field (Figure 1-1), most plants are still healthy because of their immune system, which is crucial for optimal plant responses and fitness in nature. After long-term co-evolution with pathogens, plants have formed a complex defense system. The first barrier, the cell wall composed of cellulose and pectin, can resist most pathogens (Engelsdorf et al., 2018; Malinovsky et al., 2014; Underwood, 2012).The second barrier consists of the production of reactive oxygen species (ROS), mitogen-activated protein kinase (MAPK) cascades, hypersensitive response (HR), and resistance-related hormone accumulation (Balint-Kurti, 2019; Du et al., 2009; Meng and Zhang, 2013; O'Brien et al., 2012).

Figure 1-1: Rice infected by *Xanthomonas oryzae* pv*. oryzae*

Some rice plants can resist *Xanthomonas oryzae* pv*. oryzae*, while others cannot. (https://plantvillage.psu.edu/topics/rice/infos)

1.1 The two-layered plant immune system

Unlike animals, plants lack mobile defensive cells and a somatic adaptive immune system. Over a long period of time, plants have evolved a set of defense systems that include a

two-layered innate immune system to detect and cope with diverse biotic attacks (Boller and He, 2009; Jones and Dangl, 2006; Zhou and Zhang, 2020). Therefore, investigating how plants respond to the invasion of pathogens and how their immune system works is essential to control outbreaks of severe crop diseases.

1.1.1 PTI

The first line of defense for plants against microbial invasion is activated upon perception of pathogen- or microbe-associated molecular patterns (PAMPs or MAMPs), which are a large group of conserved molecules in microbes (Medzhitov and Janeway, 1997). Plants can perceive several general microbe elicitors, which allows them to switch from growth and development into a defense mode. The general elicitors include bacterial flagellin, the elongation factor Tu (EF-Tu), peptidoglycan (PGN), β-glucans from oomycetes, the fungal cell wall component chitin and NLP20, a peptide pattern found in necrosis- and ethylene-inducing peptide 1 (Nep1)-like proteins (NLP) from different microbes (Bohm et al., 2014b; Felix et al., 1999; Kunze et al., 2004). PAMPs/MAMPs can be recognized by plant pattern-recognition receptors (PRRs) which are localized on the surface of plant cells (Figure 1-2). Dependent on the protein domain structure, plant PRRs can be classified into either receptor kinases (RKs) or receptor proteins (RPs). RKs contain a ligand-binding ectodomain, a transmembrane domain, and an intracellular kinase domain, whereas RPs contain a similar ectodomain and a short transmembrane domain but lack a cytoplasmic kinase domain. The ectodomain of RKs/RPs could be a leucine-rich repeat (LRR) or lysine motif (LysM) domain (Bohm et al., 2014a; Boutrot and Zipfel, 2017; Saijo et al., 2018; Wan et al., 2019).

When PAMPs/MAMPs are recognized by PRRs, plants can activate pattern-triggered immunity (PTI), leading to early molecular events, among which typically include a burst of reactive oxygen species (ROS), calcium influx, production of immunogenic peptides, and defense hormones (Zhou and Zhang, 2020). In many cases, plants cannot distinguish pathogenic microbial PAMPs/MAMPs from beneficial microbial PAMPs/MAMPs. The damage induced by a microbe may depend on the lifestyle of the invader in combination with PAMPs/MAMPs signals, providing clues to identify pathogenic or nonpathogenic microbes (Thoms et al., 2021). For example, some plant

pathogens use the cell wall-degrading enzymes conserved in bacteria and fungi to generate many cell wall-degradation compounds and destroy cell walls (Berlemont and Martiny, 2013). However, nematodes can release intracellular danger signals or induce plants to produce damage-associated molecular patterns (DAMPs) (Klauser et al., 2015; Lee et al., 2018; Zhang and Gleason, 2020).

1.1.2 ETI

Based on many studies on the interactions between plants and pathogens, plant immunologists proposed an arms race co-evolutionary theory. Successful pathogens use their effector repertoire to suppress PRR-dependent responses. There are many types of effectors based on diverse lifestyles of pathogens (Dangl et al., 2013). Some effectors from extracellular bacterial pathogens are delivered into plant cells by the type III secretion system (TTSS) (Baltrus et al., 2011; Block and Alfano, 2011); effectors from fungi and oomycetes are normally secreted from the so-called haustoria, a specialized feeding organelle, into plant cells (Koeck et al., 2011); salivary proteins upon aphid and nematode feeding can be delivered to plant cells (Bos et al., 2010). Pathogens deliver virulence effectors into plant cells, which can be localized into interior special compartments where they usually suppress PTI and facilitate virulence to shut down plant defense. For example, the *Arabidopsis* (*A.*) *thaliana* immune receptor FLAGELLIN-SENSING 2 (FLS2) and co-receptor brassinosteroid-insensitive 1 (BRI1) associated receptor kinase 1 (BAK1) perceive the bacterial flagellin epitope flg22 to initiate plant immunity. To impede the plant immune response, the *P. syringae* effectors AvrPto and AvrPtoB directly bind to the FLS2-BAK1 complex and inhibit their kinase activities. Effector HopB1 acts as a protease to cleave the immune-activated co-receptor BAK1 to suppress immunity activation (Li et al., 2016). Thus, some pathogenic effectors use a virulence strategy to attack the plant immune system.

While many pathogen effectors have been shown to enhance virulence by suppressing PTI signaling pathways, some of them can be recognized by the host (Feng et al., 2012; Xin and He, 2013). Not surprisingly, plants have evolved the perception mechanisms to sense the perturbation of the PTI pathway by effectors. We now know that many resistant (*R*) genes are usually present in plant multigene clusters (Dangl et al.,

2013). R proteins induce specific immune responses called effector-triggered immunity (ETI), resulting in rapid localized cell death known as hypersensitive response (HR) (Jones and Dangl, 2006). HR induced by fungi, oomycetes, bacteria, and viruses is a widespread phenomenon (Balint-Kurti, 2019). However, HR can also be induced by insects (Rossi et al., 1998). The gene-for-gene hypothesis was proposed by Flor many years ago (1942). This hypothesis stated that there is one corresponding gene controlling avirulence in the pathogen for each resistance gene controlling host defense (Bourras et al., 2016). The resistance gene in the host and the corresponding avirulence gene can be identified by this hypothesis. During that time people understood this hypothesis as a R protein directly matched with an avirulence protein. Currently, it is validated that, for example, *Pi-ta* from rice encoding an R protein has been shown to directly interact with its matching Avr protein Avr-Pita (Jia et al., 2000). Moreover, this appears to be true in several examples (Deslandes et al., 2003; Dodds et al., 2006; Jia et al., 2000; Scofield et al., 1996; Tang et al., 1996). However, effectors can be sensed indirectly in many cases, which explains that effectors cannot be detected if there is missing the host target bound by the effector. Thus, an alternative model was proposed called the “guard hypothesis”, which postulated that R proteins indirectly recognize effectors (Van der Biezen and Jones, 1998). It is described that R proteins “guard” the targets of effectors. An example is that *the P. syringae* effector protein AvrPphB, a cysteine protease, cleaves a host protein kinase PBS5. The cognate R protein (RPS5) detects the cleavage event and induces the ETI response (Ade et al., 2007; Shao et al., 2003). R proteins are activated by the perturbation of the host targets of effectors. A few effectors are now known to be indirectly recognized (Axtell and Staskawicz, 2003; Mackey et al., 2003; Mackey et al., 2002; Rooney et al., 2005). Furthermore, there is a third model that describes a specific R protein associated with a molecular decoy of the host target modified by an effector. The molecular decoy normally has no function in PTI (Dangl et al., 2013).

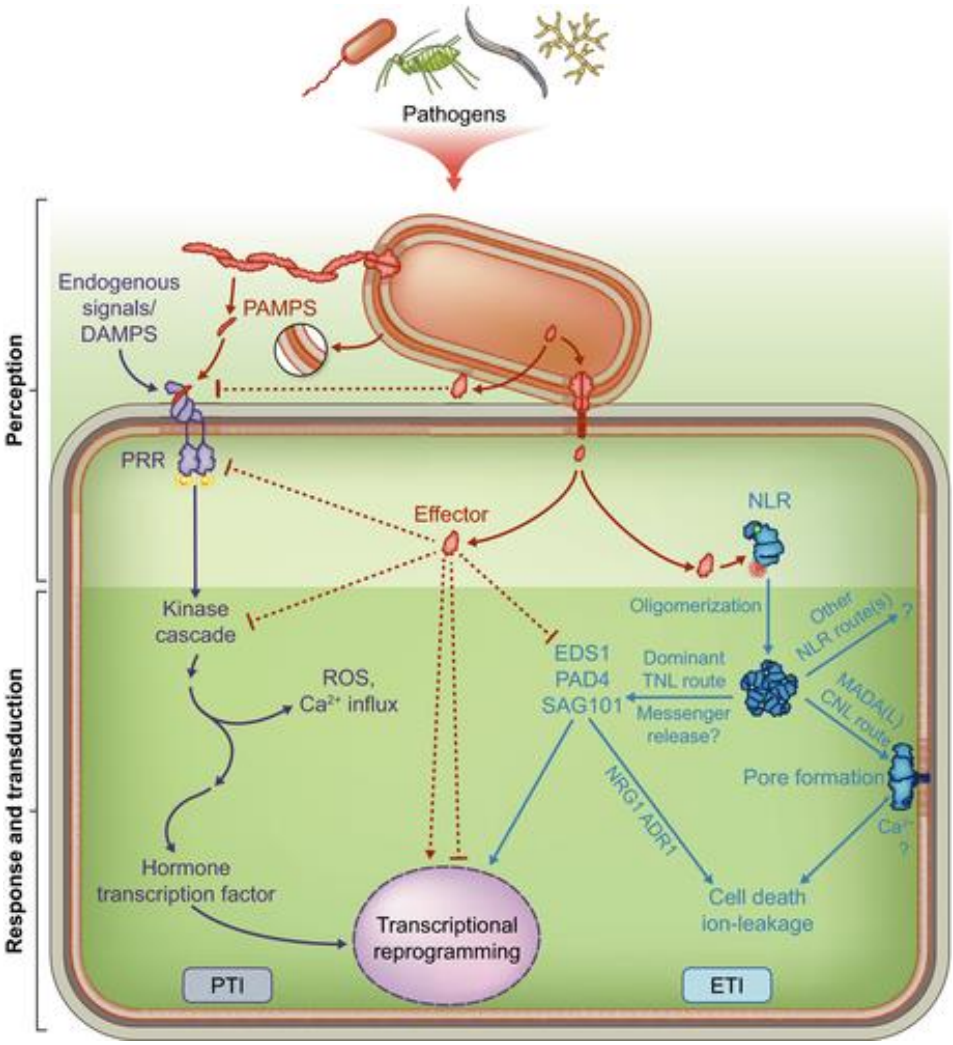

Figure 1-2: Simplified model of the plant immune system (Song et al., 2021)

The recognition of PAMPs from pathogens by extracellular PRRs initiates pattern-triggered immunity (PTI) (left). Pathogens deliver effectors into host cells to block PTI. The effectors can be recognized by intracellular NLR proteins directly or indirectly. Direct or indirect effector recognition can initiate NLR oligomerization. The oligomerization of NLR can form higher-order complexes termed resistosomes that trigger defense responses such as EDS1 signaling, transcriptional reprogramming, and ion leakage typically associated with regulated cell death, which can initiate NLR-dependent effector-triggered immunity (ETI) (right).

PTI and ETI seem to be induced by the two different classes of immune receptors that consist of different activation mechanisms and require different early signaling components. However, PTI and ETI share many common downstream responses, including ROS bursts, calcium influx, MAPK cascades activation, expression of defense-related genes and biosynthesis of defense phytohormones (Kadota et al., 2019; Tsuda et al., 2013). Recently, PTI and ETI have been reported to be mutually potentiated and required by each other (Ngou et al., 2021; Pruitt et al., 2021; Tian et al., 2021; Yuan et

al., 2021). Further studies on the mechanisms underlying signal collaboration between PTI and ETI will provide a more complete understanding of the plant immune system.

1.2 Regulation of R genes (NLRs)

1.2.1 Structures and functions of plant NLRs

Functioning intracellularly, plant R proteins constitute the second layer of the plant immune system (Chisholm et al., 2006; Dangl and Jones, 2001; Maekawa et al., 2011b). Most R genes encode members of intracellular NOD (N-terminal oligomerization domain)-like receptors, which are characterized by a nucleotide-binding domain (NBD) and a C-terminal leucine-rich repeat domain (LRR) (NLR). This kind of combination of domains is similar to that in animal NLR proteins. Due to different ancestors, it appears that NLR proteins are the product of convergent evolution (Bayless and Nishimura, 2020; Urbach and Ausubel, 2017). NLR proteins are functionally conserved in both plants and animals to some degree.

The recognition of intracellular pathogen effector molecules facilitates conformational changes in NLR proteins (Takken and Goverse, 2012). Normally, the N-terminal domain of the NLR protein plays a signaling activation role, and the C-terminal LRR domain keeps it in the resting state by negatively regulating its N-terminal domain (Bayless and Nishimura, 2020). The NBD of plant NLRs usually acts as a molecular switch to regulate NLR activation dependent on (d)ATP-bound activation or ADP-bound inactivation (Tameling et al., 2006; Williams et al., 2011). Some critical motifs are functionally conserved in the NBD domain, such as Met-His-Asp (MHD) and P-loop motifs. The NBD domain is also well known as the NB-ARC domain based on its similarity to mammalian APAF-1, plant R proteins, and nematode CED-4 (Raffaele et al., 2010; Tameling et al., 2002; Williams et al., 2011). Contrary to the relatively conserved NBD domain, the C-terminal LRR domain is a relatively variable region in different plant NLRs. The function of the LRR domain is involved in NLR autoinhibition (Ade et al., 2007; Qi et al., 2012) and effector recognition (Dodds et al., 2006; Wang et al., 1998).

The N-terminal region of plant NLRs normally could be either a Toll/Interleukin-1 receptor/resistance domain (TIR), a Coiled-coil (CC), or a non-NLR Resistance to Powdery Mildew 8 (RPW8)-like CC (CC_R) domain. Thus, the different plant NLRs are

normally divided into three subgroups, called as TNLs (or TIR-NLRs), CNLs (or CC-NLRs), and RNLs (RPW8-NLRs or CC_R-NLRs) (Collier et al., 2011; Shao et al., 2016). Some atypical plant NLRs only contain NB- and LRR-only proteins, called NLs (Van de Weyer et al., 2019). In addition, some non-canonical plant NLRs have various integrated domains (IDs) at their N-terminus or C-terminus, which are thought to allow hosts to rapidly increase their ability to recognize effector proteins. Most ID-containing NLRs encoding genes have been found in paired orientation in the genome, with one ID member functioning as a pathogen sensor and another member as a signaling executor (Cesari et al., 2014; Le Roux et al., 2015). However, both members are required for activation and repression of NLR signaling (Ma et al., 2018).

1.2.2 TNL signal

The N-terminal signaling domains are variable and distinct in both plant and animal NLRs. They are autoregulated and self-associated during signal transduction (Nanson et al., 2019; Qi and Innes, 2013). Several plant TIR domains have been reported to have a similar structure, which consists of a flavodoxin-like fold including a central β-sheet surrounded by α-helices (αA–αE). There are two TIR domains formed by self-association interfaces by the αA/αE and αD/αE helices from architecture, respectively. Both are required for self-association and cell death signaling in plant TNL signaling pathways (Bernoux et al., 2011).

The TIR domain is one of the major classes of intracellular receptors in dicots. Interestingly, while the TIR domain is found to be usually served as a scaffold for assembly of protein complexes for plant innate immune signaling in the beginning (Akira et al., 2006; O'Neill et al., 2013), it is also structurally and functionally conserved and widely distributed in archaeal, bacteria, and eukaryotic proteins (Essuman et al., 2018). For example, the TIR domain of animal SARM1 (sterile alpha and TIR motif containing 1) was recently found to act as an enzyme to cleave cellular NAD^+ (nicotinamide adenine dinucleotide) to mediate axonal cell death (Essuman et al., 2017). Plant TIR domains also have NAD^+-cleaving catalytic activity. NAD^+-cleaving activity is important for TIR-mediated cell death. Nicotinamide, adenosine diphosphate ribose (ADPR) and v-cyclic ADPR (vADPR) are produced by plant TIR domain cleavage of NAD+ (Wan et al., 2019).

This process of NAD+ cleavage by plant TIR domains may be a signaling event because cyclic ADPR is involved in Ca^{2+} signaling activation (Hunt et al., 2004). The mechanisms by which TIR-containing proteins with NADase activity in plants activate immunity are still unclear.

Many proteins that are required for plant TNL signaling have been identified from genetic screens. The first common component is called Nucleocytoplasmic lipase-like protein ENHANCED DISEASE SUSCEPTIBILITY 1 (EDS1), which is involved in TNL-mediated ETI responses (Cui et al., 2015) and is thought to work downstream of TIR NADase activity (Horsefield et al., 2019; Wan et al., 2019). Furthermore, EDS1 can functionally form exclusive heteromeric complexes with its sequence-related lipase-like SENESCENCE ASSOCIATED GENE101 (SAG101) or PHYTOALEXIN DEFICIENT 4 (PAD4), which are involved in TNL-mediated immunity (Feys et al., 2005; Lapin et al., 2019; Wagner et al., 2013). The second family of proteins functioning downstream of the EDS1 family, the RPW8-domain containing RNLs (helper NLRs) such as NRG1 (N-requirement Gene 1) and the ADR1 family (Activated Disease Resistance 1), are also required for TIR pathways (Collier et al., 2011; Jubic et al., 2019; Qi et al., 2018). EDS1 and PAD4 have been reported to play a critical role in plant basal defense and salicylate signaling (Cui et al., 2017). The binding of the N-terminal lipase-like domains to EDS1 or PAD4 establishes unique interaction interfaces at the C-terminal EP (α-helical EDS1-PAD4) domain that can also be implied from the crystal structure of the EDS1-SAG101 heterodimer (Wagner et al., 2013). The EP domain at the C-terminus of EDS1 family members harbors positively charged residues that are important for transduction of TNL signaling (Bhandari et al., 2019; Lapin et al., 2019). TNL RPS4 (Resistance to *P.syringae* 4), a particular TNL protein, is reported to interact with EDS1 as well as NRG1 (Heidrich et al., 2011; Huh et al., 2017; Qi et al., 2018). The functional consequences of these physical interactions among EDS1-PAD4, EDS1-SAG101 or EDS1-RPS4 are still unknown. Expression of the RPW8-containing domain of NRG1 or ADR1 in *eds1* null backgrounds is sufficient to trigger the hypersensitive reaction (HR), implying that the helper RNL functions downstream of EDS1 (Collier et al., 2011; Qi et al., 2018). Besides, Sun et al. (2021) determined that ADR1 proteins can associate with EDS1-PAD4, however NRG1 proteins only interact with EDS1-SAG101 (Sun et al., 2021). The

mechanisms of how plant NLRs switch on downstream immunity is an active field of plant immunity.

1.2.3 CNL signaling

Coiled-coil (CC)-containing NLRs (CNLs) can be further grouped into different subclades based on their CC or NB-ARC domains (Collier et al., 2011; Wang et al., 2021). Several conserved motifs in the CC domain were characterized. For instance, there is a conserved motif called EDVID in CC domains that is first described in a potato CNL called Resistance to Potato virus X (Rx), which can recognize the PVX coat protein (Rairdan et al., 2008). Although the EDVID motif was determined to mediate the interaction between the CC domain and the NB-ARC or NB-ARC-LRR of the CNL receptor, mutation in the EDVID motif cannot block the activation of cell death (Bai et al., 2012; Wang et al., 2015). Besides, some other domains such as the SD domain are characterized as positive regulators to relieve the inhibitory effects of the CC domain and itself on NB-ARC. In addition, the CC_R domain mentioned above in RNLs, including the NRG1 and ADR1 families, can induce defense responses and cell death (Collier et al., 2011). Recently, a MADA motif with the sequence MADA xVSFxVxKLxxLLxxEx is found to be another conserved motif in some CNL subclades such as NRC4 and ZAR1, which play a critical role in mediating cell death (Adachi et al., 2019a). Therefore, CC domains are very diverse among different plant CNL subclades.

The structure basis of CNL activation has attracted many efforts to study for a long time in the field of plant immunity. The first analyzed CC domain structure was resolved for MLA10 from Barley, which was shown to be made up of two helix-loop-helix molecules to form an intertwined dimer (Maekawa et al., 2011a). However, other CNLs such as Rx, Sr33 and the inactive form of ZAR1 have been reported as a monomeric four-helix bundle (Casey et al., 2016; Hao et al., 2013; Wang et al., 2019). One of the milestone studies in the NLR field is the first full-length structural basis of CNL, ZAR1. It was found that ZAR1 can form a pentamer complex called a resistosome upon activation. The CC domain of the active form of ZAR1 undergoes conformational changes, forming a funnel shape by five CC domains where the first α helix is released and the remaining three helices form a bundle together (Wang et al., 2019). Further investigation proved that the pentamer

complex can mediate calcium influx, a key secondary signal in the ETI response (Bi et al., 2021).

Although the CC domain of plant CNLs is thought to be the functional domain that induces cell death, CC domains from some CNLs such as RPS5 (Ade et al., 2007), Rx (Rairdan et al., 2008), and RPM1 (El Kasmi et al., 2017) cannot trigger cell death. The expression of some CC domains by itself is sufficient to induce disease resistance and mediate cell death simultaneously (Wroblewski et al., 2018). The accurate link between cell death and disease resistance signaling is mostly unknown. For example, rice NLR BROWN PLANTHOPPER RESISTANCE14 (BPH14) confers resistance to brown planthoppers. The expression of the CC or NB-ARC domains of BPH14 can show a resistance level similar to that of the full-length protein (Hu et al., 2017).

The CC domain seems to mediate the interaction between downstream components. CC-interacting proteins are often involved in defense signaling or pathogen recognition. For example, the fungal avirulence effector protein AVR_{A10} is recognized by MLA10. AVR_{A10} can induce an association between MLA10 and WRKY2 in the nucleus mediating by the CC domains of MLA10 (Shen et al., 2007). Because WRKY1/2 plays a crucial function in basal defense against *Blumeria graminis*, MLA10 may activate basal defense responses by disturbing WRKY-mediated repression (Shen et al., 2007). One more example, the CC domain of RPM1 can interact with RIN4, a key regulator in plant immunity (Mackey et al., 2002). RPM1-mediated defense responses are activated by the detection of RIN4 phosphorylation induced by T3SE (Type III secreted effector) AvrB and AvrRpm1 or RIN4 integrity induced by T3SE AvrRpt2 (Chung et al., 2011; Liu et al., 2011).

NON-RACE SPECIFIC DISEASE RESISTANCE-1(NDR1) was reported to play an essential role in the activation of plant defense (Century et al., 1997). Both NDR1 and EDS1 are characterized as central activators of defense signaling. As described above, EDS1 is involved downstream of TNL signaling. However, NDR1 participates in the activation of the CNL family of resistance (Knepper et al., 2011). Moreover, some CNLs are reported to transduce downstream signaling via helper NLR ADR1, indicating that crosstalk might occur at the late point of some particular CNL and TNL signaling pathways (Saile et al., 2020; Wu et al., 2020). However, the underlying mechanism for CNL defense

signaling is still elusive and may be diverse. For instance, some CNLs localize at other cell compartments (e.g cytosol or nucleus) and show different signaling behaviors depending on their localization (Fenyk et al., 2015; Knip et al., 2019; Slootweg et al., 2010). Thus, there might be some other signaling pathways for compartment-specific ETI responses due to the localization diversity of CNLs. It is tempting to perform further studies to investigate how CNLs mediate downstream defense signaling events.

1.3 Regulations of co-receptor BAK1

1.3.1 Biological functions of RKs

The first one of plant receptor protein kinases (RKs) identified in maize was called ZmPK1 (Walker and Zhang, 1990). More than 30 RKs have been functionally characterized in plants and a few specific ligands have been identified (Gou et al., 2010). There are at least 223 leucine-rich repeat receptor-like kinases (LRR-RKs) in *A. thaliana* (Gou et al., 2010).. Plant LRR-RKs play essential roles in plant growth, development, pathogen resistance and cell death. For instance, CLAVATA1 (CLV1) controls differentiated and undifferentiated shoot and floral meristem cells (Clark et al., 1997); HAESA/HSL2 determines floral organ abscission (Jinn et al., 2000); SOMATIC EMBRYOGENESIS RECEPTOR KINASE 1 (SERK1) and SERK2 function in microsporogenesis and male sterility (Albrecht et al., 2005; Colcombet et al., 2005; Zhao et al., 2002). LRR-RLKs RECEPTOR-LIKE PROTEIN KINASE 1 (RPK1) is involved in abscisic acid early signaling (Hong et al., 1997; Osakabe et al., 2005); FLS2 can specifically recognize bacterial flagellin (Clay and Nelson, 2002); BIR1 and SOBIR1 were identified to regulate cell death and plant innate immunity (Gao et al., 2009).

Notably, several LRR-RKs play dual or multiple roles during plant growth and development. For example, BRASSINOSTEROID INSENSITIVE (BRI1)-ASSOCIATED KINASE 1 (BAK1) is involved in Brassinosteroid (BR)-dependent cell growth, PAMP-triggered immunity, and cell death control under various stresses (He et al., 2007; Kemmerling et al., 2007).

1.3.2 Multifunction of co-receptor BAK1

As mentioned above, BAK1 is a multifunctional RK that is involved in different biological processes such as plant development, growth, cell death and immunity. BAK1 belongs to

a SOMATIC EMBRYOGENESIS RECEPTOR-like KINASE (SERK) subfamily of LRR-RKs, which has five members, SERK1 to 5 (SERK1-5) (Hecht et al., 2001). It was named BRI1-associated kinase 1 because it was first identified as a co-receptor of the Brassinolide (BL) receptor BRI1 (Li et al., 2002; Nam and Li, 2002). The following studies show that BAK1 plays an important role in plant immunity as it interacts with multiple PAMP/MAMP receptors (Figure 1-3), such as FLS2 and the Elongation Factor-Tu Receptor (EFR), the DAMP receptor PEPR1 and PEPR2, the phytosulfokine receptor PSKR1 and PSY1R (Chinchilla et al., 2007; Heese et al., 2007; Krol et al., 2010; Ladwig et al., 2015; Postel et al., 2010; Roux et al., 2011; Yamaguchi et al., 2006).

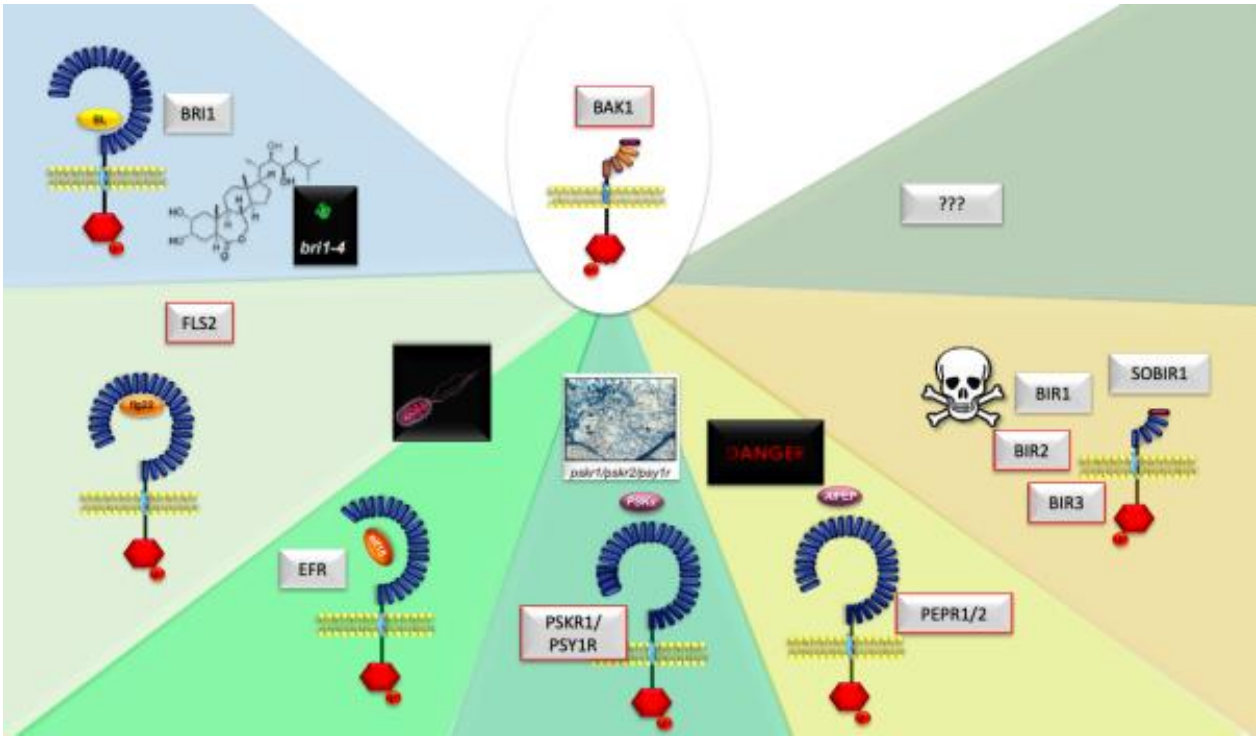

Figure 1-3: Schematic of the interaction between *A. thaliana* LRR-RKs and BAK1

Some BAK1-interacting LRR-RKs such as BRI1, FLS2, EFR, PEPR1/2 and PSKR1/PSY1R are involved in multiple pathways, for example development, and plant immunity. The BAK1-interacting receptor (BIR) family is also involved in plant immunity by negative regulation of BAK1. (picture © B.Kemmerling).

BAK1 is well-studied in that it can act as an interaction partner of either BRI1, the *A. thaliana* brassinosteroid (BR) receptor, FLS2, the immune receptor of *A. thaliana* that can perceive the bacterial flagellin epitope flg22, or EFR that can recognize the bacterial

elongation factor Tu or the minimal peptide elf18. When pathogens attack plants, BAK1 can be recruited to the FLS2 complex by recognizing the C-terminus of FLS2-bound flg22 (Sun et al., 2013b) and thus activate the innate immune response of plants (Chinchilla et al., 2007; Heese et al., 2007; Kemmerling et al., 2007; Schulze et al., 2010). Genetic and biochemical analyses reveal that BAK1 plays crucial roles in both the BRI1 and FLS2 signaling pathways as a co-receptor (Chinchilla et al., 2007; Heese et al., 2007; Li et al., 2002; Nam and Li, 2002; Sun et al., 2013a). BAK1 interacts with RKs to form complexes after treatment with their cognate ligands (Chinchilla et al., 2007; Heese et al., 2007; Santiago et al., 2013; Somssich et al., 2015; Sun et al., 2013b). RK/BAK1 complex formation is followed by a set of responses such as the transphosphorylation of both kinase domains, the internalization of the activated RK/BAK1 complex through endocytosis and the initiation of downstream signaling (Couto and Zipfel, 2016; Frescatada-Rosa et al., 2015; Schwessinger et al., 2011; Wang et al., 2008).

In addition to RKs, leucine-rich repeat (LRR) receptor-like proteins (LRR-RLPs) are universal cell surface receptors lacking a cytoplasmic kinase domain. However, RLPs constitutively interact with RK Suppressor Of BIR1-1/ EVERSHED (SOBIR1/EVR), assuming that they provide a kinase domain that is required for downstream signaling (Gao et al., 2009; Gust and Felix, 2014; Leslie et al., 2010; Liebrand et al., 2014). SOBIR1 was shown to be essential for plant defense responses by specific LRR-RLPs, which similarly act as immune receptors (Liebrand et al., 2013; Zhang et al., 2013). Similar to the situation with LRR-RKs, BAK1 was found to be required for LRR-RLPs function. It has been determined that BAK1 is recruited to RLP/SOBIR1 complexes upon RLP activation by its cognate ligand (Albert et al., 2015; Domazakis et al., 2018; Postma et al., 2016; Wang et al., 2018). For example, Albert et al. (2015) revealed that the RLP23/SOBIR1 complex mediates immunity triggered by necrosis and ethylene-inducing peptide-like 1 proteins (NLPs) in a BAK1-dependent manner. Similarly, Postma et al. (2016) showed that BAK1 was specifically recruited to the Cf-4/SOBIR1 complex when Cf-4 is activated by perception of Avr4 from *Cladosporium fulvum*. Moreover, Aranka M. Van Der Burgh et al. reported that the kinase activity of SOBIR1 and BAK1 is required for immune signaling (van der Burgh et al., 2019).

Additionally, BAK1 plays a role in cell death control since *bak1* mutants show a spreading cell death phenotype upon treatment with *P.syringae* pv*. tomato* DC3000 and *Alternaria* (*A*.) *brassicicola* (Kemmerling et al., 2007). BAK1 and its closest homolog BKK1 (BAK1-like 1 or SERK4) can negatively regulate cell death because *bak1 bkk1* double mutant shows constitutive activation of immune responses and displays spontaneous cell death and seedlings lethality (He et al., 2007). Interestingly, the 5 members of the SERK family not only have redundant roles but also specific roles in the signaling transduction. For example, SERK1, SERK3, SERK4 and SERK5 are involved in the BR-signaling pathway; both SERK3 and SERK4 are involved in MAPK activation and cell death control; both SERK1 and SERK2 are involved in somatic embryogenesis and tapetum development (Colcombet et al., 2005; Li, 2010). Therefore, the SERK family members show significant overlap in functions, but each has a specific subset of signaling. Sequence analysis for SERK family proteins from different plant species including monocots, dicots and nonvascular plants indicates that SERKs are a highly conserved protein family (Aan den Toorn et al., 2015). Some specific residues in the extracellular domain that are essential for interaction with other receptor kinases are conserved even if the SERK protein does not function in that pathway. For example, SERK2 has no function in the brassinosteroid pathway and does not interact with BRI1, but it is also conserved in its BRI1-interacting domain (Aan den Toorn et al., 2015). *SERK* family genes are ancient genes which act as co-receptors to be recruited to newly evolved signaling pathways during speciation.

More study indicates that overexpression of the *A. thaliana* BAK1 leads to cell death (Belkhadir et al., 2012). Similarly, overdose of BAK1 causes harmful effects on plants, including development, leaf necrosis, growth stagnation and reduced seed yield (Dominguez-Ferreras et al., 2015). Even without PAMP treatment, higher accumulation of BAK1 can lead to induction of MAPKs, ethylene production, and increased resistance to the pathogenic *P. syringae* pv. *tomato* DC3000. The same study also showed that the extracellular domain of BAK1 was sufficient to induce autoimmunity. Interestingly, the phenotype of BAK1 overexpression can be rescued by *sobir1* mutation. Although SOBIR1 was identified to regulate cell death (Gao et al., 2009), the molecular mechanism by which BAK1 overexpression phenotype is suppressed by *sobir1* was not clarified yet. It was

postulated that R protein might detect BAK1 accumulation because the overexpression of BAK1 could induce several redundant ETI pathways or some non-tested pathways (Dominguez-Ferreras et al., 2015). In addition, the phenotype of BAK1 overexpression can be rescued by *bir1*. It was elucidated that a well-balanced amount of BAK1 is essential for *A. thaliana* fitness, especially for repression of premature death.

One of the most interesting questions is how the signal specificity within BAK1-mediated physiological programs is maintained. BAK1 can provide signaling specificity in a phosphorylation-dependent manner on the regulation of plant growth, cell death, and innate immunity (Schwessinger et al., 2011). Albrecht et al. (2012) had shown that the activation of BAK1 by BR treatment does not lead to immune responses such as the production of ROS or MAPK activation (Albrecht et al., 2012). It implies that BAK1 is not the rate-limiting component in these two different pathways. One possibility is that the co-receptor BAK1 and these receptors are already in proximity in different membrane compartments before ligand binding, as shown for BRI1 and BAK1 (Bucherl et al., 2013). Recently, the crystal structures of the receptor complexes have provided an insight into SERK co-receptors bind to ligand-binding LRR-RKs and the receptor-bound ligands (Santiago et al., 2013; Sun et al., 2013a; Sun et al., 2013b). Thus, the signal specificity of BAK1-mediated physiological programs could be understood as differential phosphorylation of BAK1 by different ligand-binding receptors. Many studies indicate that the direction of signaling specificity, via different phosphorylation patterns in BAK1-mediated physiological processes which facilitates BAK1 as a co-receptor in plant development, defense, and cell death (Perraki et al., 2018; Schwessinger et al., 2011; Wang et al., 2014; Yan et al., 2012).

BAK1 plays essential roles as a co-receptor by interacting with many LRR-RKs which are involved in many plant signalling pathways such as plant growth and development, plant immunity and plant reproduction. Thus, identification of additional BAK1-interacting proteins that control its BL-independent activity should provide insight into how specificity in plant developmental and immunity programs is maintained.

1.4 The receptor-like kinase BIRs family

The first member in the BIR family is BIR1 which was identified by genetic screening of plants with seedling lethality phenotype at normal temperature. BIR1 can constitutively interact with BAK1 (Gao et al., 2009). Although the cell death triggered by the loss of function mutant *bir1-1* is still elusive, another RK SOBIR1, one partner in the RLP complex, seems to be required for the *bir1-1*-mediated cell death (Gao et al., 2009). Consistently, overexpression of SOBIR1 triggers cell death and defense response (Gao et al., 2009). Both BIR1 and SOBIR1 are active protein kinases because the kinase activity is very important for their function. PAD4, EDS1 and SA signaling is partially required for *bir1-1*-mediated cell death (Gao et al., 2009), indicating that NLRs probably contributes to this process.

A proteomics study by analysis of BAK1-interacting proteins using mass spectrometry in combination with bioinformatic analyses identifies more members within the BIR families: BIR2 and BIR3 (Halter et al., 2014; Imkampe et al., 2017). All the BIRs belong to a related RLK subfamily Xa in the LRR subgroup X. It was found that BIR2 plays a negative role in PAMP-triggered immunity. BIR2 is characterized to be an atypical kinase which has no autophosphorylation activity. However, BIR2 can constitutively interact with BAK1 and be phosphorylated by BAK1 (Blaum et al., 2014; Halter et al., 2014). The phosphorylated BIR2 is released from BAK1, thus relieving the negative role in PTI response. Further analysis indicates that BIR2 negatively regulates the formation of FLS2-BAK1 complexes induced by flg22 (Halter et al., 2014). Moreover, *bir2* mutant also shows enhanced cell death responses upon treatment with necrotrophic fungal pathogen *A. brassicicola*, which is similar to *bak1* and *bir1* mutant. BIR2 appears to specifically regulate PTI response in immunity because it does not affect BR signaling.

In contrast to BIR2, another BIR family member, BIR3 negatively regulates the BR, PAMP and cell death pathways (Imkampe et al., 2017). In BR signaling, BIR3 interacts with BRI1 in addition to BAK1 and competitively inhibits BRI1-mediated signaling. In PAMP-triggered immunity, BIR3 can interact with both ligand binding receptor and co-receptor BAK1, thus negatively regulates complex formation between BAK1 and ligand binding receptors, for example FLS2. Interestingly, *bir3* mutant shows very mild

phenotypes, BIR3 additionally controls the stabilization of BAK1 and other SERK proteins. *bak1 bir3* double mutant can cause very strong cell death which is reminiscent of *bak1 bkk1* double mutant (He et al., 2007; Imkampe et al., 2017). Therefore, it is tempting to investigate how BIR family proteins regulate cell death events.

1.5 Autoimmunity and cell death

Plant immunity is strictly controlled to avoid activation in the absence of pathogens. Otherwise, it will lead to autoimmunity if plant immunity is constitutively activated without pathogens. Autoimmunity usually manifests the phenotype of spontaneous cell death, growth defects such as dwarfism, and elevated resistance to pathogens. Up to date, there are many autoimmune mutants that have been identified. They involve different kinds of immune proteins as described in the following.

1.5.1 Autoimmunity caused by NLR

The most well studied autoimmune mutant in *A. thaliana* is *snc1* (*suppressor of npr1-1, constitutive 1*), which encodes a TNL protein with a point mutant in the linker region between NB and LRR domain. *snc1* exhibits very strong dwarfism phenotype in a temperature dependent manner (Jia et al., 2021; Li et al., 2001). This phenotype makes *snc1* or other autoimmune mutants to be very good tools for suppressor screens. Indeed, by screening enhancers or suppressors of *snc1*, many components which are involved in NLR protein homeostasis or signaling pathway have been determined (Cai et al., 2018; Jia et al., 2021).

Normally, autoimmune phenotype caused by NLR genes is dominant in genetics (Lolle et al., 2017). Another gain-of-function mutant of TNL, *suppressor of salicylic acid insensitive 4* (*ssi4*), similarly causes dwarfism and spontaneous cell death (Shirano et al., 2002). As stated above, some NLR proteins contain an additional domain so-called integrated domain (ID), which are usually used for effector recognition. Interestingly, several of these atypical NLRs with a mutant at ID domain were also found to cause plant autoimmunity. For example, TNL protein CHS3 contains a LIM domain at its C-terminus. *chs3-2D*, a missense mutation close to the LIM domain, can trigger very strong dwarfism and constitutive resistance. *RRS1* encodes a TNL protein containing a WRKY domain at its C-terminus (Xu et al., 2015). One allele of *RRS1*, *sensitive to low humidity 1* (*slh1*)

encodes protein with an amino acid insertion in the WRKY domain causing plant immunity as well (Newman et al., 2019). In addition, a mutation in *chs1*, a truncated TIR-NB protein, can also lead to cell death and defense response in the absence of pathogens (Liang et al., 2019).

1.5.2 Autoimmunity caused by other types of proteins

In addition to NLR, there are autoimmunity caused by mutations of other types of proteins. For example, loss-of-function of multiple members of the MAPK pathway leads to activation of defense response. Because MAPK cascade is one of the important events activated in the PTI response, it is reasonable that NLR protein monitors this pathway based on the “guard model”. Indeed, CNL protein SUMM2 was characterized to be required for mutant *mekk1*-, *mkk1/mkk2*-, and *mpk4*-mediated autoimmunity (Kong et al., 2012; Zhang et al., 2017). Likely, CNGC2/CNGC4 are the key components which mediate calcium influx in the PTI response (Tian et al., 2019). The mutant *cngc2* and *cngc4* results in constitutive defense responses in the absence of cell death (Balague et al., 2003; Clough et al., 2000; Jurkowski et al., 2004). Although the mechanism underlying is unclear, it is assumed that an unknown NLR guards these two proteins and leads to autoimmunity. Another example of autoimmunity caused by atypical immune protein is ACD6, which contains an ankyrin repeat domain and a multiple transmembrane domain (TM). *acd6-1* encodes the protein with a point mutation in a TM domain leading to constitutive cell death and enhanced resistance to pathogens (Lu et al., 2003; Lu et al., 2009; Rate et al., 1999). It was recently found that ACD6 may function as a calcium channel to be involved in plant immunity. The hyperactive form of ACD6-1 may cause elevated calcium concentration in plant cells and thus trigger plant autoimmunity (Kolodziej et al., 2021).

1.5.3 Autoimmunity in hybrid

In hybrids, a very common phenomenon is heterosis. However, not very less to be observed in hybrids is necrosis. For a very long time, it was unknown the mechanism of hybrid necrosis until scientists identified that the immune-related genes are involved in this process. Consistent with before mentioned autoimmunity caused by chemical-induced mutants or others, autoimmunity in hybrids was found to be caused by similar

proteins. For example, mismatched NLR protein from two parents DM1 and DM2 can interact with each other and can lead to hybrid necrosis (Tran et al., 2017). Atypical resistance protein RPW8 acts as a ligand to trigger a canonical CNL protein RPP7 forming a complex, by which RPW8 and RPP7 induce autoimmunity in hybrid (Li et al., 2020). Similar to *acd6-1*, two different alleles from two *A. thaliana* strains can cause plant autoimmunity, implying that ACD6 forms homooligomers in plants.

1.5.4 Autoimmunity caused by RLK/RLPs

As described above, the most well studied autoimmunity caused by mutations in RLKs/RLPs is *bak1 bkk1* double mutant. By genetic screen, several components are identified to be required for *bak1 bkk1*-mediated cell death. Du et al found a nucleoporin (NUP) 85-like protein is essential for BAK1- and BKK1-mediated cell death control, implying nucleocytoplasmic traffic may be involved in this process (Du et al., 2016). Moreover, by using virus-induced gene silencing of BAK1/BKK1, STT3a, a protein involved in N-glycosylation modification, was found to be required for activation of *bak1 bkk1* cell death (de Oliveira et al., 2016). A cysteine-rich receptor-like kinase (CRK) appears to be the client protein of protein glycosylation which is involved in regulation of cell death (Burdiak et al., 2015; Quezada et al., 2019). Using the same strategy, cyclic nucleotide-gated channel 19/20 (CNGC19/20) was revealed to regulate *bak1 bkk1* cell death. CNGC19 and CNGC20 can be phosphorylated by BAK1, and their homeostasis likely contribute to *bak1 bkk1* cell death (Yu et al., 2019). NLR protein seems to be involved in *bak1 bkk1* cell death because helper NLRs were identified to be indispensable for the autoimmune phenotype (Wu et al., 2020).

Loss of BIR1 causes plant autoimmunity as well. Although BIR2 and BIR3 negatively regulate PTI response, loss of either BIR2 or BIR3 only causes very mild phenotypes. However, double mutant *bak1 bir3* shows a very strong dwarfism phenotype. While the mechanisms underlying it are still unclear, it is not totally the same as *bak1 bkk1*.

1.6 The Aims of the thesis

The BAK1-interacting receptor kinase BIR3 can prevent interaction between BAK1 and ligand-binding receptor by directly interacting with both ligand-binding receptors and

BAK1. Double mutants in *bak1 bir3* show a severe dwarf phenotype and spontaneous cell death. To investigate the mechanism underlying it, we employed ESI-LC-MS/MS and identified a BIR3 interacting protein, *CONSTITUTIVE SHADE AVOIDANCE* 1 (CSA1) which belongs to the TNL family. We found that mutation in *csa1* can suppress *bak1 bir3*-mediated cell death. The aims of the thesis are to study (i) the downstream components that are involved in *bak1 bir3* cell death signaling, (ii) the mechanism by which CSA1 mediate cell death of the *bak1 bir3* mutants, and (iii) the function of CSA1 partner CHS3 in *bak1 bir3*-mediated cell death.

2. Materials and methods

2.1 Materials

2.1.1 Plants genotypes

Genotype	Mutation	Reference/Source
Col-0	wildtype	
bak1-4	SALK_116202, T-DNA insertion in *BAK1* (At4g33430)	(Kemmerling et al., 2007)
bir3-2	Salk_116632, T-DNA insertion in *BIR3* (At1g27190)	(Halter et al., 2014)
csa1-2	SALK_023219, T-DNA insertion in *csa1* (At5g17880)	(Faigon-Soverna et al., 2006)
chs3-3	SALK_063886, T-DNA insertion in *chs3* (At5g17890), referred to as *chs3-3*	(Alonso et al., 2003)
nahG	expression of the bacterial NahG gene, a salicylate hydroxylase	(Lawton et al., 1995)
pad4	point mutation in *pad4* (At3g52430)	(Glazebrook et al., 1996)
sag101	Col-0 dSpm transposon insertion lines in *sag101* (At5g14930)	(Feys et al., 2005)
bak1-4 bir3-2	Crossing of *bak1-4* with *bir3-2*	(Imkampe et al., 2017)
bir2-1	GABI N 733599, T-DNA insertion in *bir2* (At3g28450)	(Halter et al., 2014)
35S-BIR3-YFP	pB7YWG2-BIR3 transformed in Col-0	(Halter et al., 2014)
bak1-4 csa1-2	Crossing of *bak1-4* with *csa1-2*	(Schulze et al., 2022)
bak1-4 bir3-2 csa1-2	Crossing of *csa1-2* with *bak1-4* and *bir3-2*	(Schulze et al., 2022)
bak1-4 eds1-12	Crossing of *eds1-12* with *bak1-4*	this work
bak1-4 bir3-2 eds1-12	Crossing of *eds1-12* with *bak1-4* and *bir3-2*	(Gao et al., 2009)
bir2-1 eds1-12	Crossing of *eds1-12* with *bir2-1*	this work
bak1-4 bir3-2 pad4-1	Crossing of *pad4-1* with *bak1-4 bir3-2* (+/-)	this work
bak1-4 bir3-2 sag101	Crossing of *sag101-1* with *bak1-4 bir3-2* (+/-)	this work
bak1-4 bir3-2 NahG	Crossing of *NahG* with *bak1-4 bir3-2* (+/-)	this work
bak1-4 bir3-2 nrg1.1 nrg1.2	Crossing of *nrg1.1 nrg1.2* with *bak1-4 bir3-2* (+/-)	this work
bak1-4 chs3-3	Crossing of *chs3-3* with *bak1-4*	this work
bak1-4 bir3-2 chs3-3	Crossing of *chs3-3* with *bak1-4 bir3-2* (+/-)	this work

bak1-4 csa1-2/ pCSA1:: CSA1	expressing CSA1 genomic DNA construct under endogenous promotor in *bak1-4 csa1-2* background	(Schulze et al., 2022)
bak1-4 bir3-2 csa1-2/ pCSA1 :: CSA1	expressing CSA1 genomic DNA construct under endogenous promotor in *bak1-4 bir3-2 csa1-2* background	this work
Nicotiana benthamiana	wildtype	

2.1.2 Bacteria strains

Strain	Genotype
Escherichia coli DH5α	F-(Φ80lacZΔM15) Δ(lacZYA-argF) U169 recA1 endA1 hsdR17 (rK–, mK+) phoA supE44 λ– thi-1 gyrA96 relA1
Agrobacterium tumefaciens GV3101	T-DNA- vir+ rifr, pMP90 genr
Yeast THY. AP4	*Saccharomyces*. *Cerevisiae* MATa; *ade2* -, *his3* -, *leu2* -, *trp1* -, *ura3* -; lexA::ADE2, lexA::HIS3, lexA::lacZ)

2.1.3 Media and Antibiotics

Components of the different media are given in the below table in this study.

Medium	Components
LB	10 g/l Bacto-Trypton, 5 g/l Bacto-Yeast extract, 5 g/l NaCl, to solidify add 15 g/l Agar
½ MS	2.2 g/l MS-salts (Duchefa), 1% sucrose when indicated, set pH 5.7 with KOH, to solidify add 8 g/l Select-Agar
YPD	20 g/l peptone, 20 g/l glucose, 10 g/l yeast extract, set pH to 6-6.3, to solidify add 15 g/l oxoid agar
CSM	6.9 g/l YNB without amino acids (Formedium), synthetic complete amino acid drop out according to manufacturer's instructions (Formedium), 20 g/l glucose, set pH to 6-6.3, to solidify add 1.5 % oxoid agar

All solutions were autoclaved at 121 °C for 20 mins, then were cooled down to 60 °C and supplemented with corresponding antibiotics in the following concentrations.

Antibiotic	Stock	final concentration
Kanamycin	50 mg/ml in ddH_2O	50 µg/ml

Rifampicin	12.5 mg/ml in methanol	50 µg/ml
Spectinomycin	50 mg/ml in ddH_2O	100 µg/ml
Gentamycin	10 mg/ml in ddH_2O	25 µg/ml
Carbenicillin	50 mg/ml in ddH_2O	50 µg/ml

2.1.4 Agarose beads and antibodies

Both anti-V5 agarose and anti-HA magnetic beads are stored in 0 – 4 °C refrigerator.

Agarose	Order number	Company
anti-V5 agarose	A7345-1ml	Sigma-Aldrich
anti-HA Magnetic Beads	88836-1ml	ThermoFisher Scientific

1. Antibody	Host species	Use	Reference/Provider
α-GFP	mouse	1:3000	Abcam
α-HA	mouse	1:3000	Sigma-Aldrich
α-V5	mouse	1:2000	Sigma-Aldrich
α-Luciferase	mouse	1:3000	Sigma-Aldrich
α-VP16	mouse	1:1000	Santa Cruz (Halter et al., 2014)
α-ATPase	rabbit	1:3000	Agrisera

2. Antibody	Feature	Use	Reference/Provider
α-mouse	HRP conjugated	1:10000	Sigma-Aldrich
α-rabbit	HRP conjugated	1:50000	Sigma-Aldrich

2.1.5 Primers

Primers were synthesized by EurofinsGenomics. All Primer stocks were saved at 100 µM concentration in – 20 °C freezer and diluted in nuclease-free water. The working

concentration is 10 mM. The sequences of primers used in this study are listed in the following table.

Name	Sequence (5'-> 3')	Characteristics
CSA1-F (KpnI)	CGGGTACCTAATGACAAGCTCCTCCTCCTG	cloning for CSA1 cds, fwd
CSA1-R (SalI)	AGGGTCGACACACAAAAGAGTGGAACCAAAAC	cloning for CSA1 cds, rev
CSA1-TIR-R(187aa)	AGGGTCGACAGAAGGAGGACCCTCTGAAC	deletion constructs of CSA1, rev
CSA1-NB-F(188aa)	CGGGTACCATGAAATGTTCTGCACTACCGCCC	deletion constructs of CSA1, fwd
CSA-NB-R(586aa)	AGGGTCGACATATCTTAGATCCCTCATCATG	deletion constructs of CSA1, rev
CSA1-LRR-F(587aa)	CGGGTACCATGCTCAAAATCTACAGCACTCATTG	deletion constructs of CSA1, fwd
CSA1-LRR-R(end)	AGGGTCGACACACAAAAGAGTGGAACCAAAAC	deletion constructs of CSA1
BIR3-F (KpnI)	CGGGTACCATGAAGAAGATCTTCATCACAC	cloning for PCL-BIR3 or PNL-BIR3, fwd
BIR3-R (SalI)	AGGGTCGACAGCTTCTTGTTTGTTGAAGACC	cloning for PCL-BIR3 or PNL-BIR3, rev
CHS3-F (KpnI)	CGGGTACCATGGAACCACCAGCTGCTCG	cloning for CHS3 cds, fwd
CHS3-R (SalI)	AGGGTCGACTAACTTTGAATATTGTGGAG	cloning for CHS3 cds, rev
CHS3-TIR-R(154aa)	AGGGTCGACCTCTTCCACTAGTTCGGAGTC	deletion constructs of CHS3, rev
CHS3-NB-F(155aa)	CGGGTACCATGATCGTCAGAGATGTTTATG	deletion constructs of CHS3, fwd
CHS3-NB-R(518aa)	AGGGTCGACGTGTTCAGCGACCAGACCAG	deletion constructs of CHS3, rev
CHS3-LRR-F(519aa)	CGGGTACCATGATCGAAAGCATATTCCTG	deletion constructs of CHS3, fwd

CHS3-LRR-R(835aa)	AGGGTCGACAAGCTGCTCAAAATCCAAATTAATTG	deletion constructs of CHS3, rev
CHS3-LIM-F(836aa)	CGGGTACCATGCCTAGGCACTTCATCTTC	deletion constructs of CHS3, fwd
CHS3-LIM-R(1386aa)	AGGGTCGACCTCAAAGAATTCACGGATTTC	deletion constructs of CHS3, rev
CHS3-unkn-F(1387aa)	CGGGTACCATGGGCTTACACATGAAGATTGAG	deletion constructs of CHS3, fwd
M13F	tgtaaaacgacggccagt	sequencing for CSA1, fwd
M13R	caggaaacagctatgacc	sequencing for CSA1, fwd
CSA1-F(700)	ATGCCCGGTATAGGTAAAACC	sequencing for CSA1, fwd
CSA1-F(1400)	CTTCTTGACATAGCTTGCTTC	sequencing for CSA1, fwd
CSA1-F(2100)	ATGTGGATATGGAAAATATG	sequencing for CSA1, fwd
CHS3-F(700)	GGACTCCACCGTTTGCTC	sequencing for CHS3, fwd
CHS3-F(1397)	TGATCCAAGACACCTGCC	sequencing for CHS3, fwd
CHS3-F(2099)	TATTCAATGCGACCCATC	sequencing for CHS3, fwd
CHS3-F(2804)	TTAGGTGTGTAGGTACATG	sequencing for CHS3, fwd
CHS3-F(3508)	GAAAGCATTCCAAAGATC	sequencing for CHS3, fwd
CHS3-F(4262)	GTGTCTGATGGTAGTCAG	sequencing for CHS3, fwd
pCambia3300-DN-F	TCATTTGGAGAGGACGAC	DN construct, fwd
CSA1-NP1	CACTCAACTCTTGGCCCATC	sequencing for native promoter of CSA1, rev
CSA1-NP2	accattaaccaaatacgtgg	sequencing for native promoter of CSA1, rev
CSA1-NP3	gagaaattttacatttttta	sequencing for native promoter of CSA1, rev

CSA1-NP4	ctcgtctcatctttataggc	sequencing for native promoter of CSA1, rev
Cluc-R	CATCCATCCTTGTCAATCAAGGCG	for PCL sequncing or colony PCR, rev
Nluc-R	GCGTATCTCTTCATAGCC	for PNL sequncing or colony PCR, rev
Cluc-F	cataaaggccaagaaggg	for PCL sequncing or colony PCR, fwd
rbcs-R	AAATTACAAGCACAACAAATGG	for pUC19 sequncing or colony PCR, rev
CSA1-geno-F	CGGGTACCTAcacaattccagcatccacttgcg	cloning for CSA1 genomic DNA, fwd
CSA1-geno-R	AGGGTCGACATGGCTATACATTTCATAAAGC	cloning for CSA1 genomic DNA, rev
CHS3-geno-F	CGGGTACCATGGAACCACCAGCTGCTCG	cloning for CHS3 genomic DNA, fwd
CHS3-geno-R	ACCGCTCGAGTAACTTTGAATATTGTGGAGTCTTGG	cloning for CHS3 genomic DNA, rev
gCSA1-F(3231)	GTGTCATTTGCTTGCTAG	sequencing for gCSA1, fwd
gCHS3-R(1129)	CGGTCTCATAATATACGAAC	sequencing for gCHS3, rev
gCHS3-R(5509)	CTAGTATCTGCTTATTCAAC	sequencing for gCHS3, rev
gCHS3-F(3836)	GTTCATCTAGCGAATTACAG	sequencing for gCHS3, fwd
gCSA1-F(1971)	agGGAGGTTCTAATATCAGG	sequencing for gCSA1, fwd
gCSA1-R(3187)	CCAATTCATTGCAGTTAGTG	sequencing for gCSA1, rev
gCSA1-F(3903)	GTGCTAATGGTTGTTTCAAG	sequencing for gCSA1, fwd
gCHS3-R (4454)	ATCTTCAATTGCAGATTTGC	sequencing for gCHS3, rev
gCHS3-R (4700)	CGGAGCTCCTTGTAGCAAGG	sequencing for gCHS3, rev
gCSA1-R (2259)	TCGCTATAAGGAAGCTTAAG	sequencing for gCSA1, rev

gCSA1-F(3387)	GCTTTCCTGGATGTGAAATG	sequencing for gCSA1, fwd
gCSA1-F(3604)	GAAGGTTGGAAGTTTGATTG	sequencing for gCSA1, fwd
gCSA1-F(3824)	TTTGAACCTGAAGAGAACAG	sequencing for gCSA1, fwd
pXNubA22-F	CAAGCATACAATCAACTC	yeast cloning PCR, fwd
pXNubA22-R	ATTGATCCACCTCCACCG	yeast cloning PCR, rev
pMetYC-F	ATTCTATTACCCCCATCC	yeast cloning PCR, fwd
pMetYC-R	ATCCACCTCCACCGGATC	yeast cloning PCR, rev
USER-CSA1-F	GGCTTAAUATGACAAGCTCCTCCTCCTGGGT	cloning for CSA1, fwd
USER-CSA1-R	AACCCGAUCCACACAAAAGAGTGGAACCAAAACCAG	cloning for CSA1, rev
USER-CHS3-F	GGCTTAAUATGGAACCACCAGCTGCTCGTG	cloning for CHS3, fwd
USER-CHS3-R	AACCCGAUCCTAACTTTGAATATTGTGGAGTC	cloning for CHS3, rev
USER-V5-F	ATCGGGTUCGCATTCGGGTAAGCCAATCCC	cloning for CSA1 and CHS3, fwd
USER-V5-R	GGTTTAAUAAGCTTAGGTTGAGTCGAGTCCGAG	cloning for CSA1 and CHS3, rev
pad4-1-PflmI-F	ATGAGTCGCATAAGACTAGCCAAG	genotyping for *pad4-1*
pad4-1-PflmI-R	CCATTTCTTTCCTAAATGAAAATCA	genotyping for *pad4-1*
FP-sag101	GATCTTGGAGATACATAACCC	genotyping for *sag101-2*
BF53	ACTTCCGGGTGTTCATAAACTCGGTCAAG	genotyping for *sag101-2*
dSpm1	CTTATTTCAGTAAGAGTGTGGGGTTTTGG	genotyping for *sag101-2*
chs3-3 LP	ATTTTGAGCAGCTTCCTAGGC	genotyping *chs3-3*, fwd
chs3-3 RP	TCCTCATGATCTTTGGAATGC	genotyping *chs3-3*, rev
js1259	CTGGTTTCCACTTCACGATGA	genotyping for *eds1-12*
js959	AACTAGCATACAGAGGGGCA	genotyping for *eds1-12*
js960	GCTGAGAGAAATCGAACCGG	genotyping for *eds1-12*

At1g27190F3	CTCGCCGGTGAGATTCCTGAGTCTCTTA	genotyping *bir3-2*, fwd
At1g27190R3	ACAGACAAAGGCTTTTGCCCTGTAACCA	genotyping *bir3-2*, rev
bak1-4_LP	CATGACATCATCATCATTCGC	genotyping for *bak1-4*, fwd
bak1-4_RP	ATTTTGCAGTTTTGCCAACAC	genotyping for *bak1-4*, rev
csa1-2_LP	CATCCAGGAAAGCTAGTGCAG	genotyping for *csa1-2*, fwd
csa1-2_RP	GGCTGAAATTCCCGTTAAAAG	genotyping for *csa1-2*, rev

2.1.6 Plasmids

Plasmid	Features	reference
pCAMBIA2300-CSA1	Expression of pCSA1-gCSA1 in planta; cloning CSA1 genomic DNA in split-luciferase	Volkan Cevik
pCAMBIA2300-CHS3	cloning CHS3 genomic DNA in split-luciferase	Volkan Cevik
pCAMBIA3300-CSA1	Expression of 35S-CSA1-DN in planta	Morten Petersen
pUSER-FR-CSA1-V5	Expression of 35S-CSA1 genomic DNA in planta	Vokan Cevik
pUSER-FR-CSA1-V5	Expression of 35S-CHS3 genomic DNA in planta	Vokan Cevik
pB7FWG2-BIR3-eGFP	Expression of 35S-BIR3-eGFP in planta	Thierry Halter
pCAMBIA1300-Nluc (PNL)	Expression vector for BAK1/BIR3 in planta	this work
PCL-CSA1-TIR	Expression vector for TIR^{CSA1} in planta	this work
PCL-CSA1-NB	Expression vector for NB^{CSA1} in planta	this work
PCL-CSA1-LRR	Expression vector for LRR^{CSA1} in planta	this work
PCL-CHS3-TIR	Expression vector for TIR^{CHS3} in planta	this work
PCL-CHS3-NB	Expression vector for NB^{CHS3} in planta	this work
PCL-CHS3-LRR	Expression vector for LRR^{CHS3} in planta	this work
PCL-CHS3-LIM	Expression vector for LIM^{CHS3} in planta	this work
PCL-CHS3-DA1	Expression vector for $DA1^{CHS3}$ in planta	this work
pCAMBIA1300-Cluc (PCL)	expression vector for CSA1/CHS3 or domains in planta	this work
CSA1-pNubA22	Constitutive expression of CSA1 C-terminal NubA-3xHA in yeast	this work

CHS3-pNubA22	Constitutive expression of CHS3 C-terminal NubA-3xHA in yeast	this work
pMetYC-Dest	Expression vector in yeast	Christopher Grefen
pNubA22-Dest	Expression vector in yeast	Christopher Grefen
BIR3-pNubA22	Constitutive expression of BIR3 C-terminal NubA-3xHA in yeast	Julia Imkampe
BAK1-pMetYC	Met repressible expression of BAK1 in yeast with C-terminal Cub-ProteinA- LexA-VP16	Julia Imkampe

2.1.7 Chemicals

Chemicals and reagents were purchased from Carl Roth, Sigma-Aldrich, Fluka, Merck, NEB or Qiagen. Enzyme used for nucleic acids studies were obtained from Thermo Scientific.

2.2 Methods

2.2.1 Plant methods

2.2.1.1 *A. thaliana*

A. thaliana plants were grown on soil in 6 cm diameter round pots for 6 weeks in growth chamber under the short day conditions (at 22 °C and about 60% relative humidity and with 8 hr/ 16 hr light/dark photoperiod). The intensity of the light was set at ~ 110 $mEm^{-2}s^{-1}$. For seed production plants were grown under long day conditions (16 hours light, 8 hours dark) in green house. For Co-IP experiments with *A. thaliana* materials were grown on soil in short day chamber only for 4~5 weeks. Sterilized transgenic seeds were sown on ½ MS plates and grown for 7~10 days under long day conditions. Afterwards the positive seedlings were transferred into soil. The transgenic seeds need to be selected according to different plant expression vector.

2.2.1.2 *Nicotiana benthamiana*

Plants were grown in green house under controlled conditions at 24 °C and 40%–65% relative humidity, and a long-day photoperiod (16 hr light and 8 hr dark). The intensity of the light was set to ~130-150 $mEm^{-2}s^{-1}$. 3-week-old plants can be used later.

2.2.1.3 Crossing

To generate a double mutant plants, the corresponding single homozygous mutants were crossed. One mutant was taken as a female plant. Several buds were chosen from these plants and the petals, sepals, and stamens were removed with forceps. Only the unfertilized carpels were kept on the flower. Another mutant was chosen as a male plant. Several mature stamens were removed from this plant with forceps and spotted onto the carpel from female plant so that pollen grains remained on the carpel. The successful crossing siliques were growing up then contained the F1 seeds. Successful crossing was verified by monitoring presence of the male T-DNA insertion in the F1 generation or by observing crossing plant growth phenotype. In the F1 or F2 generation double mutants were selected by PCR-based genotyping. F3 plants were used for analysis. For the triple mutant plants, the same crossing method were used.

2.2.1.4 Transient transformation of *Nicotiana benthamiana* by *Agrobacterium tumefaciens*

For protein transient expression in Nicotiana (*N.*) *benthamiana* via *Agrobacterium* (*A.*) *tumefaciens* GV3101 was used. Firstly, *A. tumefaciens* contained goal construct grown at 28 °C for 2 days. Then single colonies were picked into 2 ml LB liquid media with appropriate antibiotics in the morning. In the evening, the 2 ml cultures were added into 5-10 ml LB medium supplemented with appropriate antibiotics were inoculated at 28 °C overnight. Cells were harvested the next morning by centrifugation at 4000 rpm for 4 mins. The cell pellets were resuspended in 2 ml 10 mM $MgCl_2$ and 10 mM MES mixture washing buffer and centrifugation was repeated one more time. The cultures were diluted for 10 times to measure OD value. All the strains were diluted into OD_{600}=0.5. The strains were mixed to the same rate, also with the silencing inhibitor p19 (Voinnet et al., 2003). 150 µM acetosyringone was added (from 150 mM stock in DMSO saved in -20 °C freezer) and the *A. tumefaciens* were incubated about 2 hours at room temperature. Tobacco leaves of 3-week-old plants were infiltrated with a needleless syringe at the infiltration side. Leaves were harvested 2 days after infiltration and used to detect protein expression in total protein extracts, protein localization analysis, split-luciferase assay or subsequent Co-IP analysis.

2.2.1.5 Seeds sterilization

Seeds sterilization was performed with chlorine gas in airing cabinet. The seeds were put into microcentrifuge tubes and the tubes with open lids were put into a glass desiccator. In the desiccator a beaker with 50 ml 12 % sodium-hypochlorite solution was placed, then 2 ml 37 % HCl were added. The desiccator was closed immediately, and the seeds were sterilized for 4 hrs to overnight. After that the tubes were placed close and transferred into the sterile bench, opening for 30 mins to allow evaporation of remaining chlorine gas. Then seeds were transferred into ½ MS media plates.

2.2.1.6 Infections with *A. brassicicola*

A. brassicicola MUCL20297 cultivation and spore production was performed as described (Thomma et al., 1998). For infection experiments 6-week-old *A. thaliana* plants were used. A glycerol stock of *A. brassicicola* spores with of $2 * 10^7$ spores/ml was diluted with sterile water to 1×10^6 spores/ml and brought to room temperature. Two leaves per plant were inoculated with 2-4 5 µl droplets of the spore solution. Plants were randomly distributed in a tray and were kept under 100 % humidity in a short day chamber. The bonitations were done after 7, 10 and 13 days according to the following scheme: 1: no symptoms, 2: light brown spots at infection site, 3: dark brown spots at infection site, 4: spreading necrosis, 5: leaf maceration, 6: sporulation. The disease index (DI) was calculated with the following formula: $DI = \Sigma\, i * n_i$. ‘‘i’’ is the symptom category, and ‘‘n_i’’ is the percentage of leaves in ‘‘i.

2.2.1.7 Trypan blue staining

Trypan blue staining of *A. brassicicola* inoculated leaves was performed as described in (Kemmerling et al., 2007). *A. thaliana* leaves were put into 6 well plate with 2 ml trypan blue staining solution (8 % (v/v) lactic acid, 8 % (v/v) glycerol, 8 % (v/v) Aqua-Phenol; 66 % (v/v) EtOH; 0.36 % (w/v) trypan blue) and incubated in a 100 °C water bath for 45 sec - 1 min. The staining solution was then replaced with chloralhydrate solution (1 g/ml) for leaves destaining. After 6 hrs the destaining solution was replaced with fresh solution and incubated again overnight. The destained leaves were placed on microscope slides with 20 % glycerol and examined under a binocular.

2.2.2 DNA analysis

2.2.2.1 Polymerase Chain Reaction (PCR)

In this study, two kinds of Polymerase Chain Reaction (PCR) were used. Plant genotyping PCR reactions were performed with a normal Taq polymerase. The PCR system was performed in a 20 µl mix: 1 x reaction buffer (67 mM Tris, 16 mM $(NH_4)_2SO_4$, 2.5 mM $MgCl_2$, 0.01 % Tween, pH 8.8), 125 µM dNTPs, 0.5 µM fwd and rev primer, 0.5 µl Taq polymerase and 2 µl DNA from Edwards protocol. The protocol was as follows: Initial denaturation for 3 mins at 95 °C, 40 cycles of 30 s 95 °C denaturation, 30s at Tm -3 annealing and 1 min/kb at 72 °C elongation, then 5 mins 72 °C final elongation. For cloning the proofreading polymerases Q5 (NEB) or Phusion (Thermo Scientific) were used according to manufacturer's instructions.

2.2.2.2 DNA agarose gel electrophoresis

DNA samples such as PCR products were mixed with 5 x DNA loading buffer (10 mM Tris pH 7.5, 60 mM EDTA, 60 % (v/v) glycerol, 0.25 % bromphenol blue) for agarose gel electrophoresis. Then they were loaded on 1 % (or higher percentage if needed for short DNA fragments) agarose gels in 1 x TAE buffer (40 mM Tris, 1 mM EDTA, pH 8.5) with ethidiumbromide (0.5 µg/ml). Gels were run at 100 - 150 V in 1x TAE buffer according to the maximum limiting voltage of the electrophoresis tank. GeneRuler 1 kb DNA ladder (Thermo Scientific) was used as DNA standard. Bands were visualized by using UV-Transilluminator (Infinity-3026 WL/26 MX, Peqlab).

2.2.2.3 Purification of DNA fragments from agarose samples

The DNA bands were cut out for purification of DNA fragments from agarose gels (the DNA band was cut as thin as possible from agarose gels). DNA was extracted by using GeneJet Gel extraction kit (Thermo Scientific) according to manufacturer's instructions.

2.2.2.4 DNA ligation

Ligation Protocol with T4 DNA Ligase (M0202) was produced by NEW ENGLAND Biolabs.Combine the following in a PCR or Eppendorf tube. For example, a 10 µl reaction

includes that 1 µl T4 DNA Ligase Buffer (10X), vector DNA (0.020 pmol, 50ng), insert DNA (0.060 pmol, 37.5ng) and 0.5 µl T4 DNA Ligase, then add Nuclease-free water up to 10 µl. Mix the reaction gently by pipetting up and down and microfuge briefly. For cohesive (sticky) ends, incubate at room temperature for 10 minutes at least or 16 °C overnight. Heat inactivate at 65 °C for 10 mins. Then chill on ice and transform 1-5 µl of the reaction into 50 µl competent cells. All competent cells are made by Dr. Kemmerling's lab.

2.2.2.5 Transformation of *E. coli* DH5α

E. coli DH5α 1 µl plasmid DNA or a cloning reaction were added to 50 µl of chemically competent cells for transformation according to the reported method (Froger and Hall, 2007). The cells were kept on ice about 5 mins and then heat shocked for 90 s at 42 °C in a water bath. 500 µl LB liquid medium without any antibiotics was added into the cells and they were incubated with shaking for 1 hr at a 37 °C incubator. Afterwards 50 and 500 µl were plated on LB plates with appropriate antibiotics and plates were incubated at 37 °C overnight. Single colonies were picked for the inoculation of liquid LB cultures. From these cultures mini preps were prepared and plasmids were checked with restriction digests and glycerol stocks (50% v/v bacteria or agrobacteria with 50% glycerol) were saved in -80 °C freezer for long term storage.

2.2.2.6 Bacterial plasmid extraction

If cleaner DNA for sequencing was needed, mini preps were performed with GeneJet plasmid mini prep kit (Thermo Scientific) according to manufacturer's instructions. If bacteria plasmid DNA need for restriction digests or *A. tumefaciens*. transformation, the process was as follows: 3 ml overnight cultures for bacterial plasmid extraction by alkaline lyses were harvested by centrifugation for 2 mins at 12000 x *g*. Bacteria cell pellets were resuspended by vortex mixer shortly in 100 µl lysis buffer (50 mM Tris/HCl pH 8, 50 mM EDTA pH 8, 15 % (w/v) sucrose, 10 µg/ml RNAse A). The suspension was mixed softly by hand for 6 times after adding 200 µl alkaline SDS solution (200 mM NaOH, 1 % (w/v) SDS). Lysis reaction was terminated by neutralisation by mixing with 150 µl potassium-acetate solution (3 M Potassium acetate, 11.5 % (v/v) acetic acid). The samples were

centrifuged for 10 mins at 14000 rpm at 4 °C. The supernatant was then transferred into a fresh microcentrifuge tube. DNA was precipitated by adding 0.6 volumes isopropanol and centrifugation for 15 mins at 14000 rpm at 4 °C. DNA pellets were washed with 500 µl 70 % EtOH and centrifuged for 5 mins at 13000 rpm. Supernatants were discarded, pellets were air dried and dissolved in 50 µl 10 mM Tris/HCl pH 8. Plasmids were stored at -20 °C.

2.2.2.7 Restriction enzyme digestion of DNA

Restriction enzyme digestion of DNA was used to analyze successful cloning of plasmids. The restriction enzyme was used to cut at least one time in the insert and one time in the vector backbone. About 500 ng plasmid DNA and 1 U enzyme were used for the restriction digest reaction as given in the manufacturer's instructions (Thermo Fisher Scientific). Fragments were analyzed by 1 % agarose gel electrophoresis.

2.2.2.8 DNA sequencing

Plasmid DNA was sequenced in LightRun Sequencing Services from GATC of Eurofins genomics. 150-200 ng plasmid DNA and 25 pM primers were mixed in a total volume of 10 µl and send for sequencing. Sequencing results were analyzed by using CLC Main workbench (CLC bio).

2.2.2.9 Gateway TOPO cloning

Gateway topo cloning technology was made by Invitrogen Life Technologies. Entry vectors were created with the pENTR™/D-TOPO™ cloning kit (Invitrogen Life Technologies). The exact coding sequence of the gene of interest was PCR amplified with proofreading enzymes (or without stop codon for use with C-terminal tags). The PCR product was purified from 1% agarose gels. An A overhang reaction was added by incubation of 0.1 µl Taq polymerase with 7.9 µl PCR product, 1 µl 10 mM dATPs and 1 µl 10 x Taq buffer for 10 mins at 72 °C. 4 µl PCR fragment with A overhang added were mixed with 1 µl salt solution and 1 µl TOPO vector (from the pENTR™/D-TOPO™ cloning kit, Invitrogen Life Technologies) and incubated for 5 mins at RT. The TOPO reaction

product was directly transformed into *E. coli* DH5α cells. Entry vectors were analyzed by restriction digestion and sequencing analysis.

2.2.2.10 Gateway LR reaction

Expression constructs were created by LR reactions between Gateway entry and destination vectors by using the Gateway® LR Clonase® II Enzyme mix (Invitrogen Life Technologies). 7 µl 50-150 ng entry and 1 µl destination vector were mixed with 1µl TE, pH 8.0 and 1 µl LR clonase II enzyme mix were added, up to 10 µl and the reaction was incubated at RT for 1 hr to 4 °C overnight. The next morning the reaction was terminated by incubation with 0.5 µl proteinase K for 10 mins at 37 °C. The reaction product was directly transformed into *E. coli* DH5α. Successful cloning was analyzed by restriction digestion reaction.

2.2.2.11 Transformation of *A. tumefaciens*

A. tumefaciens 0.5-1 µl plasmid DNA were added into 25-50 µl electro-competent cells for transformation. The cells on ice were transferred into an electroporation cuvette with a pipet and electroporated at 1500 V. 500 µl LB medium without any antibiotics were added to the cells which were transferred back into microcentrifuge tubes. Tubes were incubated at 28 °C for 1-1.5 hrs. 30-50 µl cells were plated on LB plates with appropriate antibiotics and incubated at 28 °C for 2 days.

2.2.2.12 Plant genomic DNA extraction

For plant genotyping plant genomic DNA isolation was performed according to (Edwards et al., 1991). A small leaf piece was homogenized shortly in a microcentrifuge tube by a grinding tool, then 200 µl Edwards buffer (200 mM Tris/HCl pH 7.5, 250 mM NaCl, 25 mM EDTA, and 0.5 % (w/v) SDS) was added into the microcentrifuge tubes. The homogenate was centrifuged at 14,000 rpm for 5-10 mins, then the supernatant was transferred into a new microcentrifuge tube. 200 µl isopropanol were added into the tubes and the DNA was precipitated for 3-5 mins. The samples were centrifuged 10 mins at 14,000 rpm at 4 °C and the supernatant was discarded. The DNA pellets were washed with 70 % EtOH and centrifuged 5 mins at 14,000 rpm at RT. The supernatant was discarded. The pellet

was air dried and resuspended in 30-50 µl ddH_2O. Taking 2 µl plant genomic DNA were used for genotyping PCRs.

2.2.3 Protein methods

2.2.3.1 Total protein extraction from plant materials

For total protein extraction from *A. thaliana* or *N. benthamiana* 100 mg leaf material were ground in liquid N_2. The ground material was mixed with 100 µl cold extraction buffer (50 mM Tris/HCl pH 8.0, 150 mM NaCl, 0.5 % Nonidet P40, proteinase inhibitor cocktail (Roche)) and incubated for 30 mins on ice with occasional mixing. Afterwards the samples were centrifuged for 10 mins at 14000 rpm, 4 °C and the supernatant was transferred into a fresh tube. The clear lysates were mixed with 5 x SDS loading buffer (312.5 mM Tris/HCl pH 6.8, 10 % (w/v) SDS, 25 % (v/v) β-mercaptoethanol, 50 % (v/v) glycerol, 0.05 % (w/v) bromphenol blue) and boiled for 5 mins at 95 °C. Samples were directly used for immunoblotting analysis or stored at -20 °C.

2.2.3.2 Protein concentration measurements

For protein concentration measurements the detergent compatible kit Biorad DC protein assay (Biorad, Hercules, USA) was used according to the manufacturer's instruction. All samples of one experiment were adjusted with extraction buffer to the sample with the lowest protein concentration.

2.2.3.3 SDS-PAGE

For SDS-PAGE analysis the Biorad Mini-PROTEAN Tetra Cell was used. 8% resolving gels consisting of 2.3 ml ddH_2O, 1.3 ml acrylamide-bisacrylamide mix (37.5:1), 1.3 ml 1.5 M Tris pH 8.8, 50 µl 10 % SDS, 50 µl 10 % APS and 3 µl Temed were pured between glass plates with 1 mm spacers. The surface was covered with 50 % isopropanol and the gel was let polymerize. When the gel was polymerized the isopropanol was removed and the 4 % stacking gel consisting of 1.4 ml ddH_2O, 0.17 ml acrylamide-bisacrylamide mix (37.5:1), 0.13 ml 1M Tris pH 6.8, 10 µl 10 % SDS, 10 µl 10 % APS and 1 µl Temed was poured on top. A comb for 10 or 15 slots was inserted and the gel was let polymerize. The gel was placed in the running tank and covered with 1 x SDS-running buffer (25 mM

Tris base, 192 mM glycine, 0.1 % (w/v) SDS). The samples and 5 µl PageRuler Prestained protein ladder (Thermo Scientific) were loaded. The gels were run at 100-150 V according to the size of the proteins. The gels were removed from the glass plates, the stacking gel was discarded and the resolving gel was used for immunoblot analysis.

2.2.3.4 Immunoblot analysis

For immunoblot analysis the proteins were electroblotted from the SDS-PAGE gel on PVDF membranes (Roche) using the Biorad Tetra Blotting Module machine. Blotting was performed for 1 hr per membrane or 1.5 hr for two membranes at 100V in 1 x transfer buffer (25 mM Tris base, 192 mM glycine). Afterwards the membranes were incubated in 5 % low fat milk powder with 1 x PBS-T (137 mM NaCl, 27 mM KCl, 10 mM Na_2HPO_4, 2 mM KH_2PO_4, pH 7.4, 0.1 % Tween 20) for 1 hr at RT to block unspecific binding sites. The membranes were incubated in the primary antibody in 5 % milk with 1 x PBS-T at 4 °C overnight. The next day membranes were washed 3 times for 5 mins in 1 x PBS-T and the secondary antibody was incubated in 5 % milk with 1 x PBS-T for 1 hr at RT. Afterwards the membranes were washed 3 times for 5 mins in 1 x PBS-T again. The signal of the horseradish peroxidase coupled secondary antibody was detected by using ECL reagent (GE Healthcare ECL, PRIME or SELECT) according to the manufacturer's instructions. The signal was detected on X-ray films (CL X-posure films, Thermo Fisher Scientific). Afterwards membranes were Ponceau stained to visualize equal protein loading.

2.2.3.5 Co-immunoprecipitation experiments

For Co-IP experiments 300 mg leaf material of *A. thaliana* seedlings or *N. benthamiana* were ground in liquid N_2. 800 µl plant extraction buffer (50 mM Tris pH 8.0, 150 mM NaCl, 1 % (v/v) Nonidet P40, proteinase inhibitor cocktail (Roche)) was added into the powder and incubated with gentle shaking for 1 hr at 4 °C. At the same time 15-30 µl protein A agarose beads (Roche), anti-V5 agarose beads (Sigma-Aldrich), anti-HA magnetic agarose (Piece) or GFP-trap beads (Chromotek) were washed 3 times with the appropriate volume of buffer (50 mM Tris pH 8.0, 150 mM NaCl). The antibody was added (e.g., 5 µl α-BAK1) into the protein A beads and the beads were incubated with gentle

shaking at 4 °C; the anti-V5 beads, anti-HA magnetic beads or the GFP-trap beads were used directly. The protein extracts were purified by two times centrifugation at 4 °C for 15 mins at 14,000 rpm. 60 µl protein extract was taken as input sample, mixed with 15 µl 5 x SDS- loading buffer and boiled at 95 °C for 5 mins. The rest of the protein extracts were added with the antibody beads and protein binding was rotated end-over-end for 1 hr at 4 °C. Afterwards the beads are washed 3 times with appropriate washing buffer. The IP samples were centrifugated at 1000 rpm for 30 secs. The supernatant was discarded completely and the 60 µl protein extraction buffer was added to the beads, then 15 µl 5 x SDS-Loading buffer was added, too. The IP samples were boiled at 95 °C for 5 mins. Input and IP samples were directly used for immunoblotting analysis or stored at -20 °C.

2.2.3.6 Subcellular localization

For subcellular location analysis, confocal laser scanning microscopy and microsomal fractions assay were performed, respectively.

2.2.3.6.1 Confocal laser scanning microscopy

Confocal laser scanning microscopy images of CSA1-GFP and CHS3-GFP transiently expressed in *N. benthamiana* and BRI1-RFP as a membrane localized control. 0,5M mannitol was used to induce plasmolysis. Merged figures show co-localization of CSA1 and BRI1 (or CHS3 and BRI1) (By courtesy of my colleague Alexandra Ehinger).

2.2.3.6.2 Microsomal fractions

For microsomal fractions, according to the reported method (El Kasmi et al., 2017) about 100 mg of Liquid N2 frozen leaf tissue was ground to fine powder with a grinding machine and 210 µl ice cold lysis buffer (20mM Tris pH 7.5, 0.33M sucrose, 1mM EDTA, 5mM DTT and 1x complete Ultra Plant Protease Inhibitors) was added. Samples were centrifuged in a microcentrifuge at 5000 x *g* for 5 mins at 4 °C to remove debris. 60µl of supernatant was taken as the total lysate fraction (T). The rest of the lysate was then centrifuged at 4 °C at 20000 x *g* for 60 mins. 60µl of the resulting supernatant was used as the soluble fraction (S), the membrane pellet was resuspended in 60µl of lysis buffer to yield the microsomal fraction (M). 15µL 5 x SDS loading buffer was added in three

kinds of fractions, boiled at 95 °C for 10 mins. Afterwards, western blotting analysis was performed to see how protein was localized.

2.2.3.7 Split-luciferase assay

The assay was performed as previously reported (Zhou et al., 2018). *A. tumefaciens* strain containing the indicated plasmids was infiltrated into leaves of *N. benthamiana* and incubated in the green house for 48 hrs before the LUC activity measurement. For LUC activity measurement, 1 mM luciferin was added into the leaves. Relative LUC activity per cm^2 infiltrated leaf area was calculated. Each data point contains at least four replicates, and three independent experiments were carried out.

2.2.3.8 Yeast split-ubiquitin assay

The split-ubiquitin assay was performed in yeast (Asseck and Grefen, 2018) and based on the reconstitution of the two artificially cleaved halves of ubiquitin. One protein was fused to the N-terminal half of ubiquitin (Nub) with tagged-HA and the second protein to the C-terminal part (Cub) with the reporter construct PLV (ProteinA-LexA-VP16). Interaction of the tow proteins was leading to rebinding together of the ubiquitin two parts upon which the PLV was cleaved off by ubiquitin-specific proteases and thus was able to switch on reporter genes. The use of a repressible promotor for the Cub fusion (met25) gave more reliability by reducing the artefacts of overexpression.

For the interaction assay the yeast THY.AP4 (*S. cerevisiae* MATa; *ade*$^-$, *his* $^-$, *leu2*$^-$, *trp1*$^-$, *ura3* $^-$; lexA::ADE2, lexA::HIS3, lexA::lacZ) was grown in 5 ml YPD incubating with shaking at 30 °C overnight. 5 ml of the pre-culture were transferred into fresh 50 ml YPD medium and incubated with shaking for 5 hrs until an OD_{600} of 0.5 to 0.8 was reached. Cells were harvested by centrifugation for 10 mins at 2000 x *g* at RT and the supernatant was discarded. The pellets were resuspended in 20 ml sterile ddH_2O and centrifuged again. Cells were resuspended in 1 ml 0.1 M lithium acetate pH 7.5 (LiAc) and transferred in a 2 ml microcentrifuge tube. The tubes were centrifuged for 2 mins at 1000 x *g* and the supernatant was discarded. Pellets were resuspended in 500 µl 0.1 M LiAc and incubated at RT for 30 mins. Meanwhile sterile tubes with 9 µl 2 mg/ml ssDNA and 6 µl of plasmid DNA (at least 200 ng/µl, 2µl from each clone) were prepared for each transformation. A master mix of 70 µl 50 % PEG 3350, 10 µl 1 M LiAc and 20 µl competent cells was

prepared for each transformation. The master mix was carefully mixed with the DNA and incubated at 30 °C for 30 mins. After 20 mins each reaction was mixed by pipetting carefully up and down. Heat shock was performed for 15 mins at 43 °C. Cells were centrifuged for 5 mins at 2000 x *g* and the supernatant was discarded. Pellets were washed with 100 µl sterile water and centrifuged again. Supernatants were discarded and cells were resuspended in 80 µl sterile water. Cells were plated on CSM- Leu^-, Trp^- plates and incubated at 30 °C for 3 to 4 days.

For growth assays 5 ml CSM- Leu^-, Trp^- were inoculated with 5-10 colonies per transformation. Cultures were grown overnight at 30 °C with shaking. The OD_{600} was determined. 100 µl sample were centrifuged for 2 mins at 2000 x *g,* supernatants were discarded, and pellets resuspended in a volume of sterile water to get an OD_{600} of 1.0. From this cell suspension 1:10 and 1:100 dilutions were prepared with sterile water. 7 µl droplets of all dilutions were placed on CSM- Leu^-, Trp^- (vector selective medium) and CSM-Leu^-, Trp^-, Ade^-, His^- with increasing methionine concentration (interaction selective medium) plates. Plates were incubated at 30 °C for 2 days until yeast growth became visible.

2.2.4 Statistical analysis

Statistical significance between two groups has been analyzed using Student's t-test. Asterisks represent significant differences (*p <0.05; **p <0.01; ***p <0.001). One-way ANOVA was performed for multiple comparisons combined with Tukey's honest significant difference (HSD) test. Different letters indicate significant differences ($p < 0.05$).

3. Results

3.1 NLRs downstream signaling components engage in *bak1 bir3*-mediated cell death pathway

Our previous work found that *bak1 bir3* double mutants show a severe dwarf phenotype and spontaneous cell death formation (Imkampe et al., 2017). One common downstream, the nucleocytoplasmic lipase-like protein called ENHANCED DISEASE SUSCEPTIBILITY 1 (EDS1), had been identified to involve in TIR-nucleotide binding leucine rich repeat (TNL)-mediated effector-triggered immunity (ETI) responses (Cui et al., 2015). In the EDS1 family structurally unique lipase-like proteins EDS1, PHYTOALEXIN-DEFICIENT 4 (PAD4) and SENESCENCE-ASSOCIATED GENE 101 (SAG101) cooperate with other RNLs such as *N. benthamiana* N requirement gene 1 (NRG1) and ACTIVATED DISEASE RESISTANCE 1 (ADR1) to regulate nucleotide-binding leucine-rich repeats (NLRs) signaling pathway. Proprietary heterodimers between EDS1 and SAG101 or PAD4 create the necessary surface for resistance signaling (Lapin et al., 2020; Sun et al., 2021). Therefore, we would investigate whether these downstream components involve in *bak1 bir3*-mediated cell death pathway.

3.1.1 Cell death in *bak1* single mutant is dependent on EDS1

To resolve how the absence of BAK1 and BIR3 initiates cell death, we checked if known immunity-related cell death pathways are involved in this phenomenon. Firstly, we created double mutants with an essential component, *EDS1* known in ETI pathway. The CRISPR/Cas9 line *eds1-12* does not influence *bak1* mutant growth phenotype, and the light brown spots at infection site by *Alternaria (A). brassicicola* in *bak1 eds1* double mutants are as low as in the hyper-resistant *eds1* mutant (Figure 3-1 A, B). The cell death of *bak1* mutant triggered by *A. brassicicola* infection was obviously inhibited as visible from the trypan blue staining results when single mutant *eds1-12* was introduced (Figure 3-1 C, D). These results suggest that *eds1* mutation can suppress the cell death of *bak1* single mutant after *A. brassicicola* infection.

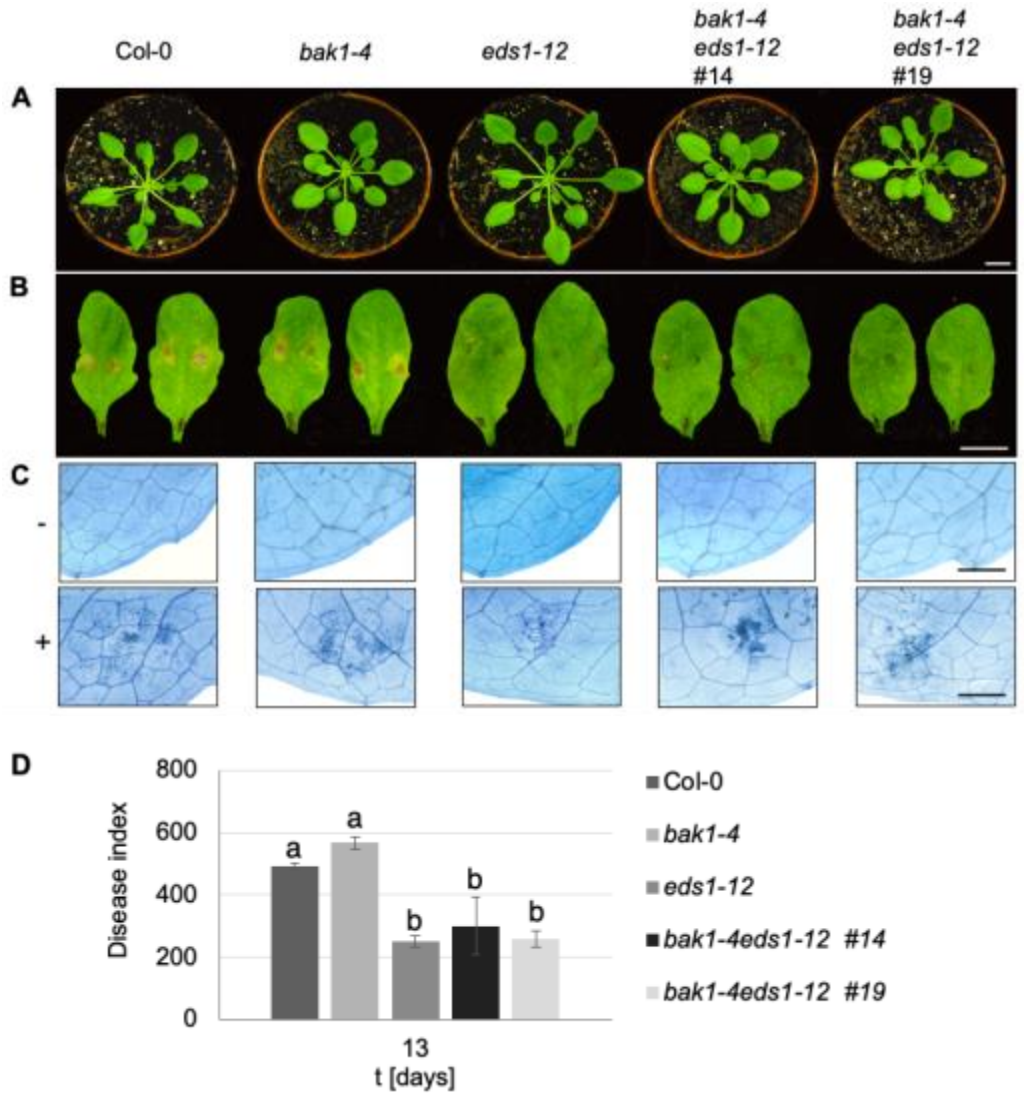

Figure 3-1: Loss of EDS1 can suppress cell death in *bak1* mutants

(A) Representative pictures of the morphological phenotypes of 6-week-old Col-0, *bak1-4, eds1-12,* the double mutant *bak1-4 eds1-12* are shown. **(B)** *A. brassicicola* droplet-infected leaves of the genotypes shown in (A) 13 days after inoculation. **(C)** Leaves of the same genotypes as in (A) and (B) droplet infected with *A. brassicicola* and trypan blue stained. The scale bar in (A), (B) and (C) represents 10 mm. **(D)** Disease indices of *A. brassicicola* infected leaves of the indicated genotypes 13 days after infection shown as mean ± SE (n=12). Different letters indicate significant differences according to one-way ANOVA and Tukey's HSD test ($p<0.05$). The experiments were repeated at least three times with similar results.

3.1.2 Cell death in *bak1 bir3* double mutant is dependent on EDS1, SA and NRGs

Double mutant *bak1 bir3* plants show autoimmune phenotypes (Figure 3-2 A), the leaves are curly and smaller than its male and female parents. Some leaf edges show yellowing when the *bak1 bir3* mutant is grown for 4 weeks. The plants are sterile. To verify how the absence of BAK1 and BIR3 initiates cell death we checked the potential immunity-related cell death pathways known in plants and created triple mutants with components of these

pathways. We used some mutants of known ETI pathway components such as *eds1, pad4, sag101* and *NahG* transgenic plants expressing a salicylic acid degrading bacterial enzyme. These mutants or transgenic plants were crossed with *bak1 bir3* mutants for epistasis analysis. The *eds1* mutant can partially block *bak1 bir3*-mediated growth phenotypes (Figure 3-2 A).

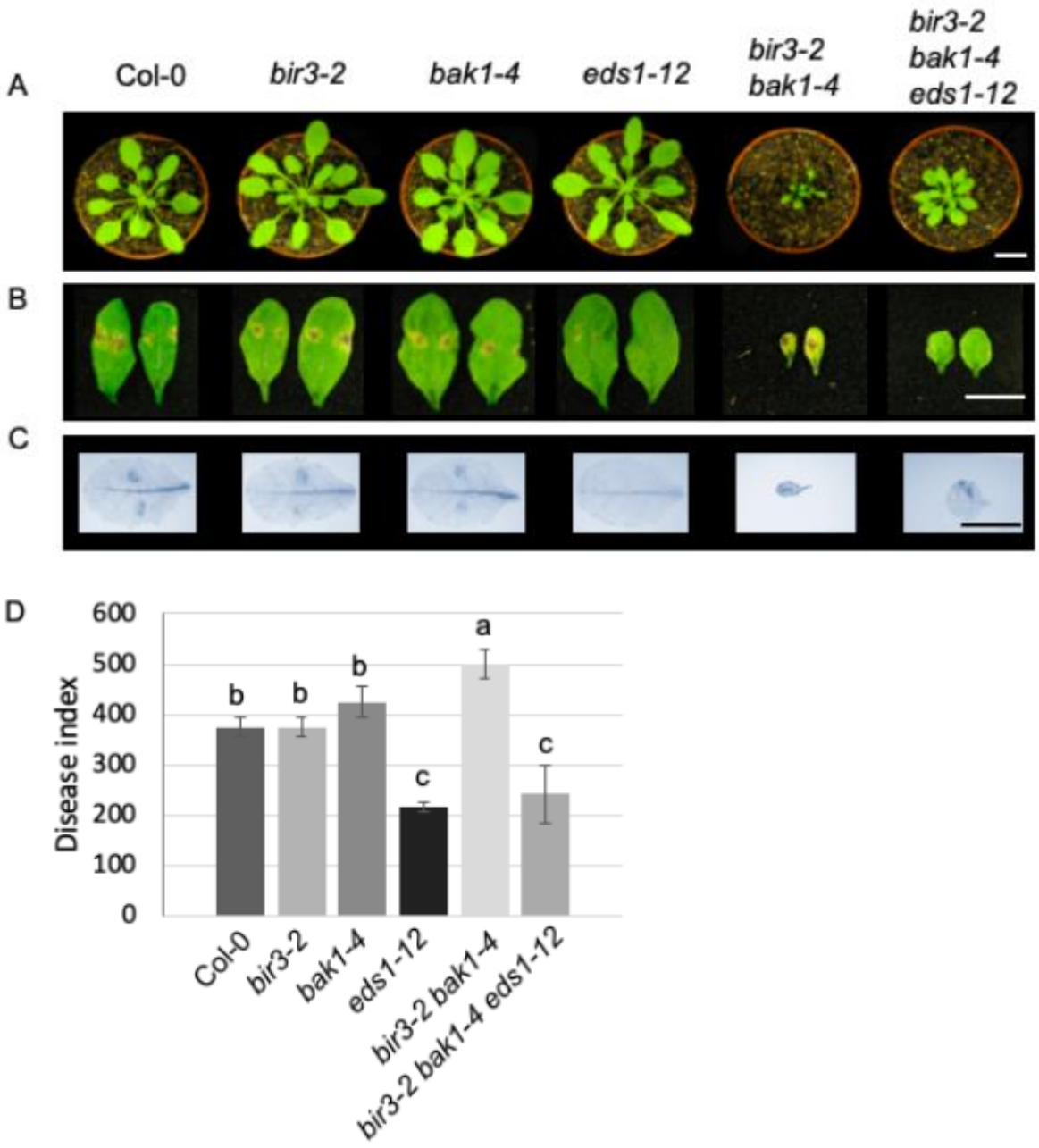

Figure 3-2: Loss of EDS1 can partially block *bak1 bir3* induced cell death

(A) Representative pictures of the morphological phenotypes of 6-week-old Col-0, *bir3-2, bak1-4, eds1-12,* the double mutant *bak1-4 bir3-2* and the triple mutant *bak1-4 bir3-2 eds1-12* are shown. **(B)** *A. brassicicola*

droplet-infected leaves of the genotypes shown in (A) 13 days after inoculation. (C) Leaves of the same genotypes as in (A) and (B) droplet-infected with *A. brassicicola* and trypan blue stained. The scale bar in (A), (B) and (C) represents 10 mm. (D) Disease indices of *A. brassicicola* infected leaves of the indicated genotypes 13 days after infection shown as mean ± SE (n=12). Different letters indicate significant differences according to one-way ANOVA and Tukey's HSD test ($p<0.05$). The experiments were repeated at least three times with similar results.

The *eds1* mutant can also partially rescue *bak1 bir3*-mediated cell death after *A. brassicicola* infection (Figure 3-2 B-D). As EDS1 is supposed to function downstream of TNL-type resistance genes, the effect of *eds1* mutation on the *bak1 bir3* phenotype suggests that a TNL might be involved in guarding the BAK1 BIR3 complex and initiates cell death when one or both components are absent. Mutation in *pad4* had a weak effect on the *bak1 bir3* growth phenotype, while mutation in *sag101* had no effect (Figure 3-3 A, C). This indicates that the EDS1 PAD4 hubs in NLR-mediated immunity downstream of TNLs are at least partially necessary for *bak1 bir3*-mediated cell death.

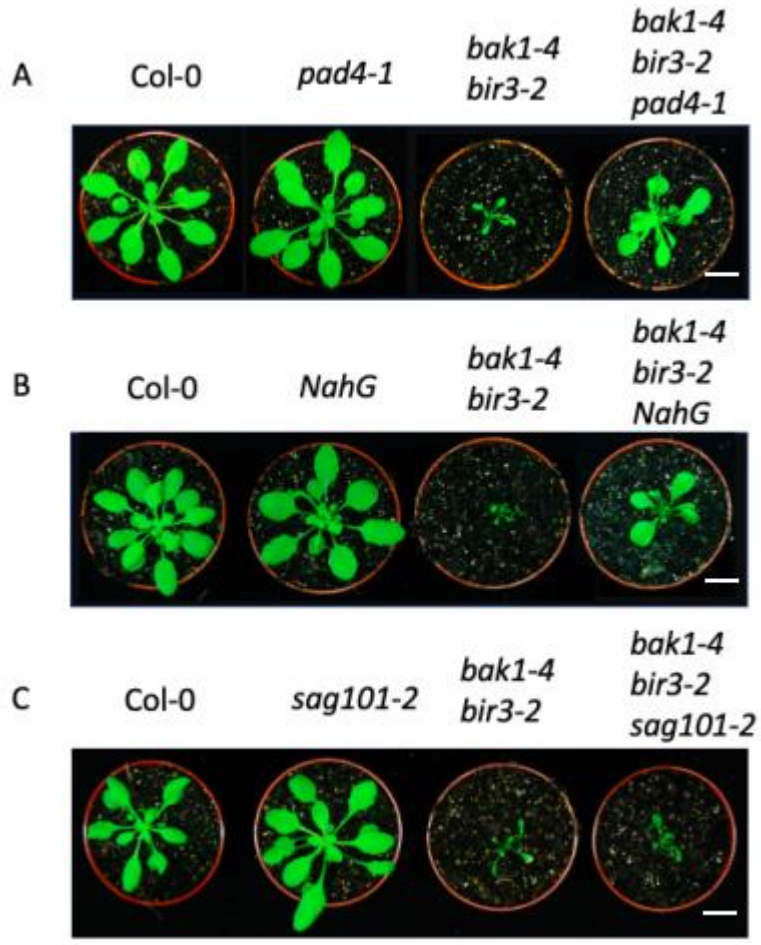

Figure 3-3: The mutation in *pad4* and the reduction of SA levels by *NahG* expression can weakly suppress the dwarf phenotype of *bak1 bir3* mutants, whereas the mutation in *sag101* cannot suppress it

Representative pictures of 6-week-old plants of the indicated genotypes are shown. The scale bar represents 1 cm.

BAK1-LIKE 1 (BKK1) functions redundantly with BAK1 in plant immunity, and double mutant *bak1 bkk1* causes severe plant cell death (He et al., 2007). SA is indispensable for *bak1 bkk1*-mediated cell death (Gao et al., 2017). Expression of *NahG*, that degrades salicylic acid, also affects *bak1 bir3*-mediated cell death (Figure 3-3 B). Our findings show that wt BAK1 and BIR3 contain cell death that is executed by EDS1-dependent complexes and SA, leading to autoimmunity-associated runaway cell death in plants lacking a functional BAK1 BIR3 complex. This suggests that components of the TNL-mediated ETI pathway contribute to and are necessary for *bak1 bir3*-mediated cell death, but the requirement of additional components for the observed phenotypes also needs to be postulated.

Lapin et al. postulated that EDS1-SAG101 and NRG1s co-evolved as a functional TNL-dependent cell-death and resistance module (Lapin et al., 2019). Since we observed a partial suppression of the *bak1 bir3* phenotype by *eds1*, we determined whether the NRG1 family is also involved in mediating *bak1 bir3* cell death. Therefore, we crossed *nrg1.1 nrg1.2* double mutants with *bak1 bir3* double mutants. The *nrg1.1 nrg1.2 bak1-4 bir3-2* mutants are larger than *bak1 bir3* mutants showing that NRG1s, as part of the TNL cell death pathway, are also contributing to the *bak1 bir3* phenotype (Figure 3-4) (we thank Svenja C. Saile from Dr. Farid El Kasmi' s group for providing the mutants and analyzes).

Figure 3-4: Helper NLRs *NRG1.1* and *NRG1.2* are necessary for *bak1 bir3* double mutant phenotypes

Representative pictures of the morphological phenotype of 6-week-old Col-0, *nrg1-1 nrg1-2* and *bir3-2 bak1-4* double mutant and the quadruple mutant *bak1-4 bir3-2 nrg1-1 nrg1-2.* The scale bar represents 1 cm. (kindly provided by S. Saile)

3.1.3 Cell death in *bir2* single mutant partially depends on EDS1

Previous studies revealed that BIR2 and BIR3 interact with BAK1 and negatively regulate BAK1 interaction with ligand binding receptors such as FLS2 and EFR. We found that the *bir2* single mutants show serious cell death after *A. brassicicola* infection. To investigate how the absence of BIR2 initiates cell death after *A. brassicicola* infection, we created double mutants with *eds1* (Figure 3-5 A). The *eds1* mutation can partially influence *bir2* mutant growth phenotypes (Figure 3-5 A), and the infection symptoms in *bir2 eds1* double mutants are also as low as in the hyper-resistant *eds1* mutant (Figure 3-5 B).

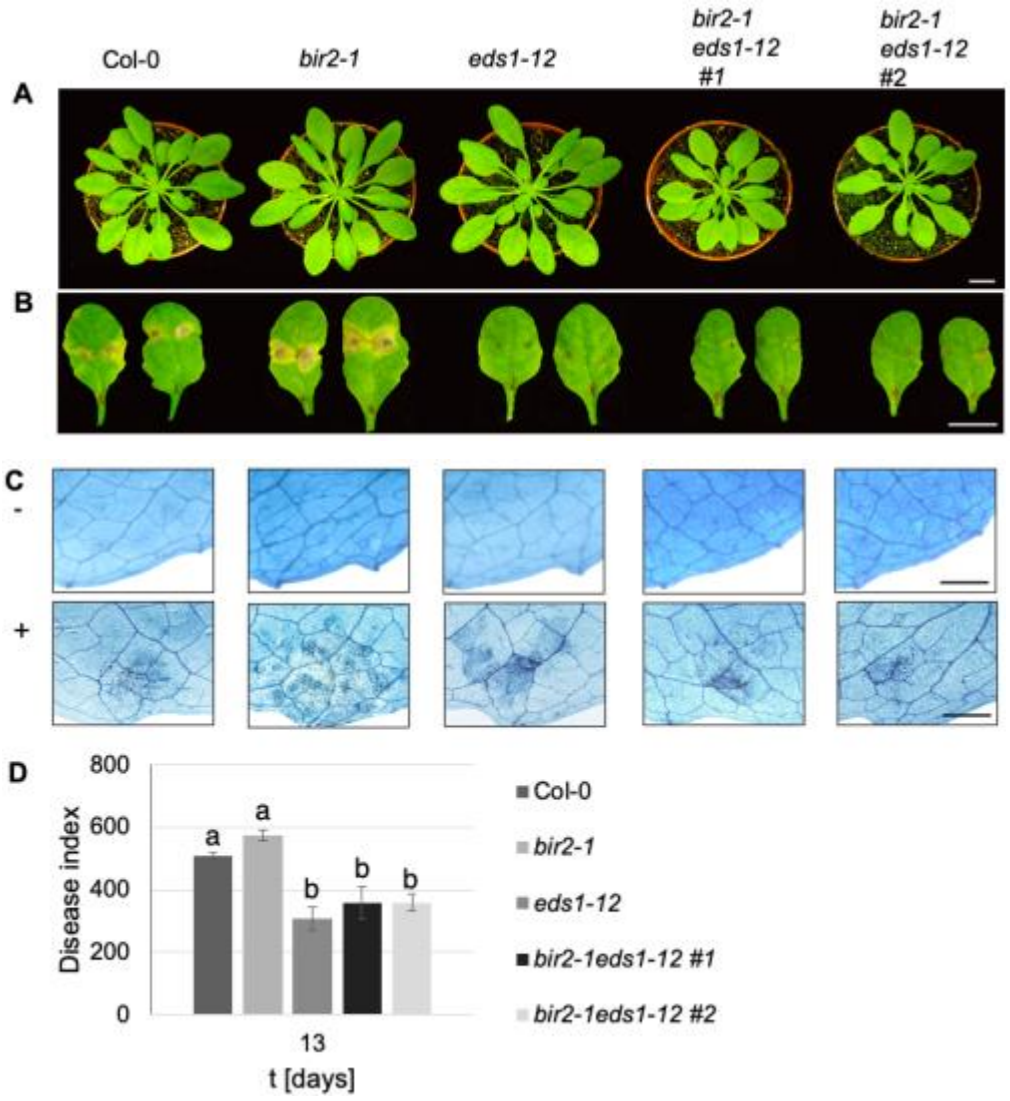

Figure 3-5: Loss of EDS1 can suppress cell death in *bir2* mutants

(A) Representative pictures of the morphological phenotypes of 6-week-old Col-0, *bir2-1, eds1-12,* the double mutant *bir2-1 eds1-12* are shown. **(B)** *A. brassicicola* droplet-infected leaves of the genotypes shown in (A) 13 days after inoculation. **(C)** Leaves of the same genotypes as in (A) and (B) droplet infected with *A. brassicicola* and trypan blue stained. The scale bar in (A), (B) and (C) represents 10 mm. **(D)** Disease indices of *A. brassicicola* infected leaves of the indicated genotypes 13 days after infection shown as mean ± SE (n=12). Different letters indicate significant differences according to one-way ANOVA and Tukey's HSD test ($p<0.05$). The experiments were repeated at least three times with similar results.

The cell death of *bir2* mutants triggered by *A. brassicicola* infection was also obviously inhibited as visible from the trypan blue staining results when the *eds1* mutation was introduced (Figure 3-5 C, D). These results suggest that *eds1* mutation can also suppress the cell death of *bir2* single mutants after *A. brassicicola* infection, implying that TNL-mediated immunity is probably involved in the cell death of *bir2*. We also tested how PAD4 and NahG involve in *bir2*-mediated cell death pathway. We found that PAD4 and NahG can block cell death in *bir2* mutants (Supplemental Figure 8-1). Therefore, EDS1 involves in both *bak1 bir3*- or *bir2*-mediated cell death pathway as a common downstream component. PAD4 and NahG are redundantly necessary for *bir2*-mediated cell death.

3.2 The identification of components involved in the BAK1/BIR3-mediated cell death pathway

BAK1 and BIR3 are two receptor kinases in *A. thaliana* that are constitutively interacting with each other before BAK1 is recruited as a co-recptor to ligand binding receptors (Imkampe et al., 2017)**.** If both genes are knocked out, the double mutants show a strong cell death phenotype. To identify potential components involved in *bak1 bir3* cell death, my former colleague Sarina Schulze determined the *in vivo* interactome of BIR3-YFP by liquid chromatography- electron spray ionization tandem mass spectrometry (LC-ESI-MS/MS) in *A. thaliana* plants. The MS analyses revealed BAK1 and other SERKs as the most abundant interaction partners of BIR3 (Schulze, 2020), confirming the strong interaction with BAK1 published previously (Gao et al., 2009; Halter et al., 2014; Imkampe et al., 2017). Besides, other known RKs for example MIK2, SOBIR1 and FERONIA, have been identified in the BIR3-YFP interactome, demonstrating that BIR3 interacts with multiple known but also with yet undescribed RKs (Liebrand et al., 2014; Stegmann et al., 2017; Van der Does et al., 2017). So BIR3 might be involved in multiple signaling pathways as a general interactor of RKs (Schulze et al., 2022).

To understand how the cell death phenotype in *bak1 bir3* is happening, we identified one protein with a unique peptide sequence LPDSLGQLK corresponding to a known NLR as a potential candidate (Figure 3-6). This peptide matches with a TNL protein *CONSTITUTIVE SHADE AVOIDANCE 1* (CSA1) which mutants displayed a constitutive shade avoidance phenotype (Faigon-Soverna et al., 2006), and affected autoimmune responses.

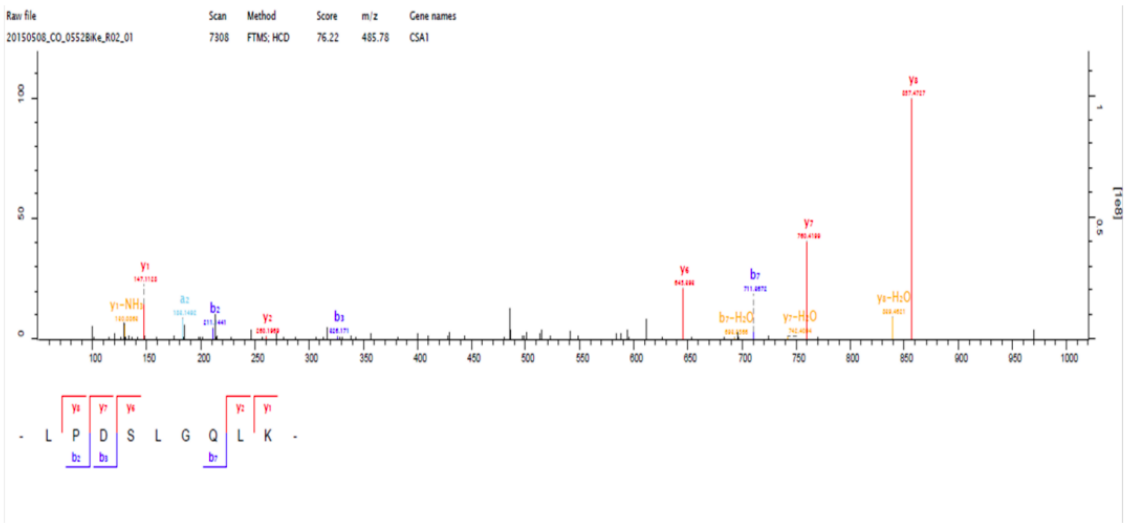

Figure 3-6: The spectrum showed the peptide LPDSLGQLK which is consistent with CSA1

Product ion spectra of CSA1 peptides generated from a tryptic digest of a BIR3-GFP IP of 6-week-old *A. thaliana* plants using ion trap LC/MS MS analysis (MSI), processed by the Proteome Center of Tübingen. All spectra were also verified by manual inspection (Schulze, 2020).

3.3 Complementation of CSA1 in *bir3 bak1 csa1* or *bak1 csa1* mutants

To confirm whether *CSA1* can really mediate cell death of *bak1* and/or *bir3* mutants, Sarina Schulze also crossed *csa1* mutant with *bak1* and *bak1 bir3* mutants. Sarina Schulze found that mutation in csa*1* can suppress the cell death phenotypes in *bak1* and *bak1 bir3* mutants (Schulze, 2020). These results confirm that CSA1 is necessary for the cell death phenotype in *bak1 bir3* mutants. Meanwhile we applied the complementation of CSA1 in *bir3 bak1 csa1* or *bak1 csa1* mutants to proof the function of CSA1 in *bak1 bir3*-mediated cell death (we thank Dr. Volkan Cevik for providing us the transgene constructs).

3.3.1 CSA1 partially restores the growth and cell death phenotype of *bak1 bir3 csa1* mutants

We have previously shown that CSA1 is required for *bak1 bir3*-mediated cell death (Schulze, 2020). To proof that CSA1 is indeed necessary to establish the autoimmune cell death phenotype in *bak1 bir3* mutants, we expressed genomic *CSA1* under its endogenous promoter in *bak1 bir3 csa1* mutants (transgenic plants kindly provided by Sarina Schulze). Due to the fact that mutants and transgene were supposed to be selected by kanamycin selection, we applied PCR with *CSA1* transgene specific primers (csa1-LP/ csa1-RP) to select positive transgenic plants.

Five-week-old soil grown transgenic plants were inoculated with *A. brassicicola*, *bak1 bir3* double mutants and *bak1 bir3 csa1* triple mutants were used as controls, as well as Col-0 plants. Plants expressing CSA1 in the *bak1 bir3 csa1* background grew much smaller than *bak1 bir3 csa1* triple mutants (Figure 3-7 A), with a size similar to *bak1 bir3* double mutants. The complementation lines also exhibited an autoimmune cell death phenotype just as *bak1 bir3* double mutants (Figure 3-7 B). After *A. brassicicola* infection, the complementation lines showed significantly more symptoms than *bak1 bir3 csa1* triple mutants even if not to the same degree as caused in *bak1 bir3* double mutants infected leaves (Figure 3-7 C). Therefore, CSA1 partially restores both the growth and cell death phenotypes of *bak1 bir3 csa1* mutants.

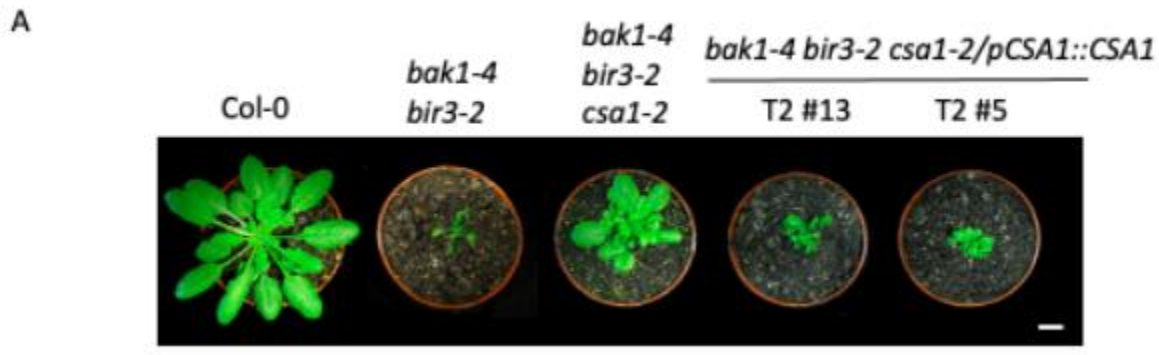

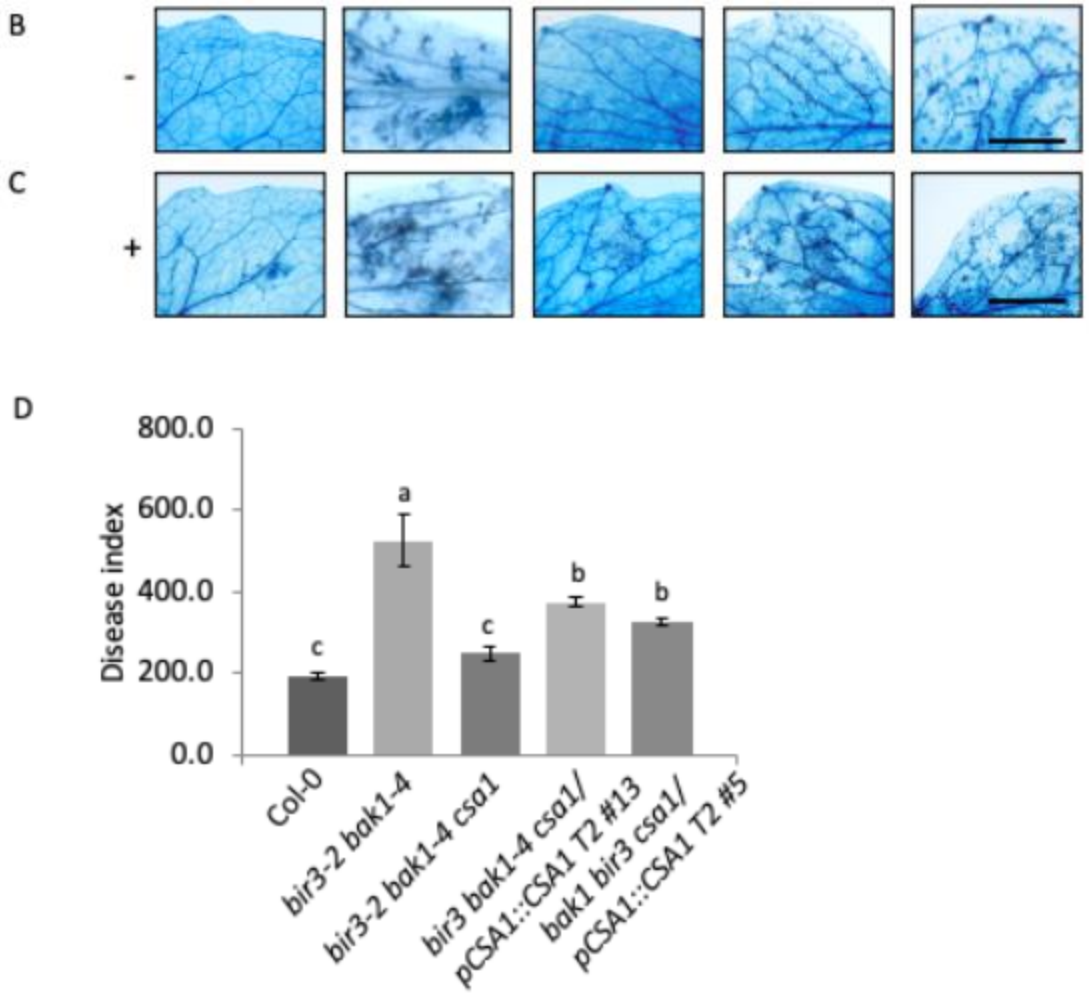

Figure 3-7: Expression of *CSA1* can complement the *bak1 bir3 csa1* triple mutant phenotype

(A) Representative pictures of the morphological phenotype of 6-week-old Col-0, *bir3-2 bak1-4,* the triple mutant *bak1-4 bir3-2 csa1-2* and the complementation lines expressing *CSA1* under the endogenous promotor in the triple mutant background. The scale bar represents 1 cm. **(B)** uninfected leaves of the genotypes shown in (A) stained with trypan blue for cell death. **(C)** Leaves of the same genotypes as in (A) and (B) droplet-infected with *A. brassicicola* and trypan blue stained. The scale bar in (B) and (C) represents 5 mm. **(D)** Disease indices of *A. brassicicola* infected leaves of the indicated genotypes 13 days after infection shown as mean ± SE (n=12). Different letters indicate significant differences according to one-way ANOVA and Tukey's HSD test ($p<0.05$). The experiments were repeated at least three times with similar results.

3.3.2 CSA1 restores the cell death of *bak1 csa1* triggered by *A. brassicicola*

As we know that *bak1* single mutants show enhanced cell death symptoms after *A. brassicicola* infection (Figure 3-1 B; Figure 3-2 B) and we previously observed that mutation in *csa1* can suppress cell death of *bak1* triggered by *A. brassicicola* infection (Schulze, 2020). We performed complementation assay in *bak1 csa1* double mutants to confirm the function of *CSA1* in *bak1*-mediated cell death. We used the same construct

in the vector pCAMBIA2300 to express CSA1 in *bak1 csa1* double mutants. With the CSA1 expressing *A. thaliana* plants, we did *A. brassicicola* infection assays (Figure 3-8). Col-0, *csa1*, *bak1* and *bak1 csa1* were used as controls. The transgenic plants restored *bak1* single mutant growth phenotypes (Figure 3-8 A). Their complementation leaves showed more cell death than *bak1 csa1* double mutant just as *bak1* single mutant 13 days after *A. brassicicola* infection (Figure 3-8 B).

Complementation of the *bak1 csa1* mutant and the *bak1 bir3 csa1* mutant with a genomic construct expressing CSA1 under its own promoter can complement mutant phenotypes and restore stronger cell death symptoms typically observed in *bak1* and *bak1 bir3* mutants (Figure 3-7; Figure 3-8). Therefore, CSA1 is confirmed to be the functional protein necessary for *bak1* and *bak1 bir3*-initiated cell death.

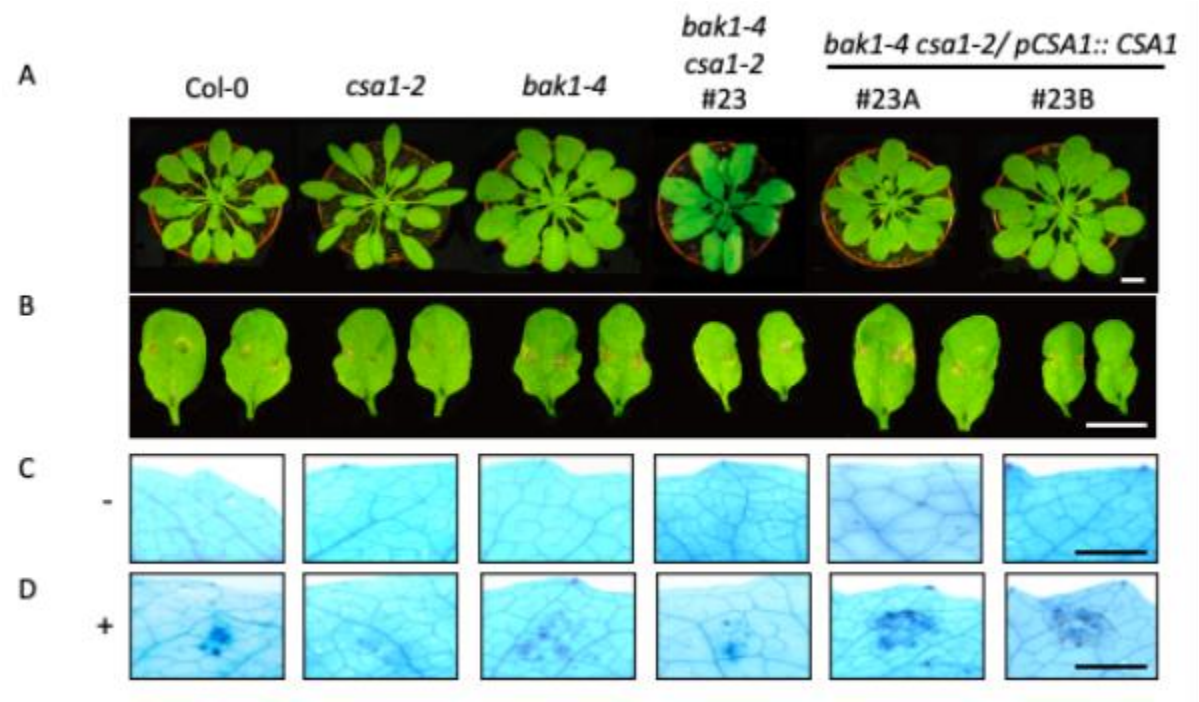

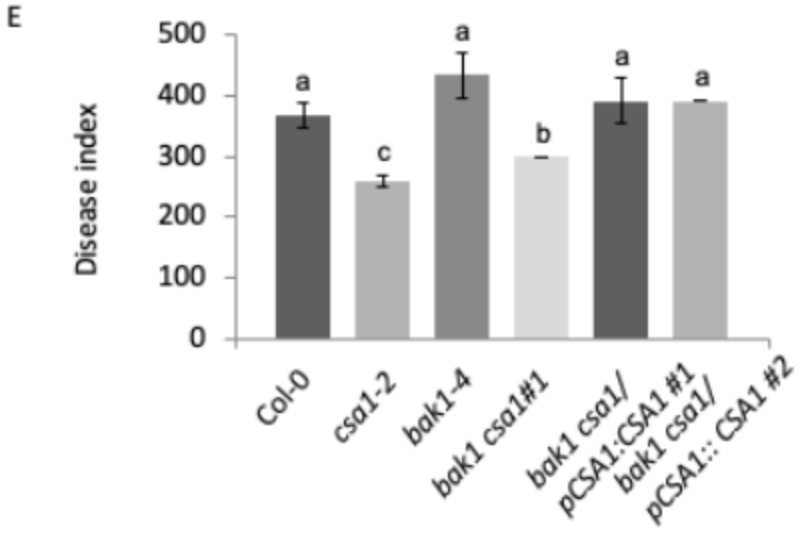

Figure 3-8: Expression of CSA1 can complement the *bak1 csa1* double mutant phenotype

(A) Representative pictures of the morphological phenotype of 6-week-old Col-0, *csa1-2*, *bak1-4, bak1-4 csa1-2* and the complementation lines expressing CSA1 under the endogenous promoter in the double mutant background. **(B)** Leaves of the same genotypes as in A and B droplet-infected with *A. brassicicola.* The scale bars in (A) and (B) represent 10 mm **(C)** Uninfected leaves of the genotypes shown in (A) stained with trypan blue for cell death. **(D)** Leaves of the same genotypes as in A droplet-infected with *A. brassicicola* and trypan blue stained. The scale bars in (C) and (D) represent 5 mm. **(E)** Disease index of *A. brassicicola* infected leaves of the indicated genotypes 13 days after infection shown as mean ± SE (n=12). Different letters indicate significant differences according to one-way ANOVA and Tukey's HSD test ($p<0.05$). The experiments were repeated at least three times with similar results.

3.4 CSA1 interacts with BIR3

Previously we have proved the function of *CSA1* in the *bak1 bir3*-mediated cell death pathway. But how does *CSA1* mediate cell death of the *bak1 bir3* mutants? We performed a set of interaction methods between CSA1 and BIR3 (or BAK1) in *planta* or yeast. Sarina Schulze found that CSA1 can interact with BIR3 (or BAK1) by Co-IP in *N. benthamiana* (Schulze, 2020). Now we want to know whether the interaction between CSA1 and BIR3 (or BAK1) is direct or indirect.

3.4.1 Subcellular localization of CSA1

To understand better how CSA1 and BIR3 are interacting, we firstly tested the localization of CSA1 in *planta*. We examined its subcellular localization by microsomal fractionation and confocal laser scanning microscopy experiments in *N. benthamiana*. CSA1-V5 and BIR3-eGFP fusion proteins were expressed under the CaMV35S promoter in *N. benthamiana.* Leaves were harvested 48 hrs after infiltration for cell fractionation and

immunoblotting. An ATPase was detected as a membrane marker as well as BIR3-eGFp which is also localized at the plasma membrane. Confocal laser scanning microscopy was applied to visualize the localization of CSA1-GFP transiently expressed in *N. benthamiana* and BRI1-RFP as a membrane localized control. Plasmolysis was performed to prove plasma membrane localization. Localization studies with fractionated plant extracts and confocal laser scanning microscopy revealed that CSA1 is predominantly localized to the microsomal fraction and the plasma membrane (Figure 3-9 A, B), which is in agreement with interaction with the plasma membrane-resident BIR3.

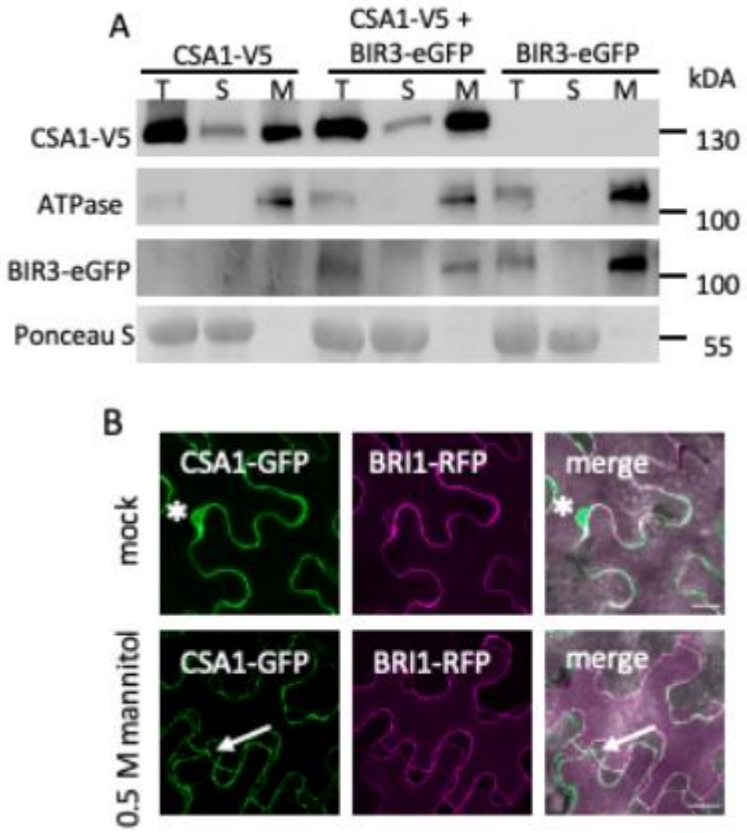

Figure 3-9: CSA1 localizes preferentially to microsomal fractions

(A) Agrobacteria containing CSA1-V5 or BIR3-eGFP, 35S-driven both constructs were transiently infiltrated either alone or both into *N. benthamiana* leaves. Tissue was harvested at 48 hpi for cell fractionation and immunoblotting with anti-V5 (CSA1), anti-ATPase (membrane marker) and anti-GFP (membrane). Ponceau S (PS) staining shows as loading control and marker for the cytosolic fraction. T, total extract; S, soluble; M, microsomal fraction. **(B)** Confocal laser scanning microscopy images of CSA1-GFP transiently expressed in *N. benthamiana* and BRI1-RFP as a membrane localized control. 0,5M mannitol was used to induce plasmolysis. Merged figures show co-localization of CSA1 and BRI1 in the red and green channel. The arrows mark Hechtian strands and asterisks the nuclei, size bars represent 20µm (Figure 3-9 B was by courtesy of my colleague Alexandra Ehinger).

3.4.2 Subcellular localization of CHS3

Previous studies show that CSA1 and CHS3 function together as a sensor and executer pair of NLRs (Adachi et al., 2019b; Castel et al., 2019). To know how the CSA1 partner CHS3 localizes, we also examined the subcellular localization by microsomal fractionation and confocal laser scanning microscopy experiments in *N. benthamiana*. Subcellular localization assays show that CHS3 is localized to the plasma membrane but also to the soluble fraction and can also be localized in the nucleus (Figure 3-10).

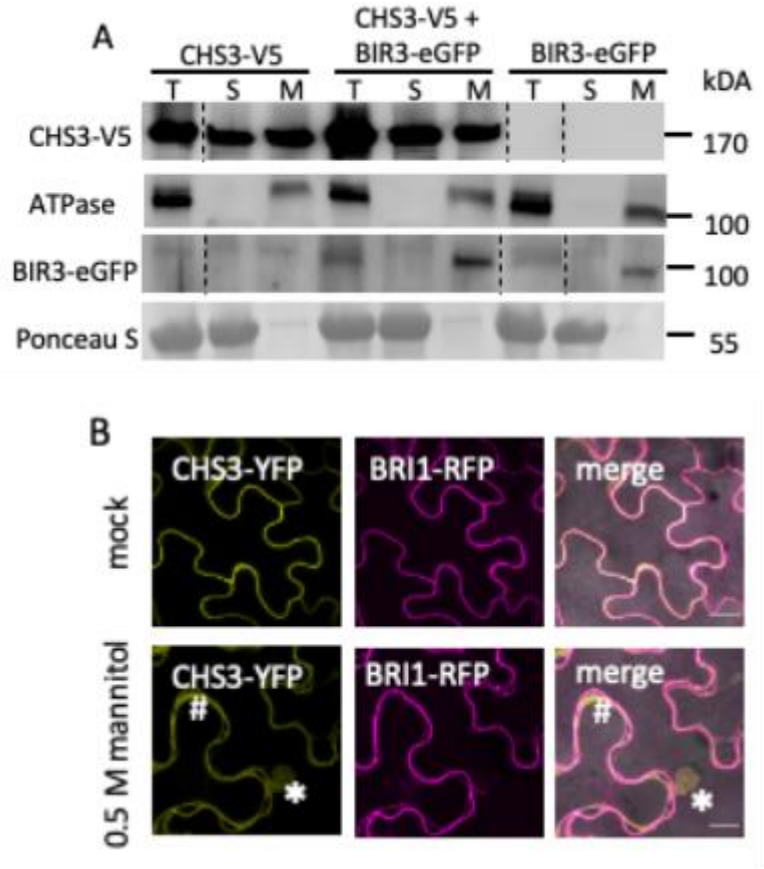

Figure 3-10: CHS3 localizes plasma membrane, cytoplasm and nucleus

(A) Agrobacteria containing CHS3-V5 or BIR3-eGFP, 35S-driven both constructs were transiently infiltrated either alone or both into *N. benthamiana* leaves. Tissue was harvested at 48 hpi for cell fractionation and immunoblotting with anti-V5 (CHS3), anti-ATPase (membrane marker) and anti-GFP (membrane localized BIR3). Ponceau S staining is shown as loading control and marker for the cytosolic fraction. T, total extract; S, soluble; M, microsomal fraction. **(B)** Confocal laser scanning microscopy images of CHS3-GFP transiently expressed in *N. benthamiana* and BRI1-RFP as a membrane localized control. 0,5M mannitol was used to induce plasmolysis. Merged figures show co-localization of CHS3 and BRI1 in the red and green channel. The asterisks mark the nuclei and hashtags cytoplasm, size bars represent 20µm (Figure 3-10 B was by courtesy of my colleague Alexandra Ehinger).

3.4.3 CSA1 interacts with BIR3 but not with BAK1 in *N. benthamiana* in split-luciferase assay

To further explore the interaction between CSA1 and BIR3 (or BAK1), we used split-luciferase (LUC) assay (Zhou et al., 2018) to detect the interaction in *planta* (*N. benthamiana*). BIR3 and BAK1 were used as positive control, while empty vectors pCAMBIA3100-Nluc (PNL) and pCAMBIA3100-Cluc (PCL) (Zhou et al., 2018) as negative controls. CSA1 and BIR3 coding sequences fused to the N- and C-terminal parts of Luciferase were cloned into PNL or PCL, respectively. Then the constructs were transiently expressed *in N. benthamiana* and tested for restoration of luciferase enzyme activity. The increase in luciferase activity, as quantified by relative light units emitted from degraded luciferin, shows that the luciferase can complement when CSA1-CLuc and BIR3-NLuc are expressed together but not when expressed with the empty vector controls, confirming that also in this experimental setup CSA1 and BIR3 are interacting in *planta* (Figure 3-11; Supplemental figure 8-2 A).

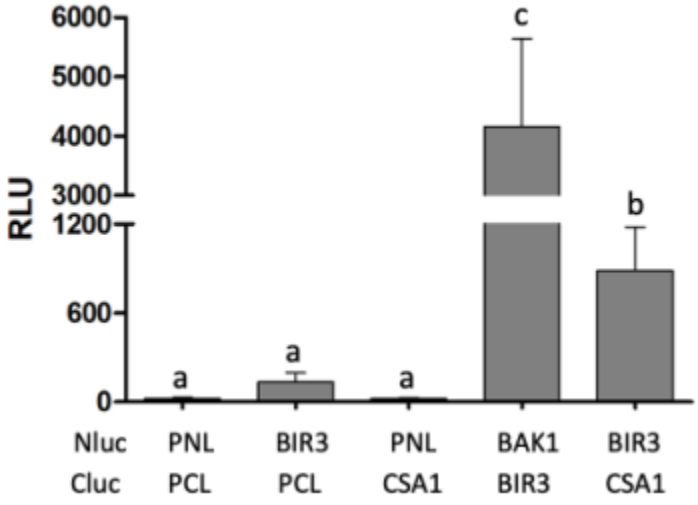

Figure 3-11: CSA1 can interact with BIR3

Split-luciferase assay with transiently expressed BIR3-Nluc and CSA1-Cluc fusion proteins show reconstituted luciferase activity measured in relative light units (RLU) indicating that the two proteins are in close vicinity. BAK1-Nluc and BIR3-Cluc constructs serve as positive controls. Empty vector controls (PNL, PCL) serve as negative controls.

To check the interaction between CSA1 and BAK1 in *planta* (*N. benthamiana*), we also did Co-IP experiments (Sarina Schulze) in *N*. *benthamiana*. Co-IP shows that CSA1 can interact with BAK1 (Schulze, 2020). To investigate whether there is interaction

between CSA1 and BAK1, we also used split-luciferase (LUC) assay to detect the interaction between CSA1 and BAK1 in *planta* (*N. benthamiana*). Similarly, CSA1 and BAK1 coding sequences fused to the N- and C-terminal parts of Luciferase were transiently expressed *in N. benthamiana* and tested for restoration of luciferase enzyme activity. The measured luciferase activity, as quantified by relative light units emitted from degraded luciferin, shows that the luciferase cannot be complemented when CSA1-CLuc and BAK1-NLuc are expressed together. The emitted light was not significantly higher than in the empty vector controls. Thus, the split-Luciferase assay does not show interaction between CSA1 and BAK1 in *N. benthamiana* (Figure 3-12; Supplemental figure 8-2 C).

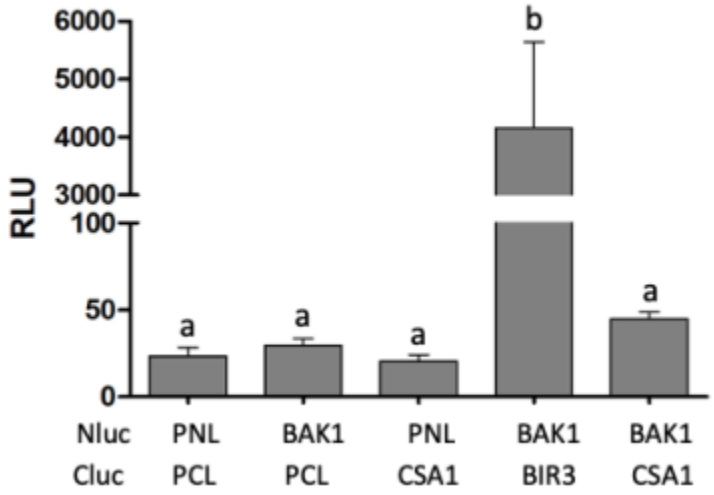

Figure 3-12: CSA1 cannot interact with BAK1 in split-luciferase assay

Split-luciferase assay with transiently expressed BAK1-Nluc and CSA1-Cluc fusion proteins show no reconstituted luciferase activity measured in relative light units (RLU) indicating that the two proteins are not in close vicinity. BAK1-Nluc and BIR3-Cluc constructs serve as positive controls. Empty vector controls (PNL, PCL) serve as negative controls. Different letters indicate significant differences according to one-way ANOVA and Tukey's HSD test ($p<0.05$).

3.4.4 The interaction of CSA1 and BIR3 is direct

Even though Co-IP and split-luciferase experiments show the interaction between CSA1 and BIR3 in *planta*, these data could not tell us if the interaction between CSA1 and BIR3 is direct or not. Thus, we performed split-ubiquitin system (SUS) assays in yeast (Asseck and Grefen, 2018), a classical two-hybrid systems that also works with membrane associated proteins. Previously we have shown that BIR3 can directly interact with BAK1

in yeast (Imkampe et al., 2017). BIR3 and BAK1 were used as a (strong) positive control, while BIR3, BAK1 and CSA1 with empty vectors either pXNubA22-dest or pMetYC-dest, respectively, were used as negative controls. To perform the interaction tests, CSA1 and BIR3 were fused to N- and C-terminal parts of ubiquitin and were cloned into empty vectors pXNubA22-dest and pMetYC-dest, respectively. Then the constructs were transformed into the yeast strain THY. AP4.

Depending on the interaction strength the yeast cells can supplement auxotrophies and can grow more or less. The growth rescue on limiting medium (CSM-Leu$^-$, Trp$^-$, Ade$^-$, His$^-$ for interaction selecting) strongly suggests that CSA1 can directly interact with BIR3 but not with BAK1 (Figure 3-13; Supplemental figure 8-3 A C). We hypothesize that CSA1 directly guards BIR3 and that cell death in *bak1* mutants may be mediated via BIR3 by CSA1.

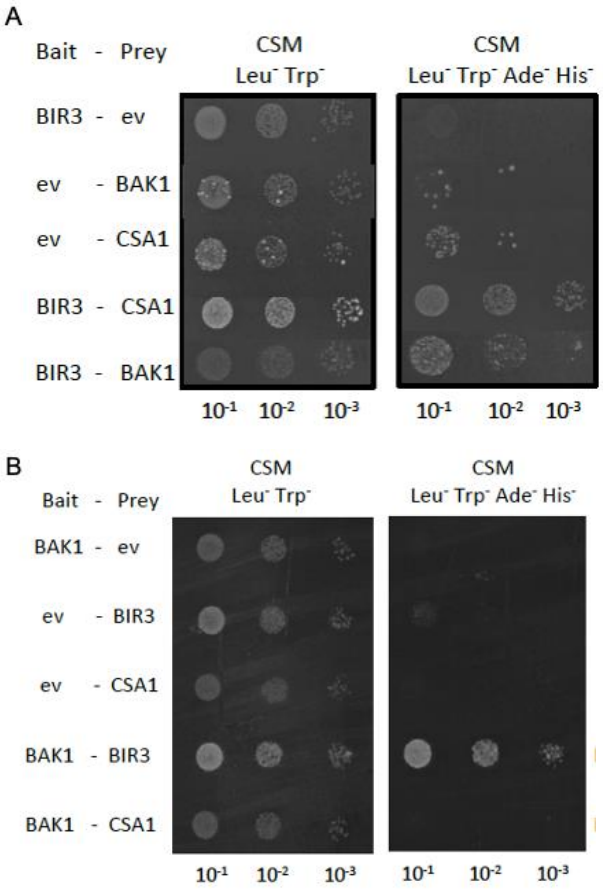

Figure 3-13: CSA1 can interact with BIR3 in yeast, but not with BAK1

Split-ubiquitin yeast growth assays containing the **(A)** CSA1 and BIR3 or **(B)** CSA1 and BAK1 proteins fused to N- and C-terminal parts of ubiquitin were performed with empty vectors either pXNubA22-dest or pMetYC-dest, respectively. Yeast was grown at three different 1 to 10 dilutions on medium selecting for

vector transformation (CSM-Leu$^-$, Trp$^-$) and for interaction (CSM-Leu$^-$, Trp$^-$, Ade$^-$, His$^-$). Growth was monitored after 1 d for the vector-selective control plates and after 3 d for the interaction plates. BIR3 and BAK1 serve as positive controls, empty vector (ev) controls as negative controls. All experiments were repeated at least three times with similar results.

3.5 The function of the CSA1 partner CHS3 in *bak1 bir3*-mediated cell death pathway

CSA1 and CHS3 form an NLR protein pair encoded adjacently on chromosome 5 (Van de Weyer et al., 2019). We have shown that CSA1 is necessary for *bak1* and *bak1 bir3* initiated cell death. It is necessary to figure out how the CSA1 partner CHS3 function in *bak1* and *bak1 bir3*-mediated cell death pathway. Thus, we would analyze the genetic functions of CHS3 in *bak1* and *bak1 bir3*-mediated cell death pathway

3.5.1 Mutation in *chs3* can partially suppress cell death in *bak1* mutants

Loss of BAK1 and BIR3 causes strong autoimmune cell death in *A. thaliana* (Imkampe et al., 2017). As we identified CSA1 in the interactome of BIR3, we generated a *bak1 bir3 csa1* triple mutant to test whether loss of CSA1 can block *bak1 bir3*-initiated cell death. As mentioned in Chapter 3.3, Sarina Schulze found that the *csa1* mutation can suppress cell death of *bak1 bir3* double mutants (Schulze, 2020). *bak1* single mutants has no macroscopically visible autoimmune cell death (Figure 3-14 A), but *bak1* shows enhanced cell death after *A. brassicicola* infection (Figure 3-14 C). Sarina Schulze generated a *bak1 csa1* double mutant and found that loss of CSA1 can suppress cell death of *bak1* mutants triggered by *A. brassicicola* infection (Schulze, 2020). Similarly, as CHS3 was reported to function as a paired NLR with CSA1 (Van de Weyer et al., 2019), and we identified CHS3 as a potential complex partner of BIR3 and/or BAK1 (Schulze, 2020), we also crossed *bak1* or *bak1 bir3* double mutant with a *chs3* mutant. We did *A. brassicicola* infection assay to check whether CHS3 is involved in the *bak1 bir3*-mediated cell death pathway. We found that *bak1 chs3* double mutant plants grew larger than *bak1* (Figure 3-14 A) and the infection spot area was smaller in *bak1 chs3* than in *bak1* after *A. brassicicola* infection (Figure 3-14 B). These results suggest that mutation in *chs3* can partially suppress the growth and immunity phenotype of *bak1* triggered by *A. brassicicola* infection and might be involved in the execution of cell death initiated in the absence of BAK1.

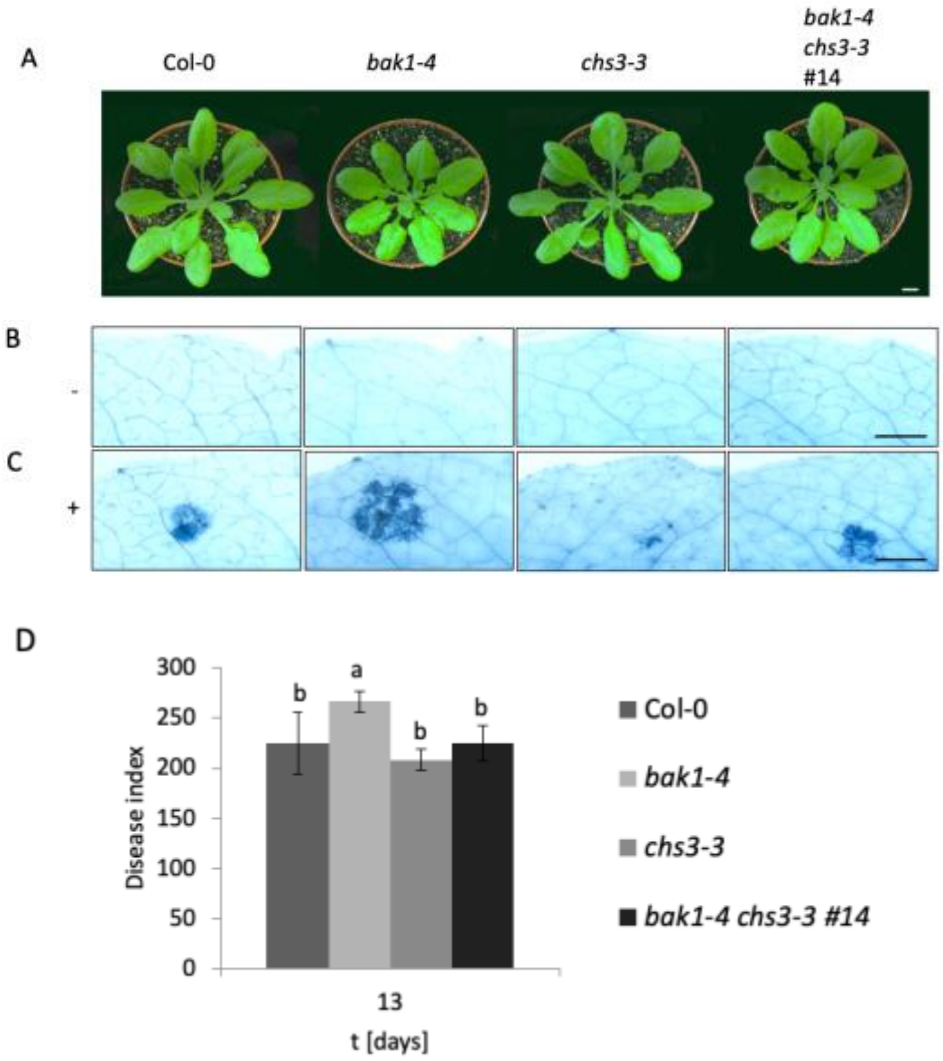

Figure 3-14: The mutation in *chs3* partially suppresses cell death phenotypes in *bak1* mutants

(A) Representative pictures of the morphological phenotype of 6-week-old Col-0, *bak1-4, chs3-2* and the double mutant *bak1-4 chs3-2.* The scale bar represents 1 cm. **(B)** Uninfected leaves of the genotypes shown in (A) stained with trypan blue for cell death. **(C)** Leaves of the same genotypes as in (A) and (B) droplet-infected with *A. brassicicola* and trypan blue stained. The scale bar in (A) and (B) represents 5 mm. **(D)** Disease indices of *A. brassicicola* infected leaves of the indicated genotypes 13 days after infection shown as mean ± SE (n=12). Different letters indicate significant differences according to one-way ANOVA and Tukey's HSD test ($p<0.05$). The experiments were repeated at least three times with similar results.

3.5.2 Mutation in *chs3* partially suppress cell death in *bak1 bir3* mutants

For the triple mutant *bak1 bir3 chs3* we generated, we also performed *A. brassicicola* infection assay. We found that introduction of a *chs3* mutation was affecting the growth phenotype of *bir3 bak1* mutants less than *csa1* mutants did (Figure 3-7 A; Figure 3-15 A). However, loss of CHS3 in the *bak1 bir3* background also affected the autoimmune cell

death shown by trypan blue staining of uninfected plants and the cell death induced by *A. brassicicola* infections (Figure 3-15 B, C). This shows that CHS3 partially contributes to the autoimmune cell death symptoms and the development of spreading cell death after *A. brassicicola* infections in the *bak1 bir3* mutant (Figure 3-15 C, D).

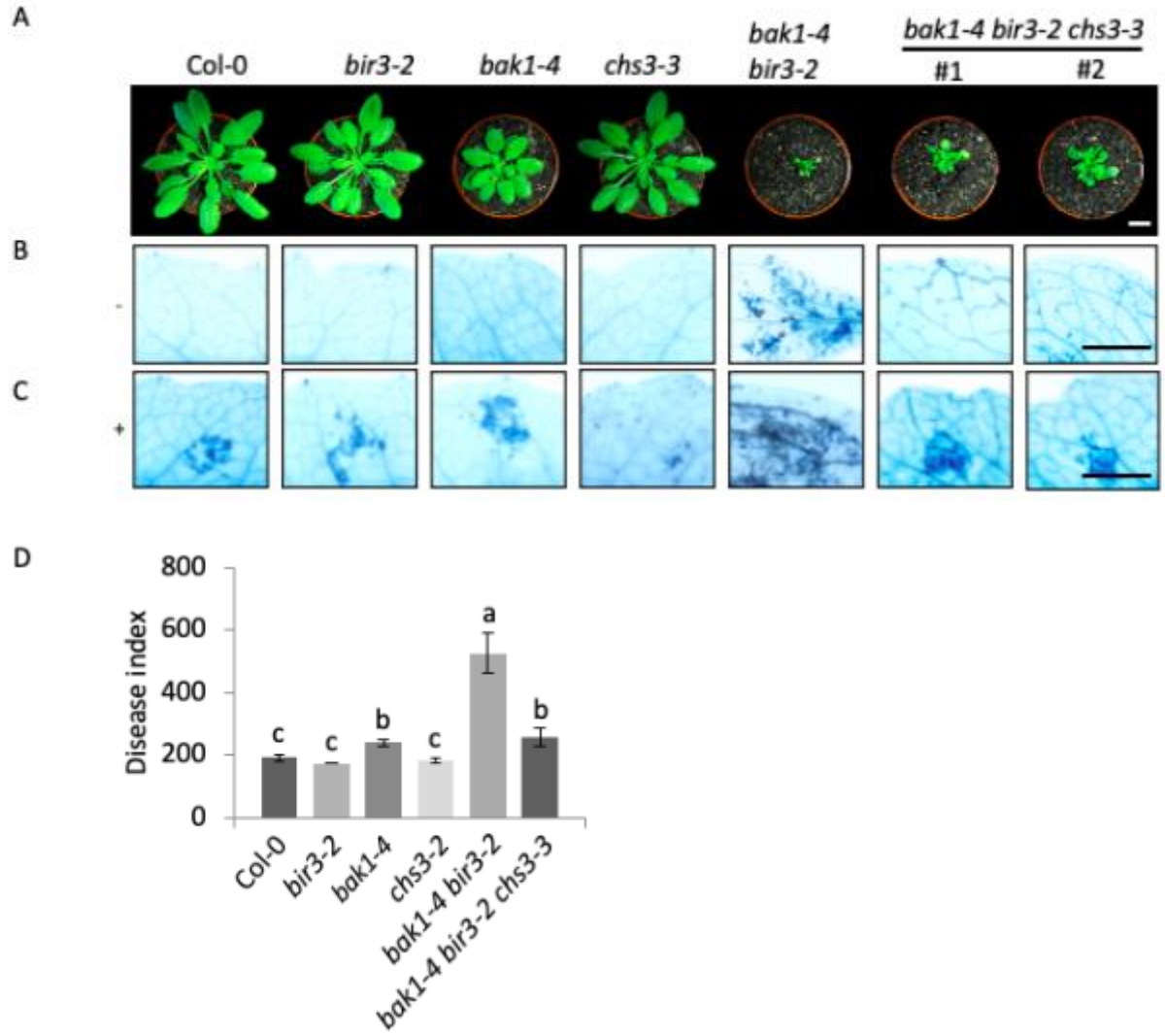

Figure 3-15: The mutation in *chs3* partially suppresses cell death phenotypes in *bak1 bir3* double mutants

(A) Representative pictures of the morphological phenotype of 5-week-old Col-0, *bir3-2*, *bak1-4*, *chs3-3* and the double mutant *bak1-4 bir3-2* and the triple mutant *bak1-4 bir3-2 chs3-3.* The scale bar represents 1 cm. (B) Uninfected leaves of the genotypes shown in (A) stained with trypan blue for cell death. (C) Leaves of the same genotypes as in (A) and (B) droplet-infected with *A. brassicicola* and trypan blue stained. The scale bar in (A) and (B) represents 5 mm. (D) Disease indices of *A. brassicico*la infected leaves of the indicated genotypes 13 days after infection shown as mean ± SE (n=12). Different letters indicate significant differences according to one-way ANOVA and Tukey's HSD test ($p<0.05$). The experiments were repeated at least three times with similar results.

3.5.3 The CSA1 partner CHS3 does not directly interact with BIR3

Recently, CSA1 and CHS3 were found to specifically associate in *A. thaliana* as well as in *N. benthamiana* plants (Parkes, 2020). We detected that CHS3 can interact in Co-IPs with BIR3 when both proteins were transiently expressed in *N. benthamiana* (Schulze, 2020). BIR1 and BIR2 can also interact in Co-IPs with CHS3 (Schulze, 2020).

To confirm this, we also performed split-luciferase assay (Figure 3-16) and split-ubiquitin system (SUS) (Figure 3-17). The constructs used in split-luciferase assay contain the genomic DNA sequence of CSA1 and CHS3 to overcome the difficulty to express NLR proteins in *plants*. We found that the interactions between CHS3 and BIR3 and CHS3 and BAK1 appeared weaker than the CSA1 BIR3 interaction in all assays (Figure 3-16; Figure 3-17).

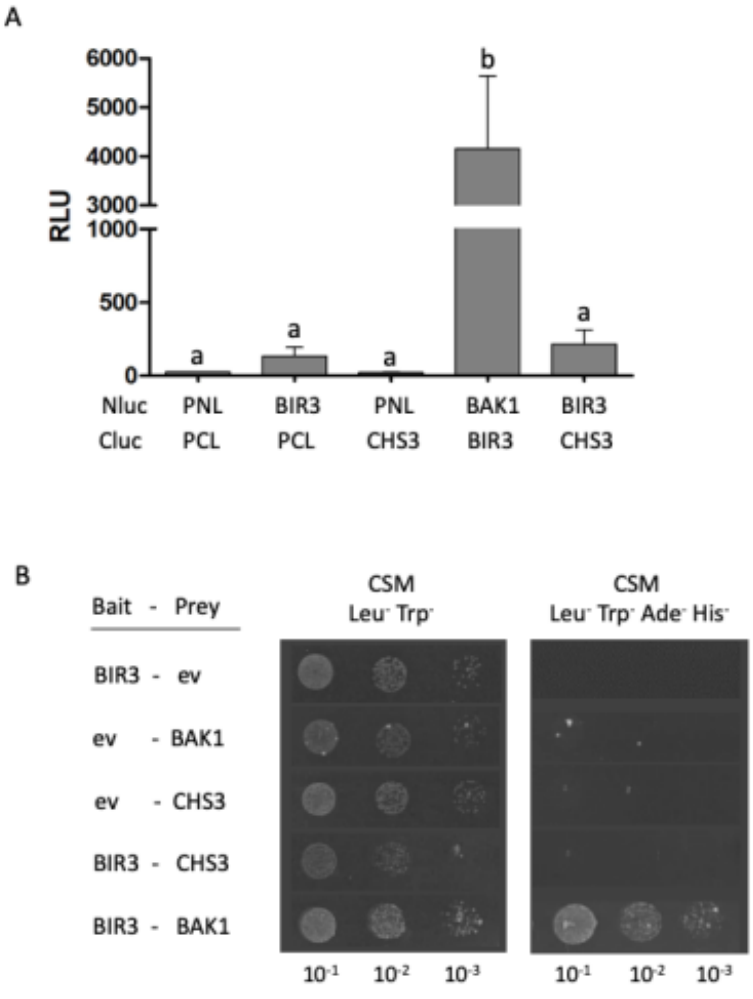

Figure 3-16: The CSA1 partner CHS3 does not directly interact with BIR3

(A) Split-luciferase assays with transiently expressed BIR3-Nluc (or BAK1-Nluc) and CHS3-Cluc (or BIR3-Cluc) fusion proteins were analyzed for reconstituted luciferase activity measured in relative light units (RLU). BAK1-Nluc and BIR3-Cluc constructs serve as positive controls. Empty vector controls (PNL, PCL) serve as negative controls. Different letters indicate significant differences according to one-way ANOVA and Tukey's HSD test ($p<0.05$).**(B)** Split-ubiquitin yeast growth assays containing the two indicated proteins fused to N- and C-terminal parts of ubiquitin were performed with empty vectors either pXNubA22-dest or pMetYC-dest, respectively (ev, empty vector). Yeast was grown at three different 1 to 10 dilutions on medium selecting for vector transformation (CSM -Leu$^-$, Trp$^-$) and for interaction (CSM-Leu$^-$, Trp$^-$, Ade$^-$, His$^-$). Growth was monitored after 1 d for the vector-selective control plates and after 3 d for the interaction plates. BIR3 and BAK1 serve as positive controls, empty vector controls as negative controls. All experiments were repeated at least three times with similar results.

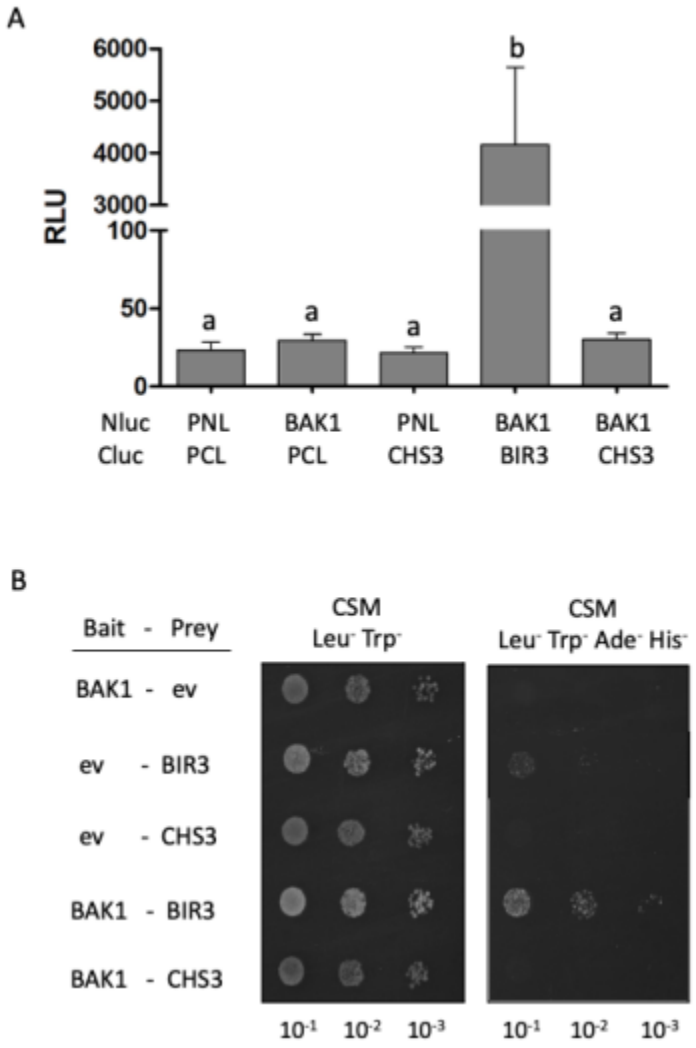

Figure 3-17: The CSA1 partner CHS3 does not interact with BAK1

(A) Split-luciferase assays with transiently expressed BAK1-Nluc and CHS3-Cluc (or BIR3-Cluc) fusion proteins were analyzed for reconstituted luciferase activity measured in relative light units (RLU). BAK1-Nluc and BIR3-Cluc constructs serve as positive controls. Empty vector controls (PNL, PCL) serve as

negative controls. Different letters indicate significant differences according to one-way ANOVA and Tukey's HSD test ($p<0.05$). **(B)** Split-ubiquitin yeast growth assays containing the two indicated proteins fused to N- and C-terminal parts of ubiquitin were performed with empty vectors either pXNubA22-dest or pMetYC-dest, respectively (ev, empty vector). Yeast was grown at three different 1 to 10 dilutions on medium selecting for vector transformation (CSM -Leu$^-$, Trp$^-$) and for interaction (CSM-Leu$^-$, Trp$^-$, Ade$^-$, His$^-$). Growth was monitored after 1 d for the vector-selective control plates and after 3 d for the interaction plates. BIR3 and BAK1 serve as positive controls, empty vector controls as negative controls. All experiments were repeated at least three times with similar results.

The interaction of BIR3 and CHS3 was neither confirmed in split-luciferase assays nor in SUS assays. The interaction of BAK1 with CHS3 was also not shown in these two assays. These data suggest that CSA1 is the direct interactor. And CHS3 might be part of the same complex with BIR3 and/or BAK1 but not in physical contact with BIR3, and we conclude that CHS3 is an indirect potential complex partner of BIR3 and/or BAK1.

3.6 Both TIR^{CSA1} and TIR^{CHS3} can directly interact with BIR3

3.6.1 Sequence and domain structure of CSA1 and CHS3

CSA1 encodes a Toll/Interleukin1 receptor–nucleotide binding site–leucine-rich repeat (TIR-NB-LRR) protein (Faigon-Soverna et al., 2006). Previous studies show that mutation in *csa1* could fully suppress cell death of the auto-active *chs3-2D* mutants indicating that CSA1 functions downstream of CHS3 (Xu et al., 2015). CHS3 encodes an atypical TNL with additional integrated domains (LIM (Lin-11, Isl-1 and Mec-3 domain) domain and putative DA-1 protease domain) at the C-terminus (Xu et al., 2015; Yang et al., 2010) (Figure 3-19).

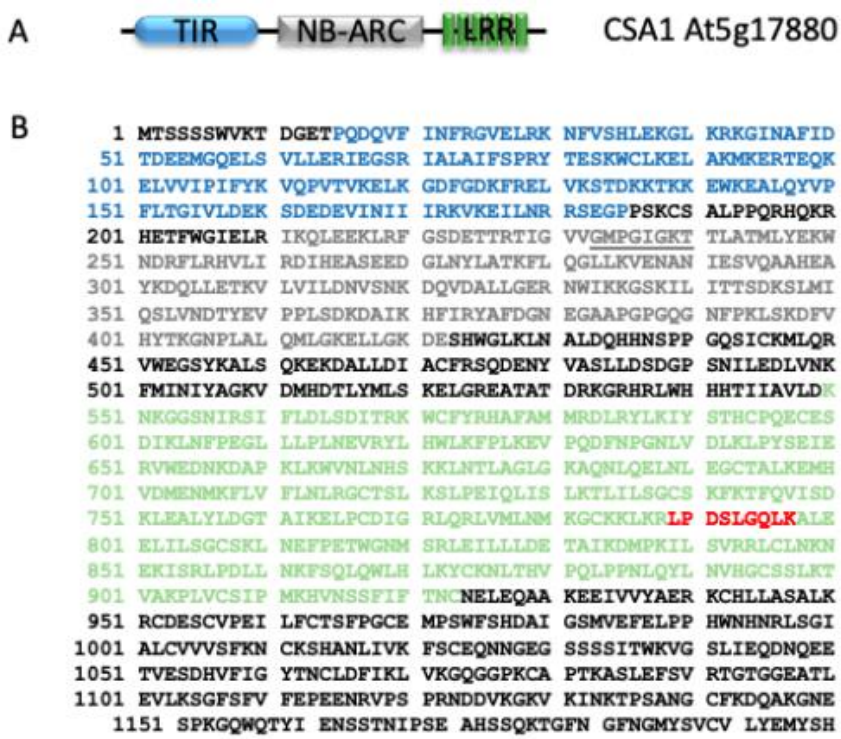

Figure 3-18: Sequence and domain structure of CSA1

(A) The schematic representation of the NLR protein CSA1 structure, containing the following domains: Toll-Interleukin receptor (TIR), nucleotide binding APAF-1 (apoptotic protease-activating factor-1), R proteins and CED-4 (*Caenorhabditis elegans* death-4 protein) (NB-ARC) and the leucine-rich repeat (LRR) domain. (**B)** Sequence of CSA1 with the domains identified with InterProScan labelled with the following color code: TIR domain (blue), NB-ARC-domain (grey) including the P-loop (underlined), LRR domain (green). The peptide identified in the Co-IPs by MS analyses is labelled in red (Schulze, 2020).

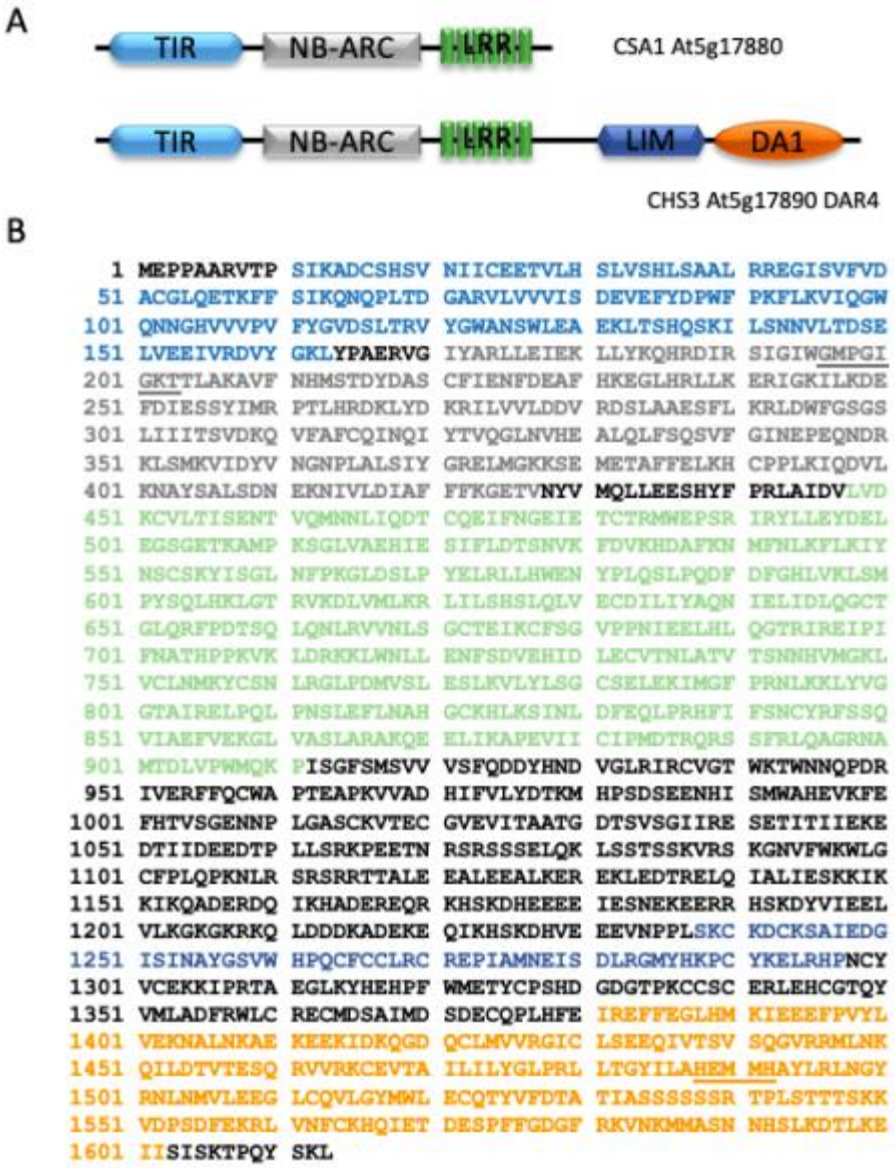

Figure 3-19: Sequence and domain structure of CHS3

(A) CHS3 contains Toll-Interleukin receptor (TIR), nucleotide binding APAF-1 (apoptotic protease-activating factor-1), R proteins and CED-4 (Caenorhabditis elegans death-4 protein) (NB-ARC) and leucine-rich repeat (LRR) domains plus integrated domains (CC: coiled coil, LIM: LIN-11, Isl-1 and MEC-3 and DA-1: DA-1-like protease domain). (**B)** Sequence of CHS3 with predicted domains based on InterProScan. Domains are marked with the following color code: TIR domain (blue), NB-ARC-domain (grey) including the P-loop (underlined), LRR-domain (LRR / green), coiled-coil domain (CC / yellow), LIM-domain (LIM / dark blue) and a zinc protease domain including the underlined HExxH motif (orange), required for protease activity.

3.6.2 Both TIR^{CSA1} and TIR^{CHS3} domains interact with BIR3 in *N. benthamiana*, but not with BAK1

CSA1 encodes a typical TNL with a Toll/Interleukin1 receptor–nucleotide binding site–leucine-rich repeat (TIR-NBS-LRR)–type gene (Figure 3-18; Figure 3-19). While CHS3 encodes an atypical TNL with additional integrated domains (LIM (Lin-11, Isl-1 and Mec-3 domain) domain and putative DA-1 protease domain) at the C-terminus (Yang et al., 2010). To know which domain mediates the interaction between these two TNLs and BIR3, we made truncated-mutants containing only the TIR domain: TIR^{CSA1} (1-187aa), nucleotide binding domain: NB^{CSA1} (188-586aa), leucine-rich repeat domain: LRR^{CSA1} (587-1185aa). And CHS3 truncated domains were generated as the following: TIR^{CHS3} (1-154aa), NB^{CHS3} (155-518aa), LRR^{CHS3} (519-835aa), LIM^{CHS3} (836-1386aa) and DA1^{CHS3} (1387-1613aa).

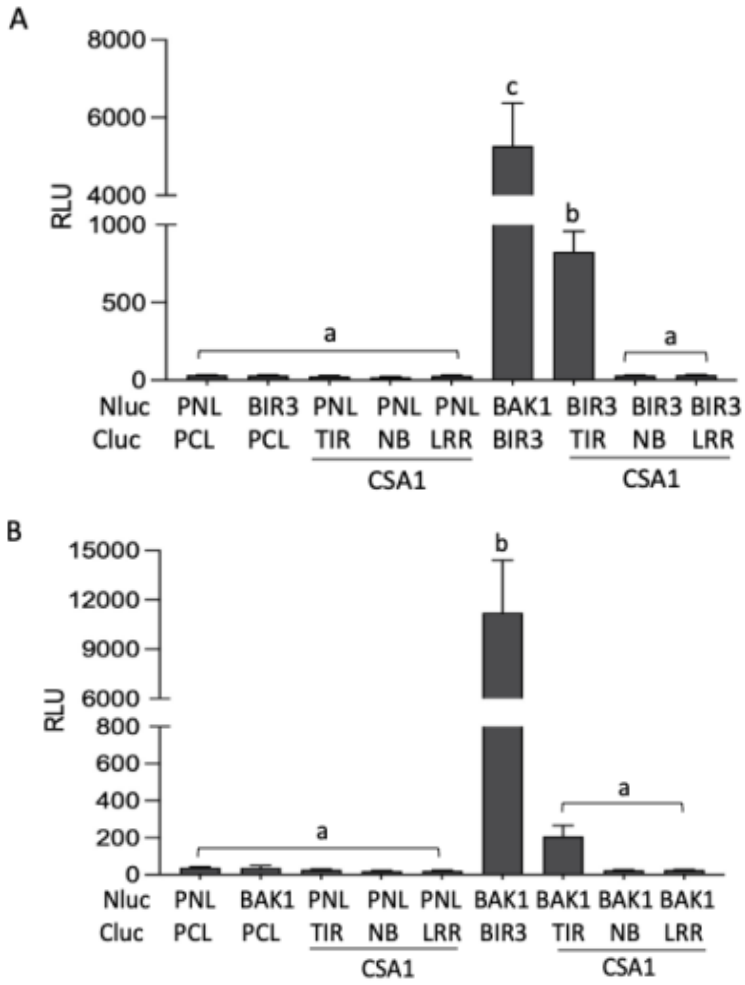

Figure 3-20: TIR^{CSA1} can interact with BIR3, but barely with BAK1

(A) and **(B),** Split-luciferase assay with transiently expressed BIR3-Nluc or BAK1-Nluc and all truncated-mutants with Cluc-tagged fusion proteins or BIR3-Cluc show reconstituted luciferase activity measured in relative light units (RLU) indicating that the two proteins are in close vicinity. BAK1-Nluc and BIR3-Cluc constructs serve as positive controls. Empty vector controls (PNL, PCL) serve as negative controls. Different letters indicate significant differences according to one-way ANOVA and Tukey's HSD test ($p<0.05$).

To detect the interaction, we performed split-luciferase complementation assay (Zhou et al., 2018). All truncated versions and BIR3 or BAK1 coding sequences fused to the N- and C-terminal parts of Luciferase were cloned into PNL or PCL vectors, respectively. We found that only both TIR^{CSA1} and TIR^{CHS3} domains can interact with BIR3 in *N. benthamiana* (Figure 3-20; Figure 3-21). All the other domains have no interaction with BIR3 (Figure 3-20; Figure 3-21; Supplemental Figure 8-4).

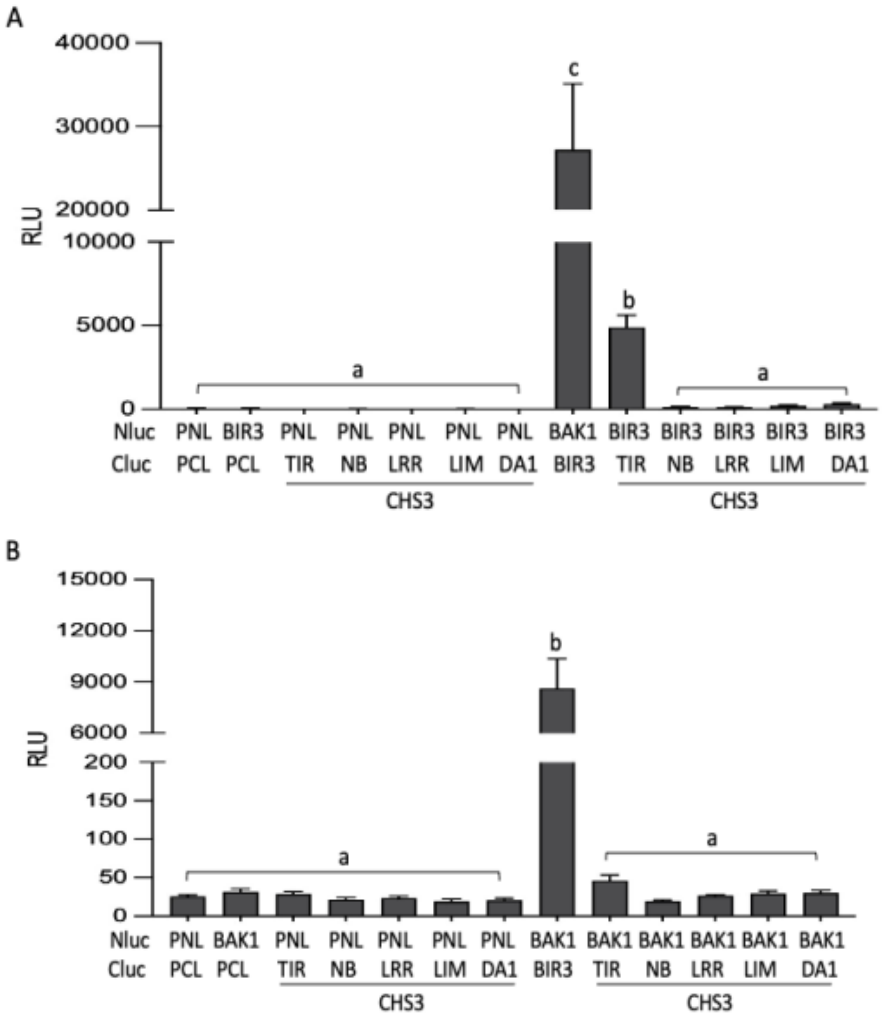

Figure 3-21: TIR^{CHS3} can interact with BIR3, but other domains cannot interact with BIR3 or BAK1

(A) and **(B),** Split-luciferase assay with transiently expressed BIR3-Nluc or BAK1-Nluc and all truncated-mutants with Cluc-tagged fusion proteins show reconstituted luciferase activity measured in relative light units (RLU) indicating that the two proteins are in close vicinity. BAK1-Nluc and BIR3-Cluc constructs serve as positive controls. Empty vector controls (PNL, PCL) serve as negative controls. Different letters indicate significant differences according to one-way ANOVA and Tukey's HSD test ($p<0.05$).

No significant differences of TIR^{CSA1} and BAK1 co-expression samples compared to the negative controls observed (Figure 3-20). For the interaction between the other truncated mutants and BAK1, no interaction was detected at all (Figure 3-21). Western blotting controls confirming the expression of proteins in the samples are shown in the supplemental data (Supplemental Figure 8-3). These data suggest that the TIR domain of CSA1 (TIR^{CSA1}), may be the region of direct association between CSA1 and BIR3.

Notably, the TIR domain of CHS3 (TIR^{CHS3}), also can interact with BIR3 by using split-luciferase assay in *N. benthamiana*, while the full-length protein of CHS3 cannot interact with BIR3 by using the same method. We cannot rule out the possibility that the non-interaction between the full length of CHS3 and BIR3 is due to the lower protein accumulation of CHS3 in *N. benthamiana*.

3.6.3 Both TIR^{CSA1} and TIR^{CHS3} domains directly interact with BIR3 in yeast

To support these findings with an independent method evaluating direct interaction of CSA1 and CHS3 domains with BIR3, we performed split-ubiquitin system (SUS) experiment. We used the same strategy to make the constructs as described above. We found that both TIR^{CSA1} and TIR^{CHS3} domains can directly interact with BIR3 in yeast. The interaction of TIR^{CSA1} domain with BIR3 is much stronger than with TIR^{CHS3} domain and BIR3 in yeast (Figure 3-22). These findings confirm that there is direct interaction of CSA1 with BIR3 via the TIR domain of CSA1 (Figure 3-22 A). However, the interaction of TIR^{CHS3} domain with BIR3 only happened with the isolated domain but not within the full-length protein (Figure 3-16; Figure 3-22 B). That the other domains accumulate extremely low level in yeast prevented us to test whether they have interaction with BIR3 or BAK1 (Figure 3-20; Figure 3-21).

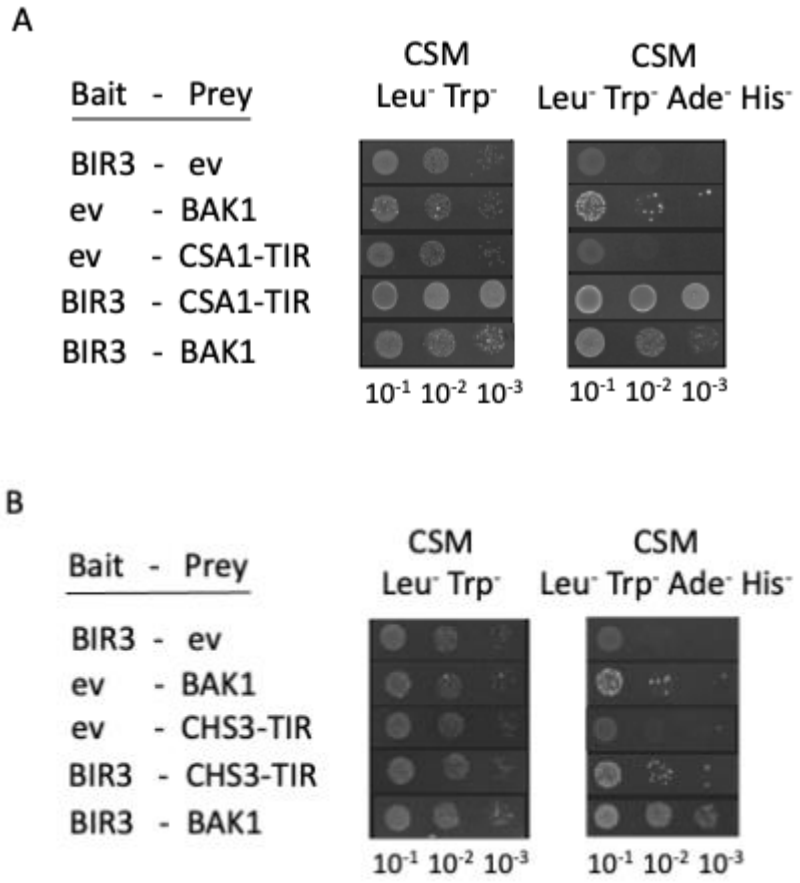

Figure 3-22: Both TIR^{CSA1} and TIR^{CHS3} directly interact with BIR3

(A) and **(B)** Split-ubiquitin yeast growth assays containing the two indicated proteins fused to N- and C-terminal parts of ubiquitin were performed with empty vectors either pXNubA22-dest or pMetYC-dest, respectively (ev, empty vector). Yeast was grown at three different 1 to 10 dilutions on medium selecting for vector transformation (CSM -Leu$^-$, Trp$^-$) and for interaction (CSM-Leu$^-$, Trp$^-$, Ade$^-$, His$^-$). Growth was monitored after 1 d for the vector-selective control plates and after 3 d for the interaction plates. BIR3 and BAK1 serve as positive controls, empty vector controls as negative controls. All experiments were repeated at least three times with similar results.

Taken together, these data indicate that CSA1 interacts with BIR3 protein by directly interacting with them via its TIR domain. CHS3 and BAK1 may be partners in a CSA1 complexes but without direct interaction of the complex partners. The role of CHS3 in this complex and whether BAK1 and CHS3 are simultaneously in complex with CSA1 needs to be studied in future experiments.

3.6.4 Interaction of CSA1 with BIR3 in *A. thaliana*

Previously, we have concluded that CSA1 interacts with BIR3 in *N. benthamiana* by Co-IP and split-luciferase experiments, and the interaction between CSA1 and BIR3 is direct

by split-ubiquitin assay in yeast. But these data could not tell us if CSA1 interacts with BIR3 in *A. thaliana* or not. We tried different methods to detect the interaction between CSA1 and BIR3 in *A. thaliana*. Firstly, we did a transient expression experiment in *A. thaliana* (Zhang et al., 2020). We used a genomic construct of CSA1 (pUSER-FR-CSA1-V5) under 35S promoter to transiently express into BIR3-GFP transgenic plants under *bir3-2* background, *bir3-2* mutant as negative control. Unfortunately, the interaction in *A. thaliana* was limited due to low expression of genomic constructs of CSA1-V5 or potentially lethal plants in Co-IP assays (Figure 3-23). We also tried to test CHS3-V5, and achieved with similar results (Figure 3-24).

Meanwhile we tried to generate double genes transgenic *A. thaliana.* We transformed the same construct of CSA1 (pUSER-FR-CSA1-V5) under 35S promoter into stable transgenic lines containing pB7FWG2-35S-BIR3-eGFP. However, interaction studies in *A. thaliana* also turned out to be limited due to low expression of CSA1-V5 and the amount of expressed and detectable immunoprecipitated CSA1 was too little to prove interaction. We also tried to directly detect expression of BIR3 in transgenic CSA1-V5 lines. But BIR3 antibody has a low affinity and is insufficient to detect co-immunoprecipitated BIR3.

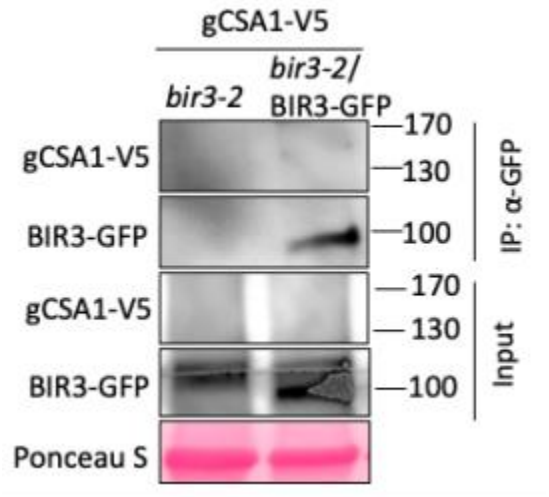

Figure 3-23: Low expression of CSA1-V5 in *A. thaliana*

Indicated constructs were transiently expressed in *A. thaliana* leaves and immunoprecipitation (IP) was performed with GFP-trap beads. Precipitated BIR3-GFP and co-immunoprecipitated CSA1-V5 were detected with α-GFP and α-V5 antibodies respectively. Protein input is shown with Western blot (WB) analysis of protein extracts before IP and α-GFP and α-HA antibodies. Ponceau S staining shows protein loading.

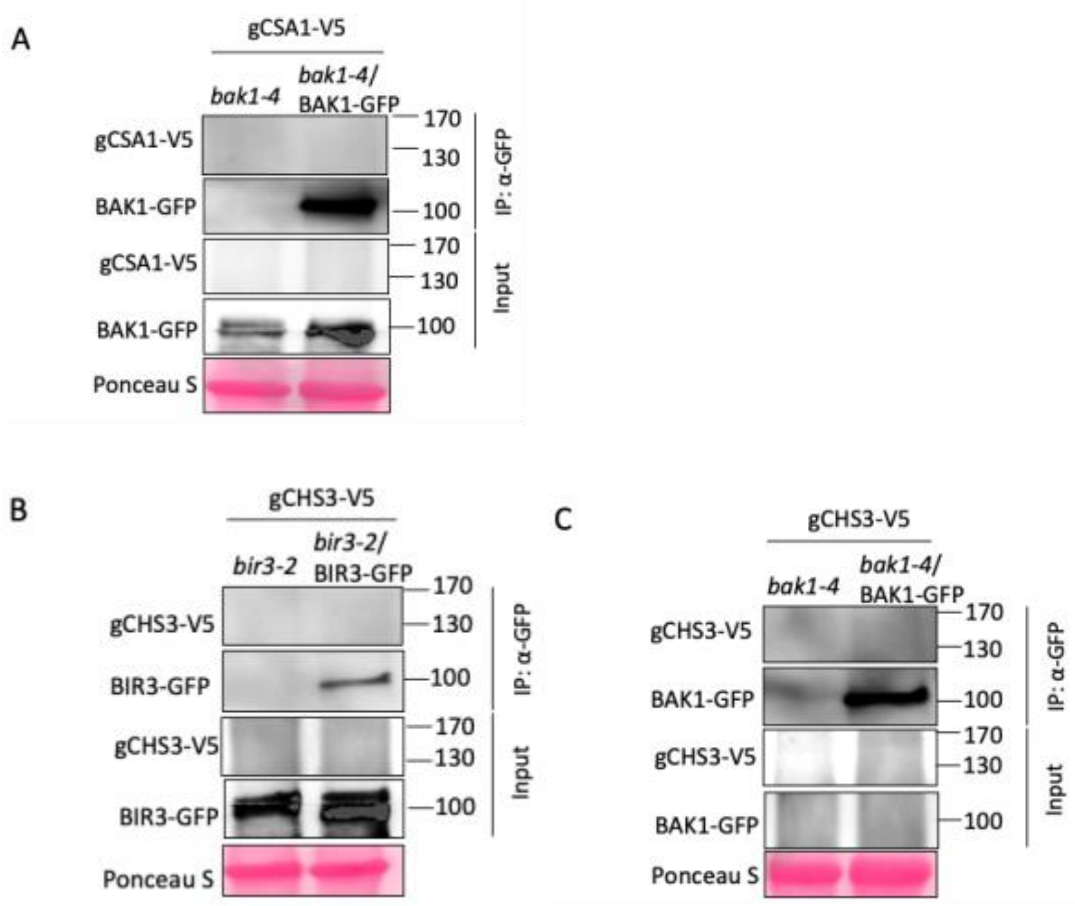

Figure 3-24: Low expression of CSA1-V5 and CHS3-V5 in *A. thaliana*

Indicated constructs were transiently expressed in *A. thaliana* leaves and immunoprecipitation (IP) was performed with GFP-trap beads. Precipitated BIR3-GFP or BAK1-GFP and co-immunoprecipitated CSA1-V5 or CHS3-V5 were detected with α-GFP and α-V5 antibodies respectively. Protein input is shown with Western blot (WB) analysis of protein extracts before IP and α-GFP and α-HA antibodies. Ponceau S staining shows protein loading.

3.6.5 The P loop function of CSA1 in *bak1 bir3*-mediated cell death

In some instances, autoimmunity is dependent on functional NLR which is well described (Lolle et al., 2017; Parkes, 2020). Previous study demonstrated that a functional P loop is required for NLR signaling (Lolle et al., 2017; Parkes, 2020). We tested mutant GXXXXGKT(T/S) to GXXXXAAT(T/S) of the P loop motif in CSA1 (hereafter CSA1-DN which is kindly provided by Dr. Morten Petersen) for suppression of *bak1 bir3* cell death. We transformed pCAMBIA3300-35S::CSA1-DN into triple mutant *bak1 bir3 csa1* plants by floral dipping (Clough and Bent, 1998). Transgenic plants were selected on soil with

BASTA (10 mg/L). Due to time constrains the work could not be finished within this thesis. My colleague Dagmar Kolb is currently continuing this work.

3.7 IP-MS/MS of CSA1

The previous work has shown that CSA1 is an essential component of cell death initiated by loss of BAK1 and BIR3. To better understand how CSA1 is functioning in this context we determined the *in vivo* interactome of CSA1-V5 by liquid chromatography- electron spray ionization tandem mass spectrometry (LC-ESI-MS/MS) in *A. thaliana* plants. Immunoprecipitations (IP) were performed with T2 *A. thaliana* plants expressing CSA1-V5 under the CaMV35S promoter, using monoclonal anti-V5 antibody coupled to agarose beads (Sigma, A7345). The immunoprecipitated proteins were eluted from agarose beads by boiling with SDS-PAGE buffer at 95 ℃ for 5 mins. Plants expressing free V5 under the same promoter (CaMV35S) in Col-0 background were supposed to be chosen as controls to detect proteins unspecifically bound to V5. The pre-experiment was done by using Col-0 as control. The workflow was: MS proteins were purified by a short SDS-PAGE gel (Figure 3-25), which was processed by the Proteome Center Tübingen. Proteins were digested In-gel with trypsin. LC-MS/MS analyzed on a Proxeon Easy-nLC coupled to QExactive HF, method: 60 mins top7 HCD. For processing of the data, the MaxQuant software (Version 1.6.7.0. with integrated Andromeda Peptide search engine) was used. The spectra were searched against a *A. thaliana* database (UP000006548_3702_ complete _2019-12-11. fasta) and a sequences database including the CSA1 sequence.

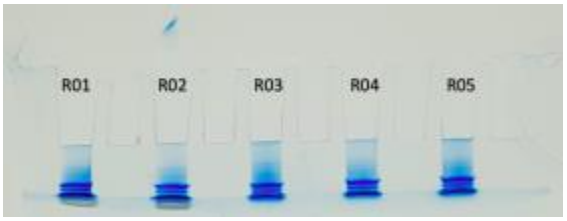

Figure 3-25: SDS-PAGE short gel with MS proteins in the IP-MS/MS of CSA1

MS protein samples were named shown on left. MS proteins were purified by a SDS-PAGE short gel. For each MS protein sample 30µl volume were loaded.

The MS analyses contained 1232 co-immunoprecipitated proteins and revealed about 43 specific kinases which included several RKs (receptor kinases) and RLKs (receptor like kinases), which could be potential interactors of CSA1 in *A. thaliana* (Table

1). Some other specific interactors including kinases and other candidate proteins were also shown in the IP-MS/MS of CSA1 compared with Col-0 (Supplemental data 8.2; Table 4). The CSA1-specific MS analyses show that Q-value of CSA1 equals zero which means the False Discovery Rate (FDR) has been adjusted to minimum. We can see that the relative abundance of CSA1 is the maximum in all MS proteins from the Table 1, which means the whole mass spectrometry experiment is correct including our CSA1 transgenic plants. However, we did not find BIR3 or CHS3 from CSA1- specific LC-MS/MS analyses. We assume that the interaction of CSA1 BIR3 and CSA1 CHS3 is dynamic. Similarly, we did not find BIR3 in the second LC-MS/MS analyses probably due to the same reason to make it hard to detect.

Table 1: The MS analyses of CSA1 interactome reveals several receptor kinases

Gene name	Protein IDs	Intensity	Q value
At5g17880	Disease resistance protein (TIR-NBS-LRR class), CSA1	$2.77x10^{10}$	0
At3g17420	Probable receptor-like protein kinase	$2.087\ x10^{8}$	0
At3g18130	RACK1C, Receptor for activated C kinase 1C	$6.27x10^{7}$	0
At1g48630	RACK1B, Receptor for activated C kinase 1B	$6.27x10^{7}$	0
At1g16260	WAKL8, Wall-associated receptor kinase-like 8	$5.33x10^{7}$	0.0026087
At1g21270	WAK2, Wall-associated receptor kinase 2	$5.33x10^{7}$	0
At3g02880	Probable inactive receptor kinase	$4.38x10^{7}$	0.0024311
At5g16590	Probable inactive receptor kinase	$4.38x10^{7}$	0.0024311
At4g04570	Cysteine-rich receptor-like protein kinase 40, CRK40	$2.69x10^{7}$	0.0024855
At4g23230	Cysteine-rich receptor-like protein kinase 15	$4.16x10^{7}$	0
At5g01850	Cysteine-rich receptor-like protein kinase 15, CPK15	$4.16x10^{7}$	0
At1g52290	Proline-rich receptor-like protein kinase PERK15	$4.16x10^{7}$	0
At4g11530	Putative cysteine-rich receptor-like protein kinase 35	$4.16x10^{7}$	0

Several RKs and RLKs were selected within CSA1-interactome of IP-MS/MS analyses, including gene names, protein IDs, ratio of intensities and Q value. The Q-value is a statistical feature to assess the probability of false positive candidates.

Since CSA1 can interact with multiple kinases, we try to find phosphorylation site of CSA1 by reprocessing of the raw files with MaxQuant1.5.2.8., iBAQ values, match between runs was selected (Col-0 samples were matched with each other and CSA1 samples were matched with each other, but no matching between groups), and Phospho (STY) as variable modification. One phosphorylation site (Ser^{1120}) was found in our pre-experiment (Figure 3-26).

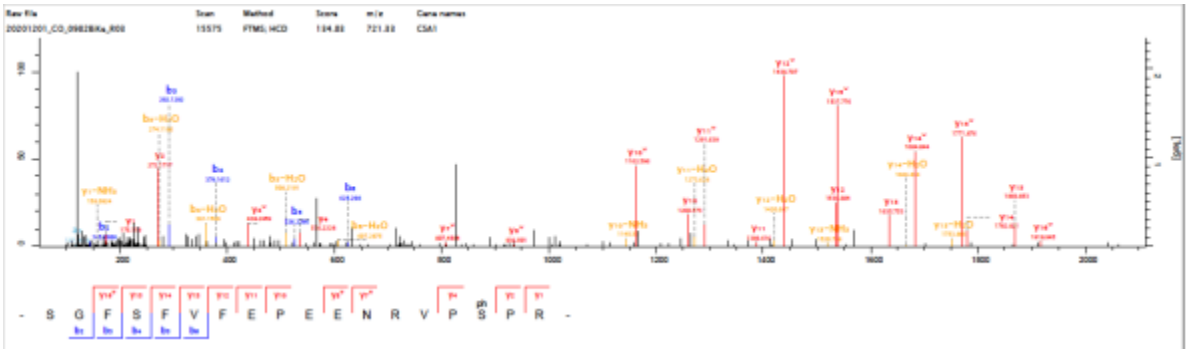

Figure 3-26: Spectrum within CSA1-interactome IP-MS/MS analyses

The only phosphorylation site for CSA1 was shown above. Ser^{1120} was marked with phosphorylation.

My colleague Dagmar Kolb did the second-round IP-MS/MS to find more potential interactors of CSA1 and CHS3 in *A. thaliana*. Plants expressing V5-YFP under the same promoter CaMV35S in Col-0 background were used to be controls this time. More information with the second-round IP-MS/MS, see Supplemental data 8.3 and 8.4. Interestingly, we find that the phosphorylation site (Ser^{1120}) of CSA1 is present in both LC-MS/MS (Supplemental Figure 8-7).

Meanwhile, we could find some enriched proteins from volcano plots of the second LC-MS/MS analyses (Figure 3-27 A, B). Figure 3-27 shows a volcano plot figure of CSA1-V5 vs control and CHS3-V5 vs control, respectively. At3g07010, F22K18.110 (NBR1, At4g24690) and K3M16_80 (At5g17510) labelled with green colors in Figure 3-27 are enriched in both CSA1 and CHS3 transgenic plants. And only two proteins, called RPL10AA and CLPP3 are enriched in control plants compared to CHS3 transgenic plants.

These data could provide us more clues for further study how CSA1 or CHS3 is activated in *bak1 bir3*-mediated cell death pathway.

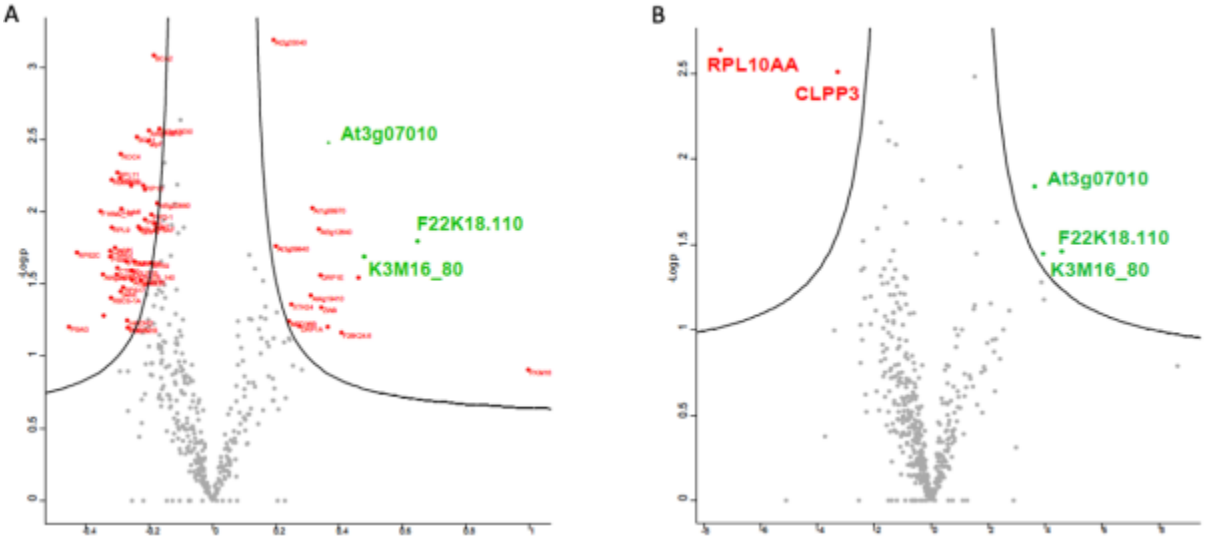

Figure 3-27: Visualization of CSA1- specific or CHS3- specific MS results with Volcano Plots

(A) and **(B)** Volcano plots with protein enrichment from mass spectrometry analyses. Left shows CSA1-specific MS analyses and right shows CHS3-specific MS analyses. In CSA1 proteome there are 42 significantly enriched proteins are downregulated and 17 proteins are upregulated. However, in CHS3 proteome there are only 2 significantly enriched proteins are downregulated and 3 proteins are upregulated.

4. Discussion

The BRI1-Associated Receptor Kinase 1 (BAK1) functions as a co-receptor that regulates BR, PAMP and MAMP signaling pathways by interacting with several well-studied RKs from *A. thaliana*, such as BRI1, FLS2, EFR and PEPR1/2 (Gomez-Gomez and Boller, 2000; Krol et al., 2010; Li and Chory, 1997; Nam and Li, 2002; van der Burgh et al., 2019; Zipfel et al., 2006). Furthermore, BAK1 is involved in the regulation of cell death pathway. In addition, BAK1 closest homolog BKK1 (BAK1-like 1 or SERK4) can additively regulate cell death because *bak1 bkk1* double mutant shows constitutive activation of immune responses and displays strong spontaneous cell death and seedlings lethality (Gao et al., 2017; He et al., 2007; Kemmerling et al., 2007; Wu et al., 2020). The BAK1 complex in vivo contains several interactors, for example BIR1, BIR2 and BIR3 (Gao et al., 2009; Halter et al., 2014; Imkampe et al., 2017). *bak1 bir3* double mutant shows a strong dwarf phenotype and spontaneous cell death formation (Imkampe et al., 2017). Therefore, this work focuses on the mechanism of *bak1 bir3*-mediated cell death.

4.1 Cell death regulation by BAK1 and BIR family proteins

BAK1 plays a role in cell death control since *bak1* mutants shows a spreading cell death phenotype upon treatment with plant pathogens (Kemmerling et al., 2007). Both BAK1 and its closest homolog BKK1 (BAK1-like 1 or SERK4) negatively regulate cell death. *bak1 bkk1* double mutant displays constitutive cell death and seedlings lethality (He et al., 2007). Although Loss of BIR1 causes plant autoimmunity as well, loss of either BIR2 or BIR3 only causes very mild cell death phenotype. However, double mutant *bak1 bir3* shows a very strong dwarfism phenotype that is reminiscent of *bak1 bkk1* double mutant.

4.1.1 Cell death regulation by BAK1

BAK1 was described as a cell death regulator because *bak1* mutants show spreading cell death when *bak1* mutant is triggered with microbial infections (Kemmerling et al., 2007). Double mutant of *bak1* and its closest homologue *bkk1* shows a seedling-lethality phenotype at an early developmental stage (He et al., 2007). Moreover, overexpression of BAK1 in *A. thaliana* plants leads to defects in cell death control (Belkhadir et al., 2012; Dominguez-Ferreras et al., 2015). BAK1 overexpressing plants mimic *bak1* mutants with spontaneous cell death. Inappropriate BAK1 mediated cell death phenotype can be

antagonized by overexpression of BRI1 (Belkhadir et al., 2012). This suggests that the amount of BAK1 needs to be proportional to its interacting partners (Belkhadir et al., 2012). And an excess of BAK1 or its ectodomain could increase resistance to *P. syringae* pv tomato DC3000 and trigger immune receptor activation but the mechanism is unclear (Dominguez-Ferreras et al., 2015). Whereas it remains elusive whether *bak1* mutant and BAK1 overexpression-mediated cell death phenotype are identical or not in downstream signaling, the dosage of BAK1 is important for the regulation of cell death.

4.1.2 Cell death regulation by BIR family proteins

Mutation in *bir1* shows strong cell death phenotypes and activation of defense responses (Gao et al., 2009). Transgenic overexpression of BIR1 leads to severe developmental defects, cell death, and premature death in virus infected tissues, which is associated with constitutive activation of plant immune responses (Guzman-Benito et al., 2019). Mutation in *bir2* shows a weak autoimmune phenotype with early senescence and slightly smaller morphology. There is spreading cell death observable in *bir2* knockouts after infection with necrotrophic fungi *A. brassicicola*, even stronger than in *bak1* knockouts (Halter et al., 2014). Halter et al. (2014) also analyzed BIR2 overexpressing plants and could demonstrate that BIR2 overexpression resulted in loss of cell death inhibition, resulting in higher disease symptoms after *A. brassicicola* infection. Therefore, the amount of BIR2 protein is essential for the cell death containment after infections. Mutation in *bir3* shows slightly larger morphology and weakest cell death after *A. brassicicola* infections (Schulze, 2020). Overexpression of BIR3 led to a strong dwarf phenotype, that is not a cell death induced dwarfism but based on blocking of the BL signaling pathway in homozygous overexpression lines, indicated that it is also working in a gene dosage-dependent manner (Imkampe et al., 2017). Therefore, loss-of-function mutants of BAK1-interacting receptors BIR1, BIR2 and BIR3 replicate autoimmune cell death phenotypes. The fact that knockdown or overexpression of a complex component results in cell death suggests that an appropriate ratio of proteins and complex integrity is necessary.

4.1.3 Rregulators of BAK1- or BIR-mediated cell death

As mentioned above, double mutant *bak1-4 bkk1* are frequently used in suppressor screens because loss of these two closest SERK family members causes a spontaneous cell death phenotype or be ultimately lethal even grown in sterilized condition (de Oliveira et al., 2016; Du et al., 2016; Gao et al., 2017; He et al., 2007; Schwessinger et al., 2011; Wu et al., 2020). Since then, multiple components necessary for the execution of BAK1- or BIR-mediated cell death have been revealed. For example, three components of ER quality control, CALRETICULIN3 (CRT3), ER-LOCALIZED DnaJ-LIKE PROTEIN 3b (ERdj3b) and STROMAL-DERIVED FACTOR-2 (SDF2) could inhibit the spontaneous cell death and constitutive defense responses in *bir1-1* (Sun et al., 2014). Furthermore, systematic studies of endoplasmic reticulum (ER) quality control (ERQC) components and glycosylation pathways revealed different and overlapping mechanisms of cell death regulated by BAK1/SERK4 and its interacting protein BIR1, such as STAUROSPORIN AND TEMPERATURE SENSITIVE3 (STT3a), a component for protein glycosylation mediated. The triple mutant *bak1-4 bkk1-1 stt3a-2* could overcome the cell death of *bak1-4 bkk1-1* and STT3a also identified to be required for *bir1* leaf chlorosis (de Oliveira et al., 2016). The cyclic nucleotide-gated channel 20 (CNGC20) specifically regulates the cell death of *bak1-4 bkk1-1*, while cyclic nucleotide-gated channel 19 (CNGC19), the closest homolog of CNGC20, makes a quantitative contribution to *bak1-4 bkk1-1* cell death only in the absence of CNGC20 (Yu et al., 2019). In addition, the nucleocytoplasmic trafficking components including SUPPRESSOR OF BAK1 BKK1/ NUCLEOPORIN 85 (SBB1/ NUP853), NUP160, NUP96 and the Dead-box RNA helicase 1 (DRH1) are required for the cell death phenotype of *bak1-3 bkk1-1* mutant, suggesting an important role for nucleocytoplasmic trafficking in BAK1- and BKK1-mediated cell death control (Du et al., 2016). Moreover, mutation in *eds1* or *pad4*, two key ETI mediators, extremely suppresses the cell death phenotype of *bak1-3 bkk1-1* (de Oliveira et al., 2016; Gao et al., 2017). And mutation in *adr1*, the helper NLR family member, could also inhibit cell death of *bak1-3 bkk1-1* (Wu et al., 2020). The last two cases suggest that the autoimmune responses in *bak1 bkk1* are caused by NLR activation.

The cell death in *bir1* could be partially suppressed by mutations in three classical ETI components such as NDR1, EDS1 and PAD4 (Gao et al., 2009). This suggests that there might be NLR protein similarly involved in the cell death control of *bir1*.

4.2 The downstream components in BAK1- or BIR-mediated cell death pathway

Mutation in *eds1*, *pad4* of known in ETI pathway and expression of *NahG* in *bir2* could partially suppress the cell death in *bir2-1* triggered by necrotrophic fungi *A. brassicicola* (Figure 3-5 B, C, D; Supplemental Figure 8-1). Therefore, we also tested multiple ETI downstream components and found that *eds1*, *pad4* and expression of NahG in *bak1-4 bir3-2* could partially suppress the cell death in *bak1-4 bir3-2* (Figure 3-3 B), indicating that TNLs could also be essential for this type of cell death. With crosses with *sag101-1*, we found that *sag101-1* is not required for cell death in *bak1 bir3* (Figure 3-3 C). This suggests that the ETI components such as *eds1*, *pad4* but not *sag101* are specifically functional in BAK1- or BIR-mediated cell death pathway. With crosses with the NRG1 family mutants, we found that mutation in *nrg1* could not suppress the cell death of *bak1-4 bir3-2*, but only has a slight contribution to the growth phenotype of *bak1-4 bir3-2* (Figure 3-4). In conclusion, the role of downstream components in cell death initiated in *bak1* mutants are summarized in table 2 (for *bir2-1*) and table 3 (for *bak1-4 bir3-2*) as follows.

Table 2: The roles of ETI pathway components and SA signaling for cell death in *bir2* triggered by *A. brassicicola*

	effects on cell death in *bir2-1**
eds1-12	yes
pad4-1	yes
NahG	yes
sag101-1	-
nrg1.1 nrg1.2	-

**A. brassicicola* Infection with 5-week-old plants of *bir2-1 eds1-12*, *bir2-1 pad4-1* and *bir2-1* NahG. It is unknown for role of *sag101-1* and *nrg1.1 nrg1.2* in *bir2-1.* Unknown results are marked with "-" sign.

Table 3: The roles of ETI pathway components, SA signaling and helper NLR NRG1 for cell death in *bak1 bir3* triggered by *A. brassicicola*

	effects on cell death in *bak1-4 bir3-2**	effects on growth in *bak1-4 bir3-2*
eds1-12	yes	yes
pad4-1	yes	yes
NahG	yes	yes
sag101-1	no	no
nrg1.1 nrg1.2	no	partial

**A. brassicicola* Infection with 5-week-old plants of *bak1-4 bir3-2 eds1-12*, *bak1-4 bir3-2 pad4-1*, *bak1-4 bir3-2* NahG, *bak1-4 bir3-2 sag101-1* and *bak1-4 bir3-2 nrg1.1 nrg1.2*.

Our data shows that the helper NLR family member NRG1 is partially required for *bak1 bir3* cell death (Figure 3-4; Table 3). Cell death in *bak1 bkk1* is significantly suppressed by the other Helper NLR ADR1 family (Saile et al., 2020; Wu et al., 2020). Whether the ADR1 helper family proteins are also required for cell death in *bak1 bir3* needs to be done in future. Therefore, *bak1 bir3*-mediated cell death might be linked to TNLs.

4.3 The NLR pair CSA1/CHS3 in *bak1 bir3*-mediated cell death

Basically, there are several methods of searching the molecular mechanism of *bak1 bir3*-mediated cell death, such as yeast-two-hybrid, IP-MS/MS and VIGS-based genetic screen and so on (Schulze, 2020; Yu et al., 2019). Although the distinctive features of *bak1 bir3* provide us with an excellent background in which to conduct genetic suppressor screens, our identified downstream components involved in *bak1 bir3*-mediated defense pathway by proteomic method differ from those involved in canonical *bak1 bkk1*-mediated signaling by genetic method (Saile et al., 2020; Wu et al., 2020).We performed IP-MS/MS analyses with BIR3-YFP transgenic *A. thaliana* plants (Schulze, 2020). The IP-MS/MS analyses of the BIR3 interactome revealed several candidates involved in cell death (Schulze, 2020). We chose CSA1 as a candidate of our further investigation with *bak1 bir3*-mediated cell death because CSA1 was the one highly enriched TNL protein

identified in IP- MS/MS of BIR3 (Schulze, 2020), that is consistent with the above finding that components of downstream TNLs play a key role in the cell death of *bak1 bir3*.

4.3.1 CSA1 and CHS3 are in the same complex with BAK1 and BIR3

As CSA1 was identified from IP- MS/MS of BIR3 interactome as a putative interaction partner of BIR3, Co-IP experiments to test the interaction of CSA1 with BIR3 or BAK1 was performed in *N. benthamiana*. All the test results from BIR1 to BIR3 shows that CSA1 can interact with all BIRs family proteins as well as with BAK1 in *N. benthamiana.* The pair of CSA1, CHS3, also shows interaction with all BIRs family members and with BAK1 in Co-IPs after transient expression in *N. benthamiana* (Schulze, 2020).

CSA1 and CHS3 are functioning as a pair in controlling autoimmune cell death response (Castel et al., 2019; Xu et al., 2015). In this study, our data shows that CSA1 can directly interact with BIR3 but not with BAK1 (Figure 3-13), which explains also why our previous interaction studies with BAK1 have not identified CSA1 as a guard of BAK1. Although the interaction between CSA1 and BIR3 is direct, CHS3 could not be able to display to directly interact with BIR3 or BAK1 (Figure 3-16; Figure 3-17). These data suggest that the NLR pair CSA1/CHS3 is present in the same complex BAK1 and BIR3 probably through direct interaction between BIR3 and CSA1. Consistently, the indirect interactions analyzed by Co-IPs reveal complex composition of more distantly related components. In this study, we also found that the subcellular localization of CSA1 and CHS3 is also different (Figure 3-9; Figure 3-10). Our study shows that CSA1 is mainly localized to the plasma membrane while CHS3 is localized to the plasma membrane but also to the soluble fraction and nuclear localization, which is in agreement with a weaker interaction with membrane-resident BIR3 or BAK1.

Since CSA1 is also required for cell death triggered by *bak1* single mutants (Schulze, 2020), we propose a model in which CSA1 directly guards BIR3 and BAK1 BIR3 complex integrity. Up to date, the activation mechanism of CSA1 by the absence of BAK1 and/or BIR3 is still unknown. *CSA1* is adjacent to and transcribed differently from *CHS3*, sharing a genomic region of approximately 3.9 kb upstream of their start codons. This genomic arrangement is reminiscent of the R gene pair *RPS4* and *RRS1*, whose protein heterodimerization is necessary for effector recognition (Williams et al., 2014). Therefore

CSA1 and CHS3 might also function as a pair. This is supported by the fact that both proteins can interact physically. A conformational change leading to NLR disinhibition by loss of the interaction interface with the receptor complex or by transphosphorylation, similar to the description of RRS1 release and RPS4 complex reorganization, seems possible. Coincidentally, we also can identify a phosphorylation site in CSA1 by MS/MS analysis (Figure 3-24). And previous studies observed that RPS4, the closest homolog of CSA1, complements phenotype of *csa1* mutant and confers resistance to *Pseudomonas syringae* (Faigon-Soverna et al., 2006). This strongly suggests that defense responses between *bak1 bir3*-mediated cell death pathway and cognate ETI pathways share similar core-signaling components.

4.3.2 The contribution of NLR pair CSA1/CHS3 in *bak1 bir3*-mediated cell death

In this study, we found that the mutation in *chs3* is less effective in suppression of *bak1*- and *bak1 bir3*-mediated cell death (Figure 3-14; Figure 3-15). However, previous studies the functions of CSA1 in *bak1* and *bak1 bir3*-mediated cell death have shown that the mutation in *csa1* is necessary for both cell death triggered in *bak1* and *bak1 bir3* (Schulze, 2020). *chs3-2D*, a missense mutation close to the LIM domain of CHS3, can trigger very strong dwarfism and constitutive resistance. The phenotype of *chs3-2D* is fully dependent on CSA1 (Xu et al., 2015). It suggests that *bak1 bir3*-mediated cell death is not totally same to the autoimmune cell death in *chs3-2D*.

In this study, we determined that *bak1 bir3*-mediated signaling relies differently on defense-related lipase-like proteins (EDS1/PAD4/SAG101) than signaling pathways downstream of *bak1-4 bkk1-1*. PAD4 and SAG101 are two known downstream components of TNL-mediated immunity. We found that mutation in *pad4* can partially suppress cell death in *bak1-4 bir3-2* mutant (Figure 3-3), while the suppression by *sag101-1* in *bak1-4 bir3-2* is marginal (Figure 3-3), suggesting that *bak1 bir3*-mediated signaling relies more strongly on PAD4. Moreover, mutation in *eds1* or *pad4*, two key ETI mediators, extremely suppresses the cell death phenotype of *bak1-3 bkk1-1* (Gao et al., 2017). In addition, the *sag101-1* mutation can completely suppress the autoimmunity of chs3-2D (Xu et al., 2015). This also indicates that *bak1 bir3*-mediated autoimmune signaling pathway is different from the autoimmune cell death pathway in *chs3-2D*. It is therefore possible that *bak1 bir3* preferentially utilizes EDS1 and PAD4 for its defense

activation, while SAG101 are marginally used. Genetic redundancy between PAD4 and SAG101 was previously proposed (Falk et al., 1999; Feys et al., 2005). However, previous studies have provided evidence that EDS1 forms distinct complexes with PAD4 and SAG101 with non-redundant signaling roles (Rietz et al., 2011). Our findings may support this model. Taken together, the role of NLR CSA1 in *bak1 bir3*-mediated cell death is different from the role in NLR pair CSA1/CHS3. Mutation in *csa1* can partially suppress cell death in *bak1-4 bir3-2* mutant (Figure 3-3), while the suppression by *chs3* in *bak1-4 bir3-2* is marginal, suggesting that *bak1 bir3*-mediated signaling relies more strongly on CSA1.

4.3.3 The complementation of CSA1 in *bak1 csa1* and *bak1 bir3 csa1* mutants

In this study, we performed the complementation experiment by expressing CSA1 in *bak1 bir3 csa1* mutants. We found that plants expressing CSA1 in *bak1 bir3 csa1* mutants grew much smaller than *bak1 bir3 csa1* triple mutants and were similar in size to the *bak1 bir3* double mutant (Figure 3-7 A). Complemented lines also exhibited an autoimmune cell death phenotype, as did the *bak1 bir3* double mutant (Figure 3-7 B). After *A. brassicicola* infection, complemented lines exhibited significantly more symptoms than *bak1 bir3 csa1* triple mutants, even to the same extent as *bak1 bir3* double mutant-infected leaves (Fig. 3-7C). This suggests that CSA1 (partially) restores both the growth and cell death phenotypes of *bak1 bir3 csa1* mutants and is therefore required and the causal gene for cell death initiation in *bak1 bir3* mutants.

In this study, we also performed the complementation experiment by expressing CSA1 in *bak1 csa1* mutants. We observed that complemented plants restored *bak1* single mutant growth phenotypes (Figure 3-8 A). And the infected leaves of complemented lines showed 13 days after *A. brassicicola* infection more cell death than *bak1 csa1* double mutant just as *bak1* single mutant infected leaves (Figure 3-8 B). This indicates that CSA1 also restores both the growth and cell death phenotypes of *bak1 csa1* mutants. Taken together, both complementation of CSA1 in *bak1 bir3 csa1* and *bak1 csa1* mutants can restore stronger cell death symptoms typically observed in *bak1* and *bak1 bir3* mutants (Figure 3-7; Figure 3-8). This suggests that CSA1 is confirmed to be the functional protein necessary for *bak1* and *bak1 bir3* initiated cell death.

4.3.4 The interaction between TIR^{CSA1} (or TIR^{CHS3}) and BIR3 (or BAK1)

Our data indicate that both TIR^{CSA1} and TIR^{CHS3} domains can interact with BIR3 in *N. benthamiana* (Figure 3-20; Figure 3-21). TIR^{CSA1} and TIR^{CHS3} contain amino acids residues 1-187 of CSA1 and 1-154 of CHS3, respectively. All the other domains including NB^{CSA1} (188-586aa), LRR^{CSA1} (587-1185aa), NB^{CHS3} (155-518aa), LRR^{CHS3} (519-835aa), LIM^{CHS3} (836-1386aa) and $DA1^{CHS3}$ (1387-1613aa) have no interaction with BIR3 at all (Figure 3-20; Figure 3-21; Supplemental Figure 8-4). The interaction between the truncated mutants of CSA1 or CHS3 and BAK1 have no significant difference with the negative control (Figure 3-20 B; Figure 3-21 B). These data suggest that the TIR domain of CSA1 might be the region of direct association between CSA1 and BIR3.

However, the full-length protein of CHS3 protein has no interaction with BIR3 by using split-luciferase assay in *N. benthamiana* and split-ubiquitin system in yeast (Figure 3-16 A B), while the TIR domain of CHS3 can interact with BIR3 (Figure 3-21 A; Figure 3-22 B) even though not as strong as the interaction between TIR^{CSA1} and BIR3 (Figure 3-22 A B). We cannot exclude the possibility that the non-interaction between full-length protein of CHS3 and BIR3 is due to lower protein accumulation of CHS3 in *N. benthamiana* and yeast. And another reason might be the low expression of some truncated mutants in *planta* that results in undetectable interaction (Supplemental Figure 8-4). Another possibility is that the NB^{CHS3} or LRR^{CHS3} (or LIM^{CHS3}, $DA1^{CHS3}$) domain in the full length of CHS3 affects the interaction between TIR^{CHS3} and BIR3, or other unknown components involve in the interaction between CHS3 and BIR3.

4.3.5 IP-MS/MS analysis of CSA1 and CHS3 in *A. thaliana*

The two independent IP-MS/MS analyses of CSA1 and CHS3 in *A. thaliana* revealed the same phosphorylation site of CSA1 (Ser^{1120}) (Figure 3-24; Supplemental Figure 8-7). Meanwhile, we discovered some more or less interacting proteins from volcano plots of the second LC-MS/MS analyses (Figure 3-25 A B). Compared with control, we find that there are three proteins, At3g07010, NBR1(At4g24690) and At5g17510 which are enriched obviously by both CSA1 and CHS3 in CSA1 or CHS3 transgenic plants. And there are only two proteins, called RPL10AA and CLPP3 are downregulated by CHS3 in CHS3 transgenic plants. NBR1 is a selective autophagy substrate, underlying the autophagy pathway is probably involved in CHS3/CSA1-regulated signaling. In addition,

RPL10 a ribosomal protein, and CLPP3 a protease, seemingly protein homeostasis also plays key roles in the CSA1-mediated cell death pathway.

4.4 Proposed working model for *bak1 bir3*-mediated defense pathway

Previous data revealed that *eds1*, *pad4* and expression of *NahG* in *bak1 bir3* could partially suppress the cell death in *bak1 bir3* while *sag101* is not required for cell death in *bak1 bir3*. And mutation in *nrg1* could not suppress the cell death in *bak1 bir3*, but only has a slight function in the growth phenotype of *bak1 bir3.* Our data shows that *bak1 bir3*-mediated signaling relies more strongly on CSA1 than CHS3. Based on our current data, we propose a model of CSA1 function in the *bak1 bir3*-mediated pathway (Figure 4-1). BIR3 constitutively interacts with BAK1 and ligand binding receptors PRRs. In the absence of ligands, BIR3 can prevent unwanted interactions of BAK1 and ligand binding receptors to block downstream signaling activation. After ligand activation, for example flg22, BIR3 is released from the BIR3/BAK1 complex, then BAK1 associates with ligand binding receptors successfully. Once BIR3/BAK1 complex is breakdown, the intracellular receptor CSA1/CHS3 will guard the integrity of BIR3/BAK1 complex. CSA1 and its partner CHS3 are in complex with BAK1 and BIR3, and CSA1 directly interacts with BIR3. In the absence of BAK1 and BIR3, CSA1/CHS3 are activated to initiate the downstream ETI signaling pathway through the components EDS1/PAD4/ADR1.

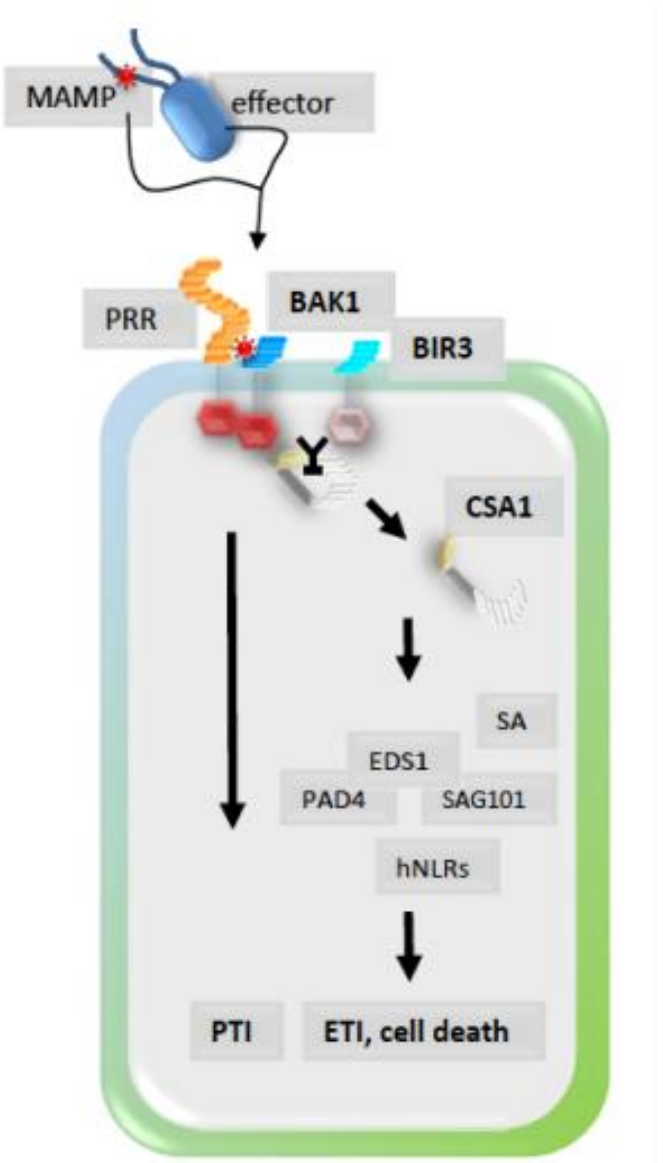

Figure 4-1: Proposed working model of CSA1 function in the *bak1 bir3*-mediated defense pathway (Schulze et al., 2022)

BIR3 functions by constitutively interacting with BAK1 and ligand binding receptors PRRs. CSA1-mediated cell death can be negatively regulated by both BAK1 and BIR3. The intergrity of BAK1 and BIR3 can be guarded by CSA1 through directly interact with BIR3 and indirectly with BAK1. The ETI pathway components such as EDS1, PAD4 and SA are partially required for cell death induced in *bak1-4 bir3-2* mutants.

5. Conclusions

As a co-receptor of leucine-rich repeat pattern recognition receptors (PRRs), *A. thaliana* BAK1/SERK3 can mediate pattern-triggered immunity (PTI). The absence in BAK1 or BAK1-interacting receptor-like kinases (BIRs) leads to spontaneous cell death formation. A TIR-NBS-LRR protein CONSTITUTIVE SHADE-AVOIDANCE 1 (CSA1) was identified by mass spectrometry in the interactome of BIR3. In this study, we found that CSA1 directly interacts with BIR3, and indirectly with BAK1. The double mutant *bak1 bir3* shows cell death symptoms and strong dwarfism that are dependent on ETI pathway components EDS1 and PAD4 and also salicylic acid, but not SAG101. We also find that NRG1 has a slight contribution to the growth phenotype of *bak1 bir3*. CSA1 mediates cell death in *bak1-4* and *bak1-4 bir3-2* mutants via effector-triggered immunity (ETI) pathways components. Thus, we propose that CSA1 guards homeostasis of BIR3 BAK1 proteins and initiates autoimmune cell death that is observed when BAK1 BIR complexes are impaired. The absence of intact BAK1 and BIR3 activates CSA1-triggering ETI cell death. This suggests that downstream of BAK1 defense responses are activated by both PTI and ETI pathways for efficient plant immunity.

6. Zusammenfassung

Als Co-Rezeptor von Mustererkennungsrezeptoren mit Leucin-reichen Wiederholungen (PRRs) kann BAK1/SERK3 in *A. thaliana* die Muster-ausgelöste Immunität (PTI) vermitteln. Das Fehlen von BAK1 oder BAK1-interagierenden rezeptorähnlichen Kinasen (BIRs) führt zur spontanen Zelltodbildung. Ein TIR-NBS-LRR-Protein CONSTITUTIVE SHADE-AVOIDANCE 1 (CSA1) wurde durch Massenspektrometrie im Interaktom von BIR3 identifiziert. In dieser Studie haben wir festgestellt, dass CSA1 direkt mit BIR3 und indirekt mit BAK1 interagiert. Die Doppelmutante *bak1 bir3* zeigt Zelltodsymptome und starken Zwergwuchs, die von den ETI-Signalwegkomponenten EDS1 und PAD4 sowie von Salicylsäure, nicht aber von SAG101 abhängig sind. Wir stellen außerdem fest, dass NRG1 einen geringen Beitrag zum Wachstumsphänotyp von *bak1 bir3* leistet. CSA1 vermittelt den Zelltod in *bak1-4*- und *bak1-4 bir3-2*-Mutanten über Komponenten des Effektor-getriggerten Immunitätsweges (ETI). Wir vermuten daher, dass CSA1 die Homöostase der BIR3-BAK1-Proteine überwacht und den autoimmunen Zelltod auslöst, der beobachtet wird, wenn die BAK1-BIR-Komplexe gestört sind. Das Fehlen von intaktem BAK1 und BIR3 aktiviert CSA1 und löst den ETI-Zelltod aus. Dies deutet darauf hin, dass BAK1-Proteine durch PTI- und ETI-Wege für eine effiziente Pflanzenimmunität aktiviert werden.

7. References

Aan den Toorn, M., Albrecht, C., and de Vries, S. (2015). On the Origin of SERKs: Bioinformatics Analysis of the Somatic Embryogenesis Receptor Kinases. Mol Plant *8*, 762-782.

Adachi, H., Contreras, M.P., Harant, A., Wu, C.H., Derevnina, L., Sakai, T., Duggan, C., Moratto, E., Bozkurt, T.O., Maqbool, A.*, et al.* (2019a). An N-terminal motif in NLR immune receptors is functionally conserved across distantly related plant species. Elife *8*.

Adachi, H., Derevnina, L., and Kamoun, S. (2019b). NLR singletons, pairs, and networks: evolution, assembly, and regulation of the intracellular immunoreceptor circuitry of plants. Curr Opin Plant Biol *50*, 121-131.

Ade, J., DeYoung, B.J., Golstein, C., and Innes, R.W. (2007). Indirect activation of a plant nucleotide binding site-leucine-rich repeat protein by a bacterial protease. Proc Natl Acad Sci U S A *104*, 2531-2536.

Akira, S., Uematsu, S., and Takeuchi, O. (2006). Pathogen recognition and innate immunity. Cell *124*, 783-801.

Albert, I., Bohm, H., Albert, M., Feiler, C.E., Imkampe, J., Wallmeroth, N., Brancato, C., Raaymakers, T.M., Oome, S., Zhang, H.*, et al.* (2015). An RLP23-SOBIR1-BAK1 complex mediates NLP-triggered immunity. Nat Plants *1*, 15140.

Albrecht, C., Boutrot, F., Segonzac, C., Schwessinger, B., Gimenez-Ibanez, S., Chinchilla, D., Rathjen, J.P., de Vries, S.C., and Zipfel, C. (2012). Brassinosteroids inhibit pathogen-associated molecular pattern-triggered immune signaling independent of the receptor kinase BAK1. Proc Natl Acad Sci U S A *109*, 303-308.

Albrecht, C., Russinova, E., Hecht, V., Baaijens, E., and de Vries, S. (2005). The Arabidopsis thaliana SOMATIC EMBRYOGENESIS RECEPTOR-LIKE KINASES1 and 2 control male sporogenesis. Plant Cell *17*, 3337-3349.

Alonso, J.M., Stepanova, A.N., Leisse, T.J., Kim, C.J., Chen, H., Shinn, P., Stevenson, D.K., Zimmerman, J., Barajas, P., Cheuk, R.*, et al.* (2003). Genome-wide insertional mutagenesis of Arabidopsis thaliana. Science *301*, 653-657.

Asseck, L.Y., and Grefen, C. (2018). Detecting Interactions of Membrane Proteins: The Split-Ubiquitin System. Methods Mol Biol *1794*, 49-60.

Axtell, M.J., and Staskawicz, B.J. (2003). Initiation of RPS2-specified disease resistance in Arabidopsis is coupled to the AvrRpt2-directed elimination of RIN4. Cell *112*, 369-377.

Bai, S., Liu, J., Chang, C., Zhang, L., Maekawa, T., Wang, Q., Xiao, W., Liu, Y., Chai, J., Takken, F.L.*, et al.* (2012). Structure-function analysis of barley NLR immune receptor MLA10

reveals its cell compartment specific activity in cell death and disease resistance. PLoS Pathog *8*, e1002752.

Balague, C., Lin, B., Alcon, C., Flottes, G., Malmstrom, S., Kohler, C., Neuhaus, G., Pelletier, G., Gaymard, F., and Roby, D. (2003). HLM1, an essential signaling component in the hypersensitive response, is a member of the cyclic nucleotide-gated channel ion channel family. Plant Cell *15*, 365-379.

Balint-Kurti, P. (2019). The plant hypersensitive response: concepts, control and consequences. Mol Plant Pathol *20*, 1163-1178.

Baltrus, D.A., Nishimura, M.T., Romanchuk, A., Chang, J.H., Mukhtar, M.S., Cherkis, K., Roach, J., Grant, S.R., Jones, C.D., and Dangl, J.L. (2011). Dynamic evolution of pathogenicity revealed by sequencing and comparative genomics of 19 Pseudomonas syringae isolates. PLoS Pathog *7*, e1002132.

Bayless, A.M., and Nishimura, M.T. (2020). Enzymatic Functions for Toll/Interleukin-1 Receptor Domain Proteins in the Plant Immune System. Front Genet *11*, 539.

Belkhadir, Y., Jaillais, Y., Epple, P., Balsemao-Pires, E., Dangl, J.L., and Chory, J. (2012). Brassinosteroids modulate the efficiency of plant immune responses to microbe-associated molecular patterns. Proc Natl Acad Sci U S A *109*, 297-302.

Berlemont, R., and Martiny, A.C. (2013). Phylogenetic distribution of potential cellulases in bacteria. Appl Environ Microbiol *79*, 1545-1554.

Bernoux, M., Ve, T., Williams, S., Warren, C., Hatters, D., Valkov, E., Zhang, X., Ellis, J.G., Kobe, B., and Dodds, P.N. (2011). Structural and functional analysis of a plant resistance protein TIR domain reveals interfaces for self-association, signaling, and autoregulation. Cell Host Microbe *9*, 200-211.

Bhandari, D.D., Lapin, D., Kracher, B., von Born, P., Bautor, J., Niefind, K., and Parker, J.E. (2019). An EDS1 heterodimer signalling surface enforces timely reprogramming of immunity genes in Arabidopsis. Nat Commun *10*, 772.

Bi, G., Su, M., Li, N., Liang, Y., Dang, S., Xu, J., Hu, M., Wang, J., Zou, M., Deng, Y.*, et al.* (2021). The ZAR1 resistosome is a calcium-permeable channel triggering plant immune signaling. Cell *184*, 3528-3541 e3512.

Blaum, B.S., Mazzotta, S., Noldeke, E.R., Halter, T., Madlung, J., Kemmerling, B., and Stehle, T. (2014). Structure of the pseudokinase domain of BIR2, a regulator of BAK1-mediated immune signaling in Arabidopsis. J Struct Biol *186*, 112-121.

Block, A., and Alfano, J.R. (2011). Plant targets for Pseudomonas syringae type III effectors: virulence targets or guarded decoys? Curr Opin Microbiol *14*, 39-46.

Bohm, H., Albert, I., Fan, L., Reinhard, A., and Nurnberger, T. (2014a). Immune receptor complexes at the plant cell surface. Curr Opin Plant Biol *20*, 47-54.

Bohm, H., Albert, I., Oome, S., Raaymakers, T.M., Van den Ackerveken, G., and Nurnberger, T. (2014b). A conserved peptide pattern from a widespread microbial virulence factor triggers pattern-induced immunity in Arabidopsis. PLoS Pathog *10*, e1004491.

Boller, T., and He, S.Y. (2009). Innate immunity in plants: an arms race between pattern recognition receptors in plants and effectors in microbial pathogens. Science *324*, 742-744.

Bos, J.I., Prince, D., Pitino, M., Maffei, M.E., Win, J., and Hogenhout, S.A. (2010). A functional genomics approach identifies candidate effectors from the aphid species Myzus persicae (green peach aphid). PLoS Genet *6*, e1001216.

Bourras, S., McNally, K.E., Muller, M.C., Wicker, T., and Keller, B. (2016). Avirulence Genes in Cereal Powdery Mildews: The Gene-for-Gene Hypothesis 2.0. Front Plant Sci *7*, 241.

Boutrot, F., and Zipfel, C. (2017). Function, Discovery, and Exploitation of Plant Pattern Recognition Receptors for Broad-Spectrum Disease Resistance. Annu Rev Phytopathol *55*, 257-286.

Bucherl, C.A., van Esse, G.W., Kruis, A., Luchtenberg, J., Westphal, A.H., Aker, J., van Hoek, A., Albrecht, C., Borst, J.W., and de Vries, S.C. (2013). Visualization of BRI1 and BAK1(SERK3) membrane receptor heterooligomers during brassinosteroid signaling. Plant Physiol *162*, 1911-1925.

Burdiak, P., Rusaczonek, A., Witon, D., Glow, D., and Karpinski, S. (2015). Cysteine-rich receptor-like kinase CRK5 as a regulator of growth, development, and ultraviolet radiation responses in Arabidopsis thaliana. J Exp Bot *66*, 3325-3337.

Cai, Q., Liang, C., Wang, S., Hou, Y., Gao, L., Liu, L., He, W., Ma, W., Mo, B., and Chen, X. (2018). The disease resistance protein SNC1 represses the biogenesis of microRNAs and phased siRNAs. Nat Commun *9*, 5080.

Casey, L.W., Lavrencic, P., Bentham, A.R., Cesari, S., Ericsson, D.J., Croll, T., Turk, D., Anderson, P.A., Mark, A.E., Dodds, P.N.*, et al.* (2016). The CC domain structure from the wheat stem rust resistance protein Sr33 challenges paradigms for dimerization in plant NLR proteins. Proc Natl Acad Sci U S A *113*, 12856-12861.

Castel, B., Ngou, P.M., Cevik, V., Redkar, A., Kim, D.S., Yang, Y., Ding, P., and Jones, J.D.G. (2019). Diverse NLR immune receptors activate defence via the RPW8-NLR NRG1. New Phytol *222*, 966-980.

Century, K.S., Shapiro, A.D., Repetti, P.P., Dahlbeck, D., Holub, E., and Staskawicz, B.J. (1997). NDR1, a pathogen-induced component required for Arabidopsis disease resistance. Science *278*, 1963-1965.

Cesari, S., Kanzaki, H., Fujiwara, T., Bernoux, M., Chalvon, V., Kawano, Y., Shimamoto, K., Dodds, P., Terauchi, R., and Kroj, T. (2014). The NB-LRR proteins RGA4 and RGA5 interact functionally and physically to confer disease resistance. EMBO J *33*, 1941-1959.

Chinchilla, D., Zipfel, C., Robatzek, S., Kemmerling, B., Nurnberger, T., Jones, J.D., Felix, G., and Boller, T. (2007). A flagellin-induced complex of the receptor FLS2 and BAK1 initiates plant defence. Nature *448*, 497-500.

Chisholm, S.T., Coaker, G., Day, B., and Staskawicz, B.J. (2006). Host-microbe interactions: shaping the evolution of the plant immune response. Cell *124*, 803-814.

Chung, E.H., da Cunha, L., Wu, A.J., Gao, Z., Cherkis, K., Afzal, A.J., Mackey, D., and Dangl, J.L. (2011). Specific threonine phosphorylation of a host target by two unrelated type III effectors activates a host innate immune receptor in plants. Cell Host Microbe *9*, 125-136.

Clay, N.K., and Nelson, T. (2002). VH1, a provascular cell-specific receptor kinase that influences leaf cell patterns in Arabidopsis. Plant Cell *14*, 2707-2722.

Clough, S.J., and Bent, A.F. (1998). Floral dip: a simplified method for Agrobacterium-mediated transformation of Arabidopsis thaliana. Plant J *16*, 735-743.

Clough, S.J., Fengler, K.A., Yu, I.C., Lippok, B., Smith, R.K., Jr., and Bent, A.F. (2000). The Arabidopsis dnd1 "defense, no death" gene encodes a mutated cyclic nucleotide-gated ion channel. Proc Natl Acad Sci U S A *97*, 9323-9328.

Colcombet, J., Boisson-Dernier, A., Ros-Palau, R., Vera, C.E., and Schroeder, J.I. (2005). Arabidopsis SOMATIC EMBRYOGENESIS RECEPTOR KINASES1 and 2 are essential for tapetum development and microspore maturation. Plant Cell *17*, 3350-3361.

Collier, S.M., Hamel, L.P., and Moffett, P. (2011). Cell death mediated by the N-terminal domains of a unique and highly conserved class of NB-LRR protein. Mol Plant Microbe Interact *24*, 918-931.

Couto, D., and Zipfel, C. (2016). Regulation of pattern recognition receptor signalling in plants. Nat Rev Immunol *16*, 537-552.

Cui, H., Gobbato, E., Kracher, B., Qiu, J., Bautor, J., and Parker, J.E. (2017). A core function of EDS1 with PAD4 is to protect the salicylic acid defense sector in Arabidopsis immunity. New Phytol *213*, 1802-1817.

Cui, H., Tsuda, K., and Parker, J.E. (2015). Effector-triggered immunity: from pathogen perception to robust defense. Annu Rev Plant Biol *66*, 487-511.

Dangl, J.L., Horvath, D.M., and Staskawicz, B.J. (2013). Pivoting the plant immune system from dissection to deployment. Science *341*, 746-751.

Dangl, J.L., and Jones, J.D. (2001). Plant pathogens and integrated defence responses to infection. Nature *411*, 826-833.

de Oliveira, M.V., Xu, G., Li, B., de Souza Vespoli, L., Meng, X., Chen, X., Yu, X., de Souza, S.A., Intorne, A.C., de, A.M.A.M.*, et al.* (2016). Specific control of Arabidopsis BAK1/SERK4-regulated cell death by protein glycosylation. Nat Plants *2*, 15218.

Deslandes, L., Olivier, J., Peeters, N., Feng, D.X., Khounlotham, M., Boucher, C., Somssich, I., Genin, S., and Marco, Y. (2003). Physical interaction between RRS1-R, a protein conferring resistance to bacterial wilt, and PopP2, a type III effector targeted to the plant nucleus. Proc Natl Acad Sci U S A *100*, 8024-8029.

Dodds, P.N., Lawrence, G.J., Catanzariti, A.M., Teh, T., Wang, C.I., Ayliffe, M.A., Kobe, B., and Ellis, J.G. (2006). Direct protein interaction underlies gene-for-gene specificity and coevolution of the flax resistance genes and flax rust avirulence genes. Proc Natl Acad Sci U S A *103*, 8888-8893.

Domazakis, E., Wouters, D., Visser, R.G.F., Kamoun, S., Joosten, M., and Vleeshouwers, V. (2018). The ELR-SOBIR1 Complex Functions as a Two-Component Receptor-Like Kinase to Mount Defense Against Phytophthora infestans. Mol Plant Microbe Interact *31*, 795-802.

Dominguez-Ferreras, A., Kiss-Papp, M., Jehle, A.K., Felix, G., and Chinchilla, D. (2015). An Overdose of the Arabidopsis Coreceptor BRASSINOSTEROID INSENSITIVE1-ASSOCIATED RECEPTOR KINASE1 or Its Ectodomain Causes Autoimmunity in a SUPPRESSOR OF BIR1-1-Dependent Manner. Plant Physiol *168*, 1106-1121.

Du, J., Gao, Y., Zhan, Y., Zhang, S., Wu, Y., Xiao, Y., Zou, B., He, K., Gou, X., Li, G.*, et al.* (2016). Nucleocytoplasmic trafficking is essential for BAK1- and BKK1-mediated cell-death control. Plant J *85*, 520-531.

Du, L., Ali, G.S., Simons, K.A., Hou, J., Yang, T., Reddy, A.S., and Poovaiah, B.W. (2009). $Ca(^{2+})$/calmodulin regulates salicylic-acid-mediated plant immunity. Nature *457*, 1154-1158.

El Kasmi, F., Chung, E.H., Anderson, R.G., Li, J., Wan, L., Eitas, T.K., Gao, Z., and Dangl, J.L. (2017). Signaling from the plasma-membrane localized plant immune receptor RPM1 requires self-association of the full-length protein. Proc Natl Acad Sci U S A *114*, E7385-E7394.

Engelsdorf, T., Gigli-Bisceglia, N., Veerabagu, M., McKenna, J.F., Vaahtera, L., Augstein, F., Van der Does, D., Zipfel, C., and Hamann, T. (2018). The plant cell wall integrity maintenance and immune signaling systems cooperate to control stress responses in Arabidopsis thaliana. Sci Signal *11*.

Essuman, K., Summers, D.W., Sasaki, Y., Mao, X., DiAntonio, A., and Milbrandt, J. (2017). The SARM1 Toll/Interleukin-1 Receptor Domain Possesses Intrinsic NAD(+) Cleavage Activity that Promotes Pathological Axonal Degeneration. Neuron *93*, 1334-1343 e1335.

Essuman, K., Summers, D.W., Sasaki, Y., Mao, X., Yim, A.K.Y., DiAntonio, A., and Milbrandt, J. (2018). TIR Domain Proteins Are an Ancient Family of NAD(+)-Consuming Enzymes. Curr Biol *28*, 421-430 e424.

Faigon-Soverna, A., Harmon, F.G., Storani, L., Karayekov, E., Staneloni, R.J., Gassmann, W., Mas, P., Casal, J.J., Kay, S.A., and Yanovsky, M.J. (2006). A constitutive shade-avoidance mutant implicates TIR-NBS-LRR proteins in Arabidopsis photomorphogenic development. Plant Cell *18*, 2919-2928.

Falk, A., Feys, B.J., Frost, L.N., Jones, J.D., Daniels, M.J., and Parker, J.E. (1999). EDS1, an essential component of R gene-mediated disease resistance in Arabidopsis has homology to eukaryotic lipases. Proc Natl Acad Sci U S A *96*, 3292-3297.

Felix, G., Duran, J.D., Volko, S., and Boller, T. (1999). Plants have a sensitive perception system for the most conserved domain of bacterial flagellin. Plant J *18*, 265-276.

Feng, F., Yang, F., Rong, W., Wu, X., Zhang, J., Chen, S., He, C., and Zhou, J.M. (2012). A Xanthomonas uridine 5'-monophosphate transferase inhibits plant immune kinases. Nature *485*, 114-118.

Fenyk, S., Townsend, P.D., Dixon, C.H., Spies, G.B., de San Eustaquio Campillo, A., Slootweg, E.J., Westerhof, L.B., Gawehns, F.K., Knight, M.R., Sharples, G.J.*, et al.* (2015). The Potato Nucleotide-binding Leucine-rich Repeat (NLR) Immune Receptor Rx1 Is a Pathogen-dependent DNA-deforming Protein. J Biol Chem *290*, 24945-24960.

Feys, B.J., Wiermer, M., Bhat, R.A., Moisan, L.J., Medina-Escobar, N., Neu, C., Cabral, A., and Parker, J.E. (2005). Arabidopsis SENESCENCE-ASSOCIATED GENE101 stabilizes and signals within an ENHANCED DISEASE SUSCEPTIBILITY1 complex in plant innate immunity. Plant Cell *17*, 2601-2613.

Frescatada-Rosa, M., Robatzek, S., and Kuhn, H. (2015). Should I stay or should I go? Traffic control for plant pattern recognition receptors. Curr Opin Plant Biol *28*, 23-29.

Froger, A., and Hall, J.E. (2007). Transformation of plasmid DNA into E. coli using the heat shock method. J Vis Exp, 253.

Gao, M., Wang, X., Wang, D., Xu, F., Ding, X., Zhang, Z., Bi, D., Cheng, Y.T., Chen, S., Li, X., *et al.* (2009). Regulation of cell death and innate immunity by two receptor-like kinases in Arabidopsis. Cell Host Microbe *6*, 34-44.

Gao, Y., Wu, Y., Du, J., Zhan, Y., Sun, D., Zhao, J., Zhang, S., Li, J., and He, K. (2017). Both Light-Induced SA Accumulation and ETI Mediators Contribute to the Cell Death Regulated by BAK1 and BKK1. Front Plant Sci *8*, 622.

Glazebrook, J., Rogers, E.E., and Ausubel, F.M. (1996). Isolation of Arabidopsis mutants with enhanced disease susceptibility by direct screening. Genetics *143*, 973-982.

Gomez-Gomez, L., and Boller, T. (2000). FLS2: an LRR receptor-like kinase involved in the perception of the bacterial elicitor flagellin in Arabidopsis. Mol Cell *5*, 1003-1011.

Gou, X., He, K., Yang, H., Yuan, T., Lin, H., Clouse, S.D., and Li, J. (2010). Genome-wide cloning and sequence analysis of leucine-rich repeat receptor-like protein kinase genes in Arabidopsis thaliana. BMC Genomics *11*, 19.

Gust, A.A., and Felix, G. (2014). Receptor like proteins associate with SOBIR1-type of adaptors to form bimolecular receptor kinases. Curr Opin Plant Biol *21*, 104-111.

Guzman-Benito, I., Donaire, L., Amorim-Silva, V., Vallarino, J.G., Esteban, A., Wierzbicki, A.T., Ruiz-Ferrer, V., and Llave, C. (2019). The immune repressor BIR1 contributes to antiviral defense and undergoes transcriptional and post-transcriptional regulation during viral infections. New Phytol *224*, 421-438.

Halter, T., Imkampe, J., Mazzotta, S., Wierzba, M., Postel, S., Bucherl, C., Kiefer, C., Stahl, M., Chinchilla, D., Wang, X*., et al.* (2014). The leucine-rich repeat receptor kinase BIR2 is a negative regulator of BAK1 in plant immunity. Curr Biol *24*, 134-143.

Hao, W., Collier, S.M., Moffett, P., and Chai, J. (2013). Structural basis for the interaction between the potato virus X resistance protein (Rx) and its cofactor Ran GTPase-activating protein 2 (RanGAP2). J Biol Chem *288*, 35868-35876.

He, K., Gou, X., Yuan, T., Lin, H., Asami, T., Yoshida, S., Russell, S.D., and Li, J. (2007). BAK1 and BKK1 regulate brassinosteroid-dependent growth and brassinosteroid-independent cell-death pathways. Curr Biol *17*, 1109-1115.

Hecht, V., Vielle-Calzada, J.P., Hartog, M.V., Schmidt, E.D., Boutilier, K., Grossniklaus, U., and de Vries, S.C. (2001). The Arabidopsis SOMATIC EMBRYOGENESIS RECEPTOR KINASE 1 gene is expressed in developing ovules and embryos and enhances embryogenic competence in culture. Plant Physiol *127*, 803-816.

Heese, A., Hann, D.R., Gimenez-Ibanez, S., Jones, A.M., He, K., Li, J., Schroeder, J.I., Peck, S.C., and Rathjen, J.P. (2007). The receptor-like kinase SERK3/BAK1 is a central regulator of innate immunity in plants. Proc Natl Acad Sci U S A *104*, 12217-12222.

Heidrich, K., Wirthmueller, L., Tasset, C., Pouzet, C., Deslandes, L., and Parker, J.E. (2011). Arabidopsis EDS1 connects pathogen effector recognition to cell compartment-specific immune responses. Science *334*, 1401-1404.

Hong, S.W., Jon, J.H., Kwak, J.M., and Nam, H.G. (1997). Identification of a receptor-like protein kinase gene rapidly induced by abscisic acid, dehydration, high salt, and cold treatments in Arabidopsis thaliana. Plant Physiol *113*, 1203-1212.

Horsefield, S., Burdett, H., Zhang, X., Manik, M.K., Shi, Y., Chen, J., Qi, T., Gilley, J., Lai, J.S., Rank, M.X.*, et al.* (2019). NAD(+) cleavage activity by animal and plant TIR domains in cell death pathways. Science *365*, 793-799.

Hu, L., Wu, Y., Wu, D., Rao, W., Guo, J., Ma, Y., Wang, Z., Shangguan, X., Wang, H., Xu, C., *et al.* (2017). The Coiled-Coil and Nucleotide Binding Domains of BROWN PLANTHOPPER RESISTANCE14 Function in Signaling and Resistance against Planthopper in Rice. Plant Cell *29*, 3157-3185.

Huh, S.U., Cevik, V., Ding, P., Duxbury, Z., Ma, Y., Tomlinson, L., Sarris, P.F., and Jones, J.D.G. (2017). Protein-protein interactions in the RPS4/RRS1 immune receptor complex. PLoS Pathog *13*, e1006376.

Hunt, L., Lerner, F., and Ziegler, M. (2004). NAD - new roles in signalling and gene regulation in plants. New Phytol *163*, 31-44.

Imkampe, J., Halter, T., Huang, S., Schulze, S., Mazzotta, S., Schmidt, N., Manstretta, R., Postel, S., Wierzba, M., Yang, Y.*, et al.* (2017). The Arabidopsis Leucine-Rich Repeat Receptor Kinase BIR3 Negatively Regulates BAK1 Receptor Complex Formation and Stabilizes BAK1. Plant Cell *29*, 2285-2303.

Jia, M., Shen, X., Tang, Y., Shi, X., and Gu, Y. (2021). A karyopherin constrains nuclear activity of the NLR protein SNC1 and is essential to prevent autoimmunity in Arabidopsis. Mol Plant *14*, 1733-1744.

Jia, Y., McAdams, S.A., Bryan, G.T., Hershey, H.P., and Valent, B. (2000). Direct interaction of resistance gene and avirulence gene products confers rice blast resistance. EMBO J *19*, 4004-4014.

Jinn, T.L., Stone, J.M., and Walker, J.C. (2000). HAESA, an Arabidopsis leucine-rich repeat receptor kinase, controls floral organ abscission. Genes Dev *14*, 108-117.

Jones, J.D., and Dangl, J.L. (2006). The plant immune system. Nature *444*, 323-329.

Jubic, L.M., Saile, S., Furzer, O.J., El Kasmi, F., and Dangl, J.L. (2019). Help wanted: helper NLRs and plant immune responses. Curr Opin Plant Biol *50*, 82-94.

Jurkowski, G.I., Smith, R.K., Jr., Yu, I.C., Ham, J.H., Sharma, S.B., Klessig, D.F., Fengler, K.A., and Bent, A.F. (2004). Arabidopsis DND2, a second cyclic nucleotide-gated ion channel gene for which mutation causes the "defense, no death" phenotype. Mol Plant Microbe Interact *17*, 511-520.

Kadota, Y., Liebrand, T.W.H., Goto, Y., Sklenar, J., Derbyshire, P., Menke, F.L.H., Torres, M.A., Molina, A., Zipfel, C., Coaker, G.*, et al.* (2019). Quantitative phosphoproteomic analysis reveals common regulatory mechanisms between effector- and PAMP-triggered immunity in plants. New Phytol *221*, 2160-2175.

Kemmerling, B., Schwedt, A., Rodriguez, P., Mazzotta, S., Frank, M., Qamar, S.A., Mengiste, T., Betsuyaku, S., Parker, J.E., Mussig, C.*, et al.* (2007). The BRI1-associated kinase 1, BAK1, has a brassinolide-independent role in plant cell-death control. Curr Biol *17*, 1116-1122.

Klauser, D., Desurmont, G.A., Glauser, G., Vallat, A., Flury, P., Boller, T., Turlings, T.C., and Bartels, S. (2015). The Arabidopsis Pep-PEPR system is induced by herbivore feeding and contributes to JA-mediated plant defence against herbivory. J Exp Bot *66*, 5327-5336.

Knepper, C., Savory, E.A., and Day, B. (2011). The role of NDR1 in pathogen perception and plant defense signaling. Plant Signal Behav *6*, 1114-1116.

Knip, M., Richard, M.M.S., Oskam, L., van Engelen, H.T.D., Aalders, T., and Takken, F.L.W. (2019). Activation of immune receptor Rx1 triggers distinct immune responses culminating in cell death after 4 hours. Mol Plant Pathol *20*, 575-588.

Koeck, M., Hardham, A.R., and Dodds, P.N. (2011). The role of effectors of biotrophic and hemibiotrophic fungi in infection. Cell Microbiol *13*, 1849-1857.

Kolodziej, M.C., Singla, J., Sanchez-Martin, J., Zbinden, H., Simkova, H., Karafiatova, M., Dolezel, J., Gronnier, J., Poretti, M., Glauser, G.*, et al.* (2021). A membrane-bound ankyrin repeat protein confers race-specific leaf rust disease resistance in wheat. Nat Commun *12*, 956.

Kong, Q., Qu, N., Gao, M., Zhang, Z., Ding, X., Yang, F., Li, Y., Dong, O.X., Chen, S., Li, X., *et al.* (2012). The MEKK1-MKK1/MKK2-MPK4 kinase cascade negatively regulates immunity mediated by a mitogen-activated protein kinase kinase kinase in Arabidopsis. Plant Cell *24*, 2225-2236.

Krol, E., Mentzel, T., Chinchilla, D., Boller, T., Felix, G., Kemmerling, B., Postel, S., Arents, M., Jeworutzki, E., Al-Rasheid, K.A.*, et al.* (2010). Perception of the Arabidopsis danger signal peptide 1 involves the pattern recognition receptor AtPEPR1 and its close homologue AtPEPR2. J Biol Chem *285*, 13471-13479.

Kunze, G., Zipfel, C., Robatzek, S., Niehaus, K., Boller, T., and Felix, G. (2004). The N terminus of bacterial elongation factor Tu elicits innate immunity in Arabidopsis plants. Plant Cell *16*, 3496-3507.

Ladwig, F., Dahlke, R.I., Stuhrwohldt, N., Hartmann, J., Harter, K., and Sauter, M. (2015). Phytosulfokine Regulates Growth in Arabidopsis through a Response Module at the Plasma Membrane That Includes CYCLIC NUCLEOTIDE-GATED CHANNEL17, H+-ATPase, and BAK1. Plant Cell *27*, 1718-1729.

Lapin, D., Bhandari, D.D., and Parker, J.E. (2020). Origins and Immunity Networking Functions of EDS1 Family Proteins. Annu Rev Phytopathol *58*, 253-276.

Lapin, D., Kovacova, V., Sun, X., Dongus, J.A., Bhandari, D., von Born, P., Bautor, J., Guarneri, N., Rzemieniewski, J., Stuttmann, J.*, et al.* (2019). A Coevolved EDS1-SAG101-NRG1 Module Mediates Cell Death Signaling by TIR-Domain Immune Receptors. Plant Cell *31*, 2430-2455.

Lawton, K., Weymann, K., Friedrich, L., Vernooij, B., Uknes, S., and Ryals, J. (1995). Systemic acquired resistance in Arabidopsis requires salicylic acid but not ethylene. Mol Plant Microbe Interact *8*, 863-870.

Le Roux, C., Huet, G., Jauneau, A., Camborde, L., Tremousaygue, D., Kraut, A., Zhou, B., Levaillant, M., Adachi, H., Yoshioka, H.*, et al.* (2015). A receptor pair with an integrated decoy converts pathogen disabling of transcription factors to immunity. Cell *161*, 1074-1088.

Lee, M.W., Huffaker, A., Crippen, D., Robbins, R.T., and Goggin, F.L. (2018). Plant elicitor peptides promote plant defences against nematodes in soybean. Mol Plant Pathol *19*, 858-869.

Leslie, M.E., Lewis, M.W., Youn, J.Y., Daniels, M.J., and Liljegren, S.J. (2010). The EVERSHED receptor-like kinase modulates floral organ shedding in Arabidopsis. Development *137*, 467-476.

Li, J. (2010). Multi-tasking of somatic embryogenesis receptor-like protein kinases. Curr Opin Plant Biol *13*, 509-514.

Li, J., and Chory, J. (1997). A putative leucine-rich repeat receptor kinase involved in brassinosteroid signal transduction. Cell *90*, 929-938.

Li, J., Wen, J., Lease, K.A., Doke, J.T., Tax, F.E., and Walker, J.C. (2002). BAK1, an Arabidopsis LRR receptor-like protein kinase, interacts with BRI1 and modulates brassinosteroid signaling. Cell *110*, 213-222.

Li, L., Habring, A., Wang, K., and Weigel, D. (2020). Atypical Resistance Protein RPW8/HR Triggers Oligomerization of the NLR Immune Receptor RPP7 and Autoimmunity. Cell Host Microbe *27*, 405-417 e406.

Li, L., Kim, P., Yu, L., Cai, G., Chen, S., Alfano, J.R., and Zhou, J.M. (2016). Activation-Dependent Destruction of a Co-receptor by a Pseudomonas syringae Effector Dampens Plant Immunity. Cell Host Microbe *20*, 504-514.

Li, X., Clarke, J.D., Zhang, Y., and Dong, X. (2001). Activation of an EDS1-mediated R-gene pathway in the snc1 mutant leads to constitutive, NPR1-independent pathogen resistance. Mol Plant Microbe Interact *14*, 1131-1139.

Liang, W., van Wersch, S., Tong, M., and Li, X. (2019). TIR-NB-LRR immune receptor SOC3 pairs with truncated TIR-NB protein CHS1 or TN2 to monitor the homeostasis of E3 ligase SAUL1. New Phytol *221*, 2054-2066.

Liebrand, T.W., van den Berg, G.C., Zhang, Z., Smit, P., Cordewener, J.H., America, A.H., Sklenar, J., Jones, A.M., Tameling, W.I., Robatzek, S.*, et al.* (2013). Receptor-like kinase SOBIR1/EVR interacts with receptor-like proteins in plant immunity against fungal infection. Proc Natl Acad Sci U S A *110*, 10010-10015.

Liebrand, T.W., van den Burg, H.A., and Joosten, M.H. (2014). Two for all: receptor-associated kinases SOBIR1 and BAK1. Trends Plant Sci *19*, 123-132.

Liu, J., Elmore, J.M., Lin, Z.J., and Coaker, G. (2011). A receptor-like cytoplasmic kinase phosphorylates the host target RIN4, leading to the activation of a plant innate immune receptor. Cell Host Microbe *9*, 137-146.

Lolle, S., Greeff, C., Petersen, K., Roux, M., Jensen, M.K., Bressendorff, S., Rodriguez, E., Somark, K., Mundy, J., and Petersen, M. (2017). Matching NLR Immune Receptors to Autoimmunity in camta3 Mutants Using Antimorphic NLR Alleles. Cell Host Microbe *21*, 518-529 e514.

Lu, H., Rate, D.N., Song, J.T., and Greenberg, J.T. (2003). ACD6, a novel ankyrin protein, is a regulator and an effector of salicylic acid signaling in the Arabidopsis defense response. Plant Cell *15*, 2408-2420.

Lu, H., Salimian, S., Gamelin, E., Wang, G., Fedorowski, J., LaCourse, W., and Greenberg, J.T. (2009). Genetic analysis of acd6-1 reveals complex defense networks and leads to identification of novel defense genes in Arabidopsis. Plant J *58*, 401-412.

Ma, Y., Guo, H., Hu, L., Martinez, P.P., Moschou, P.N., Cevik, V., Ding, P., Duxbury, Z., Sarris, P.F., and Jones, J.D.G. (2018). Distinct modes of derepression of an Arabidopsis immune receptor complex by two different bacterial effectors. Proc Natl Acad Sci U S A *115*, 10218-10227.

Mackey, D., Belkhadir, Y., Alonso, J.M., Ecker, J.R., and Dangl, J.L. (2003). Arabidopsis RIN4 is a target of the type III virulence effector AvrRpt2 and modulates RPS2-mediated resistance. Cell *112*, 379-389.

Mackey, D., Holt, B.F., 3rd, Wiig, A., and Dangl, J.L. (2002). RIN4 interacts with Pseudomonas syringae type III effector molecules and is required for RPM1-mediated resistance in Arabidopsis. Cell *108*, 743-754.

Maekawa, T., Cheng, W., Spiridon, L.N., Toller, A., Lukasik, E., Saijo, Y., Liu, P., Shen, Q.H., Micluta, M.A., Somssich, I.E.*, et al.* (2011a). Coiled-coil domain-dependent homodimerization of intracellular barley immune receptors defines a minimal functional module for triggering cell death. Cell Host Microbe *9*, 187-199.

Maekawa, T., Kufer, T.A., and Schulze-Lefert, P. (2011b). NLR functions in plant and animal immune systems: so far and yet so close. Nat Immunol *12*, 817-826.

Malinovsky, F.G., Fangel, J.U., and Willats, W.G. (2014). The role of the cell wall in plant immunity. Front Plant Sci *5*, 178.

Medzhitov, R., and Janeway, C.A., Jr. (1997). Innate immunity: impact on the adaptive immune response. Curr Opin Immunol *9*, 4-9.

Meng, X., and Zhang, S. (2013). MAPK cascades in plant disease resistance signaling. Annu Rev Phytopathol *51*, 245-266.

Nam, K.H., and Li, J. (2002). BRI1/BAK1, a receptor kinase pair mediating brassinosteroid signaling. Cell *110*, 203-212.

Nanson, J.D., Kobe, B., and Ve, T. (2019). Death, TIR, and RHIM: Self-assembling domains involved in innate immunity and cell-death signaling. J Leukoc Biol *105*, 363-375.

Newman, T.E., Lee, J., Williams, S.J., Choi, S., Halane, M.K., Zhou, J., Solomon, P., Kobe, B., Jones, J.D.G., Segonzac, C.*, et al.* (2019). Autoimmunity and effector recognition in Arabidopsis thaliana can be uncoupled by mutations in the RRS1-R immune receptor. New Phytol *222*, 954-965.

Ngou, B.P.M., Ahn, H.K., Ding, P., and Jones, J.D.G. (2021). Mutual potentiation of plant immunity by cell-surface and intracellular receptors. Nature *592*, 110-115.

O'Brien, J.A., Daudi, A., Butt, V.S., and Bolwell, G.P. (2012). Reactive oxygen species and their role in plant defence and cell wall metabolism. Planta *236*, 765-779.

O'Neill, L.A., Golenbock, D., and Bowie, A.G. (2013). The history of Toll-like receptors - redefining innate immunity. Nat Rev Immunol *13*, 453-460.

Osakabe, Y., Maruyama, K., Seki, M., Satou, M., Shinozaki, K., and Yamaguchi-Shinozaki, K. (2005). Leucine-rich repeat receptor-like kinase1 is a key membrane-bound regulator of abscisic acid early signaling in Arabidopsis. Plant Cell *17*, 1105-1119.

Parkes, T. (2020). From Recognition to Susceptibility- Functional characterization of Plant-specific LIMdomain containing proteins in plant-microbe interactions. PhD thesis.

Perraki, A., DeFalco, T.A., Derbyshire, P., Avila, J., Sere, D., Sklenar, J., Qi, X., Stransfeld, L., Schwessinger, B., Kadota, Y.*, et al.* (2018). Phosphocode-dependent functional dichotomy of a common co-receptor in plant signalling. Nature *561*, 248-252.

Postel, S., Kufner, I., Beuter, C., Mazzotta, S., Schwedt, A., Borlotti, A., Halter, T., Kemmerling, B., and Nurnberger, T. (2010). The multifunctional leucine-rich repeat receptor kinase BAK1 is implicated in Arabidopsis development and immunity. Eur J Cell Biol *89*, 169-174.

Postma, J., Liebrand, T.W., Bi, G., Evrard, A., Bye, R.R., Mbengue, M., Kuhn, H., Joosten, M.H., and Robatzek, S. (2016). Avr4 promotes Cf-4 receptor-like protein association with the BAK1/SERK3 receptor-like kinase to initiate receptor endocytosis and plant immunity. New Phytol *210*, 627-642.

Pruitt, R.N., Locci, F., Wanke, F., Zhang, L., Saile, S.C., Joe, A., Karelina, D., Hua, C., Frohlich, K., Wan, W.L.*, et al.* (2021). The EDS1-PAD4-ADR1 node mediates Arabidopsis pattern-triggered immunity. Nature *598*, 495-499.

Qi, D., DeYoung, B.J., and Innes, R.W. (2012). Structure-function analysis of the coiled-coil and leucine-rich repeat domains of the RPS5 disease resistance protein. Plant Physiol *158*, 1819-1832.

Qi, D., and Innes, R.W. (2013). Recent Advances in Plant NLR Structure, Function, Localization, and Signaling. Front Immunol *4*, 348.

Qi, T., Seong, K., Thomazella, D.P.T., Kim, J.R., Pham, J., Seo, E., Cho, M.J., Schultink, A., and Staskawicz, B.J. (2018). NRG1 functions downstream of EDS1 to regulate TIR-NLR-mediated plant immunity in Nicotiana benthamiana. Proc Natl Acad Sci U S A *115*, E10979-E10987.

Quezada, E.H., Garcia, G.X., Arthikala, M.K., Melappa, G., Lara, M., and Nanjareddy, K. (2019). Cysteine-Rich Receptor-Like Kinase Gene Family Identification in the Phaseolus Genome and Comparative Analysis of Their Expression Profiles Specific to Mycorrhizal and Rhizobial Symbiosis. Genes (Basel) *10*.

Raffaele, S., Farrer, R.A., Cano, L.M., Studholme, D.J., MacLean, D., Thines, M., Jiang, R.H., Zody, M.C., Kunjeti, S.G., Donofrio, N.M.*, et al.* (2010). Genome evolution following host jumps in the Irish potato famine pathogen lineage. Science *330*, 1540-1543.

Rairdan, G.J., Collier, S.M., Sacco, M.A., Baldwin, T.T., Boettrich, T., and Moffett, P. (2008). The coiled-coil and nucleotide binding domains of the Potato Rx disease resistance protein function in pathogen recognition and signaling. Plant Cell *20*, 739-751.

Rate, D.N., Cuenca, J.V., Bowman, G.R., Guttman, D.S., and Greenberg, J.T. (1999). The gain-of-function Arabidopsis acd6 mutant reveals novel regulation and function of the salicylic

acid signaling pathway in controlling cell death, defenses, and cell growth. Plant Cell *11*, 1695-1708.

Rietz, S., Stamm, A., Malonek, S., Wagner, S., Becker, D., Medina-Escobar, N., Corina Vlot, A., Feys, B.J., Niefind, K., and Parker, J.E. (2011). Different roles of Enhanced Disease Susceptibility1 (EDS1) bound to and dissociated from Phytoalexin Deficient4 (PAD4) in Arabidopsis immunity. New Phytol *191*, 107-119.

Rooney, H.C., Van't Klooster, J.W., van der Hoorn, R.A., Joosten, M.H., Jones, J.D., and de Wit, P.J. (2005). Cladosporium Avr2 inhibits tomato Rcr3 protease required for Cf-2-dependent disease resistance. Science *308*, 1783-1786.

Rossi, M., Goggin, F.L., Milligan, S.B., Kaloshian, I., Ullman, D.E., and Williamson, V.M. (1998). The nematode resistance gene Mi of tomato confers resistance against the potato aphid. Proc Natl Acad Sci U S A *95*, 9750-9754.

Roux, M., Schwessinger, B., Albrecht, C., Chinchilla, D., Jones, A., Holton, N., Malinovsky, F.G., Tor, M., de Vries, S., and Zipfel, C. (2011). The Arabidopsis leucine-rich repeat receptor-like kinases BAK1/SERK3 and BKK1/SERK4 are required for innate immunity to hemibiotrophic and biotrophic pathogens. Plant Cell *23*, 2440-2455.

Saijo, Y., Loo, E.P., and Yasuda, S. (2018). Pattern recognition receptors and signaling in plant-microbe interactions. Plant J *93*, 592-613.

Saile, S.C., Jacob, P., Castel, B., Jubic, L.M., Salas-Gonzales, I., Backer, M., Jones, J.D.G., Dangl, J.L., and El Kasmi, F. (2020). Two unequally redundant "helper" immune receptor families mediate Arabidopsis thaliana intracellular "sensor" immune receptor functions. PLoS Biol *18*, e3000783.

Santiago, J., Henzler, C., and Hothorn, M. (2013). Molecular mechanism for plant steroid receptor activation by somatic embryogenesis co-receptor kinases. Science *341*, 889-892.

Schulze, B., Mentzel, T., Jehle, A.K., Mueller, K., Beeler, S., Boller, T., Felix, G., and Chinchilla, D. (2010). Rapid heteromerization and phosphorylation of ligand-activated plant transmembrane receptors and their associated kinase BAK1. J Biol Chem *285*, 9444-9451.

Schulze, S. (2020). The BIR3 interactome revealed the NLR CSA1 as a component necessary for BIR- and BAK1-mediated cell death. PhD thesis.

Schulze, S., Yu, L., Hua, C., Zhang, L., Kolb, D., Weber, H., Ehinger, A., Saile, S.C., Stahl, M., Franz-Wachtel, M.*, et al*. (2022). The Arabidopsis TIR-NBS-LRR protein CSA1 guards BAK1-BIR3 homeostasis and mediates convergence of pattern- and effector-induced immune responses. Cell Host Microbe *30*, 1717-1731 e1716.

Schwessinger, B., Roux, M., Kadota, Y., Ntoukakis, V., Sklenar, J., Jones, A., and Zipfel, C. (2011). Phosphorylation-dependent differential regulation of plant growth, cell death, and innate immunity by the regulatory receptor-like kinase BAK1. PLoS Genet *7*, e1002046.

Scofield, S.R., Tobias, C.M., Rathjen, J.P., Chang, J.H., Lavelle, D.T., Michelmore, R.W., and Staskawicz, B.J. (1996). Molecular Basis of Gene-for-Gene Specificity in Bacterial Speck Disease of Tomato. Science *274*, 2063-2065.

Shao, F., Golstein, C., Ade, J., Stoutemyer, M., Dixon, J.E., and Innes, R.W. (2003). Cleavage of Arabidopsis PBS1 by a bacterial type III effector. Science *301*, 1230-1233.

Shao, Z.Q., Xue, J.Y., Wu, P., Zhang, Y.M., Wu, Y., Hang, Y.Y., Wang, B., and Chen, J.Q. (2016). Large-Scale Analyses of Angiosperm Nucleotide-Binding Site-Leucine-Rich Repeat Genes Reveal Three Anciently Diverged Classes with Distinct Evolutionary Patterns. Plant Physiol *170*, 2095-2109.

Shen, Q.H., Saijo, Y., Mauch, S., Biskup, C., Bieri, S., Keller, B., Seki, H., Ulker, B., Somssich, I.E., and Schulze-Lefert, P. (2007). Nuclear activity of MLA immune receptors links isolate-specific and basal disease-resistance responses. Science *315*, 1098-1103.

Shirano, Y., Kachroo, P., Shah, J., and Klessig, D.F. (2002). A gain-of-function mutation in an Arabidopsis Toll Interleukin1 receptor-nucleotide binding site-leucine-rich repeat type R gene triggers defense responses and results in enhanced disease resistance. Plant Cell *14*, 3149-3162.

Slootweg, E., Roosien, J., Spiridon, L.N., Petrescu, A.J., Tameling, W., Joosten, M., Pomp, R., van Schaik, C., Dees, R., Borst, J.W.*, et al*. (2010). Nucleocytoplasmic distribution is required for activation of resistance by the potato NB-LRR receptor Rx1 and is balanced by its functional domains. Plant Cell *22*, 4195-4215.

Somssich, M., Ma, Q., Weidtkamp-Peters, S., Stahl, Y., Felekyan, S., Bleckmann, A., Seidel, C.A., and Simon, R. (2015). Real-time dynamics of peptide ligand-dependent receptor complex formation in planta. Sci Signal *8*, ra76.

Song, W., Forderer, A., Yu, D., and Chai, J. (2021). Structural biology of plant defence. New Phytol *229*, 692-711.

Stegmann, M., Monaghan, J., Smakowska-Luzan, E., Rovenich, H., Lehner, A., Holton, N., Belkhadir, Y., and Zipfel, C. (2017). The receptor kinase FER is a RALF-regulated scaffold controlling plant immune signaling. Science *355*, 287-289.

Sun, T., Zhang, Q., Gao, M., and Zhang, Y. (2014). Regulation of SOBIR1 accumulation and activation of defense responses in bir1-1 by specific components of ER quality control. Plant J *77*, 748-756.

Sun, X., Lapin, D., Feehan, J.M., Stolze, S.C., Kramer, K., Dongus, J.A., Rzemieniewski, J., Blanvillain-Baufume, S., Harzen, A., Bautor, J.*, et al.* (2021). Pathogen effector recognition-dependent association of NRG1 with EDS1 and SAG101 in TNL receptor immunity. Nat Commun *12*, 3335.

Sun, Y., Han, Z., Tang, J., Hu, Z., Chai, C., Zhou, B., and Chai, J. (2013a). Structure reveals that BAK1 as a co-receptor recognizes the BRI1-bound brassinolide. Cell Res *23*, 1326-1329.

Sun, Y., Li, L., Macho, A.P., Han, Z., Hu, Z., Zipfel, C., Zhou, J.M., and Chai, J. (2013b). Structural basis for flg22-induced activation of the Arabidopsis FLS2-BAK1 immune complex. Science *342*, 624-628.

Takken, F.L., and Goverse, A. (2012). How to build a pathogen detector: structural basis of NB-LRR function. Curr Opin Plant Biol *15*, 375-384.

Tameling, W.I., Elzinga, S.D., Darmin, P.S., Vossen, J.H., Takken, F.L., Haring, M.A., and Cornelissen, B.J. (2002). The tomato R gene products I-2 and MI-1 are functional ATP binding proteins with ATPase activity. Plant Cell *14*, 2929-2939.

Tameling, W.I., Vossen, J.H., Albrecht, M., Lengauer, T., Berden, J.A., Haring, M.A., Cornelissen, B.J., and Takken, F.L. (2006). Mutations in the NB-ARC domain of I-2 that impair ATP hydrolysis cause autoactivation. Plant Physiol *140*, 1233-1245.

Tang, X., Frederick, R.D., Zhou, J., Halterman, D.A., Jia, Y., and Martin, G.B. (1996). Initiation of Plant Disease Resistance by Physical Interaction of AvrPto and Pto Kinase. Science *274*, 2060-2063.

Thomma, B.P., Eggermont, K., Penninckx, I.A., Mauch-Mani, B., Vogelsang, R., Cammue, B.P., and Broekaert, W.F. (1998). Separate jasmonate-dependent and salicylate-dependent defense-response pathways in Arabidopsis are essential for resistance to distinct microbial pathogens. Proc Natl Acad Sci U S A *95*, 15107-15111.

Thoms, D., Liang, Y., and Haney, C.H. (2021). Maintaining Symbiotic Homeostasis: How Do Plants Engage With Beneficial Microorganisms While at the Same Time Restricting Pathogens? Mol Plant Microbe Interact *34*, 462-469.

Tian, H., Wu, Z., Chen, S., Ao, K., Huang, W., Yaghmaiean, H., Sun, T., Xu, F., Zhang, Y., Wang, S.*, et al.* (2021). Activation of TIR signalling boosts pattern-triggered immunity. Nature *598*, 500-503.

Tian, W., Hou, C., Ren, Z., Wang, C., Zhao, F., Dahlbeck, D., Hu, S., Zhang, L., Niu, Q., Li, L., *et al.* (2019). A calmodulin-gated calcium channel links pathogen patterns to plant immunity. Nature *572*, 131-135.

Tran, D.T.N., Chung, E.H., Habring-Muller, A., Demar, M., Schwab, R., Dangl, J.L., Weigel, D., and Chae, E. (2017). Activation of a Plant NLR Complex through Heteromeric Association with an Autoimmune Risk Variant of Another NLR. Curr Biol *27*, 1148-1160.

Tsuda, K., Mine, A., Bethke, G., Igarashi, D., Botanga, C.J., Tsuda, Y., Glazebrook, J., Sato, M., and Katagiri, F. (2013). Dual regulation of gene expression mediated by extended MAPK activation and salicylic acid contributes to robust innate immunity in Arabidopsis thaliana. PLoS Genet *9*, e1004015.

Underwood, W. (2012). The plant cell wall: a dynamic barrier against pathogen invasion. Front Plant Sci *3*, 85.

Urbach, J.M., and Ausubel, F.M. (2017). The NBS-LRR architectures of plant R-proteins and metazoan NLRs evolved in independent events. Proc Natl Acad Sci U S A *114*, 1063-1068.

Van de Weyer, A.L., Monteiro, F., Furzer, O.J., Nishimura, M.T., Cevik, V., Witek, K., Jones, J.D.G., Dangl, J.L., Weigel, D., and Bemm, F. (2019). A Species-Wide Inventory of NLR Genes and Alleles in Arabidopsis thaliana. Cell *178*, 1260-1272 e1214.

Van der Biezen, E.A., and Jones, J.D. (1998). Plant disease-resistance proteins and the gene-for-gene concept. Trends Biochem Sci *23*, 454-456.

van der Burgh, A.M., Postma, J., Robatzek, S., and Joosten, M. (2019). Kinase activity of SOBIR1 and BAK1 is required for immune signalling. Mol Plant Pathol *20*, 410-422.

Van der Does, D., Boutrot, F., Engelsdorf, T., Rhodes, J., McKenna, J.F., Vernhettes, S., Koevoets, I., Tintor, N., Veerabagu, M., Miedes, E.*, et al.* (2017). The Arabidopsis leucine-rich repeat receptor kinase MIK2/LRR-KISS connects cell wall integrity sensing, root growth and response to abiotic and biotic stresses. PLoS Genet *13*, e1006832.

Voinnet, O., Rivas, S., Mestre, P., and Baulcombe, D. (2003). An enhanced transient expression system in plants based on suppression of gene silencing by the p19 protein of tomato bushy stunt virus. Plant J *33*, 949-956.

Wagner, S., Stuttmann, J., Rietz, S., Guerois, R., Brunstein, E., Bautor, J., Niefind, K., and Parker, J.E. (2013). Structural basis for signaling by exclusive EDS1 heteromeric complexes with SAG101 or PAD4 in plant innate immunity. Cell Host Microbe *14*, 619-630.

Walker, J.C., and Zhang, R. (1990). Relationship of a putative receptor protein kinase from maize to the S-locus glycoproteins of Brassica. Nature *345*, 743-746.

Wan, L., Essuman, K., Anderson, R.G., Sasaki, Y., Monteiro, F., Chung, E.H., Osborne Nishimura, E., DiAntonio, A., Milbrandt, J., Dangl, J.L.*, et al.* (2019). TIR domains of plant immune receptors are NAD(+)-cleaving enzymes that promote cell death. Science *365*, 799-803.

Wang, G.F., Ji, J., Ei-Kasmi, F., Dangl, J.L., Johal, G., and Balint-Kurti, P.J. (2015). Correction: Molecular and functional analyses of a maize autoactive NB-LRR protein identify precise structural requirements for activity. PLoS Pathog *11*, e1004830.

Wang, G.L., Ruan, D.L., Song, W.Y., Sideris, S., Chen, L., Pi, L.Y., Zhang, S., Zhang, Z., Fauquet, C., Gaut, B.S.*, et al.* (1998). Xa21D encodes a receptor-like molecule with a leucine-rich repeat domain that determines race-specific recognition and is subject to adaptive evolution. Plant Cell *10*, 765-779.

Wang, J., Han, M., and Liu, Y. (2021). Diversity, structure and function of the coiled-coil domains of plant NLR immune receptors. J Integr Plant Biol *63*, 283-296.

Wang, J., Hu, M., Wang, J., Qi, J., Han, Z., Wang, G., Qi, Y., Wang, H.W., Zhou, J.M., and Chai, J. (2019). Reconstitution and structure of a plant NLR resistosome conferring immunity. Science *364*.

Wang, X., Kota, U., He, K., Blackburn, K., Li, J., Goshe, M.B., Huber, S.C., and Clouse, S.D. (2008). Sequential transphosphorylation of the BRI1/BAK1 receptor kinase complex impacts early events in brassinosteroid signaling. Dev Cell *15*, 220-235.

Wang, Y., Li, Z., Liu, D., Xu, J., Wei, X., Yan, L., Yang, C., Lou, Z., and Shui, W. (2014). Assessment of BAK1 activity in different plant receptor-like kinase complexes by quantitative profiling of phosphorylation patterns. J Proteomics *108*, 484-493.

Wang, Y., Xu, Y., Sun, Y., Wang, H., Qi, J., Wan, B., Ye, W., Lin, Y., Shao, Y., Dong, S.*, et al.* (2018). Leucine-rich repeat receptor-like gene screen reveals that Nicotiana RXEG1 regulates glycoside hydrolase 12 MAMP detection. Nat Commun *9*, 594.

Williams, S.J., Sohn, K.H., Wan, L., Bernoux, M., Sarris, P.F., Segonzac, C., Ve, T., Ma, Y., Saucet, S.B., Ericsson, D.J.*, et al.* (2014). Structural basis for assembly and function of a heterodimeric plant immune receptor. Science *344*, 299-303.

Williams, S.J., Sornaraj, P., deCourcy-Ireland, E., Menz, R.I., Kobe, B., Ellis, J.G., Dodds, P.N., and Anderson, P.A. (2011). An autoactive mutant of the M flax rust resistance protein has a preference for binding ATP, whereas wild-type M protein binds ADP. Mol Plant Microbe Interact *24*, 897-906.

Wroblewski, T., Spiridon, L., Martin, E.C., Petrescu, A.J., Cavanaugh, K., Truco, M.J., Xu, H., Gozdowski, D., Pawlowski, K., Michelmore, R.W.*, et al.* (2018). Genome-wide functional analyses of plant coiled-coil NLR-type pathogen receptors reveal essential roles of their N-terminal domain in oligomerization, networking, and immunity. PLoS Biol *16*, e2005821.

Wu, Y., Gao, Y., Zhan, Y., Kui, H., Liu, H., Yan, L., Kemmerling, B., Zhou, J.M., He, K., and Li, J. (2020). Loss of the common immune coreceptor BAK1 leads to NLR-dependent cell death. Proc Natl Acad Sci U S A *117*, 27044-27053.

Xin, X.F., and He, S.Y. (2013). Pseudomonas syringae pv. tomato DC3000: a model pathogen for probing disease susceptibility and hormone signaling in plants. Annu Rev Phytopathol *51*, 473-498.

Xu, F., Zhu, C., Cevik, V., Johnson, K., Liu, Y., Sohn, K., Jones, J.D., Holub, E.B., and Li, X. (2015). Autoimmunity conferred by chs3-2D relies on CSA1, its adjacent TNL-encoding neighbour. Sci Rep *5*, 8792.

Yamaguchi, Y., Pearce, G., and Ryan, C.A. (2006). The cell surface leucine-rich repeat receptor for AtPep1, an endogenous peptide elicitor in Arabidopsis, is functional in transgenic tobacco cells. Proc Natl Acad Sci U S A *103*, 10104-10109.

Yan, L., Ma, Y., Liu, D., Wei, X., Sun, Y., Chen, X., Zhao, H., Zhou, J., Wang, Z., Shui, W.*, et al.* (2012). Structural basis for the impact of phosphorylation on the activation of plant receptor-like kinase BAK1. Cell Res *22*, 1304-1308.

Yang, H., Gou, X., He, K., Xi, D., Du, J., Lin, H., and Li, J. (2010). BAK1 and BKK1 in Arabidopsis thaliana confer reduced susceptibility to turnip crinkle virus. European Journal of Plant Pathology *127*, 149-156.

Yu, X., Xu, G., Li, B., de Souza Vespoli, L., Liu, H., Moeder, W., Chen, S., de Oliveira, M.V.V., Ariadina de Souza, S., Shao, W.*, et al.* (2019). The Receptor Kinases BAK1/SERK4 Regulate Ca($^{2+}$) Channel-Mediated Cellular Homeostasis for Cell Death Containment. Curr Biol *29*, 3778-3790 e3778.

Yuan, M., Jiang, Z., Bi, G., Nomura, K., Liu, M., Wang, Y., Cai, B., Zhou, J.M., He, S.Y., and Xin, X.F. (2021). Pattern-recognition receptors are required for NLR-mediated plant immunity. Nature *592*, 105-109.

Zhang, L., and Gleason, C. (2020). Enhancing potato resistance against root-knot nematodes using a plant-defence elicitor delivered by bacteria. Nat Plants *6*, 625-629.

Zhang, N., Zhang, D., and Li, J.F. (2017). A Simple Protoplast-Based Method for Screening Potent Artificial miRNA for Maximal Gene Silencing in Arabidopsis. Curr Protoc Mol Biol *117*, 26 29 21-26 29 10.

Zhang, W., Fraiture, M., Kolb, D., Loffelhardt, B., Desaki, Y., Boutrot, F.F., Tor, M., Zipfel, C., Gust, A.A., and Brunner, F. (2013). Arabidopsis receptor-like protein30 and receptor-like kinase suppressor of BIR1-1/EVERSHED mediate innate immunity to necrotrophic fungi. Plant Cell *25*, 4227-4241.

Zhang, Y., Chen, M., Siemiatkowska, B., Toleco, M.R., Jing, Y., Strotmann, V., Zhang, J., Stahl, Y., and Fernie, A.R. (2020). A Highly Efficient Agrobacterium-Mediated Method for Transient Gene Expression and Functional Studies in Multiple Plant Species. Plant Commun *1*, 100028.

Zhao, D.Z., Wang, G.F., Speal, B., and Ma, H. (2002). The excess microsporocytes1 gene encodes a putative leucine-rich repeat receptor protein kinase that controls somatic and reproductive cell fates in the Arabidopsis anther. Genes Dev *16*, 2021-2031.

Zhou, J.M., and Zhang, Y. (2020). Plant Immunity: Danger Perception and Signaling. Cell *181*, 978-989.

Zhou, Z., Bi, G., and Zhou, J.M. (2018). Luciferase Complementation Assay for Protein-Protein Interactions in Plants. Curr Protoc Plant Biol *3*, 42-50.

Zipfel, C., Kunze, G., Chinchilla, D., Caniard, A., Jones, J.D., Boller, T., and Felix, G. (2006). Perception of the bacterial PAMP EF-Tu by the receptor EFR restricts Agrobacterium-mediated transformation. Cell *125*, 749-760.

8. Supplemental data

8.1 PAD4 and NahG can block cell death in *bir2* mutants

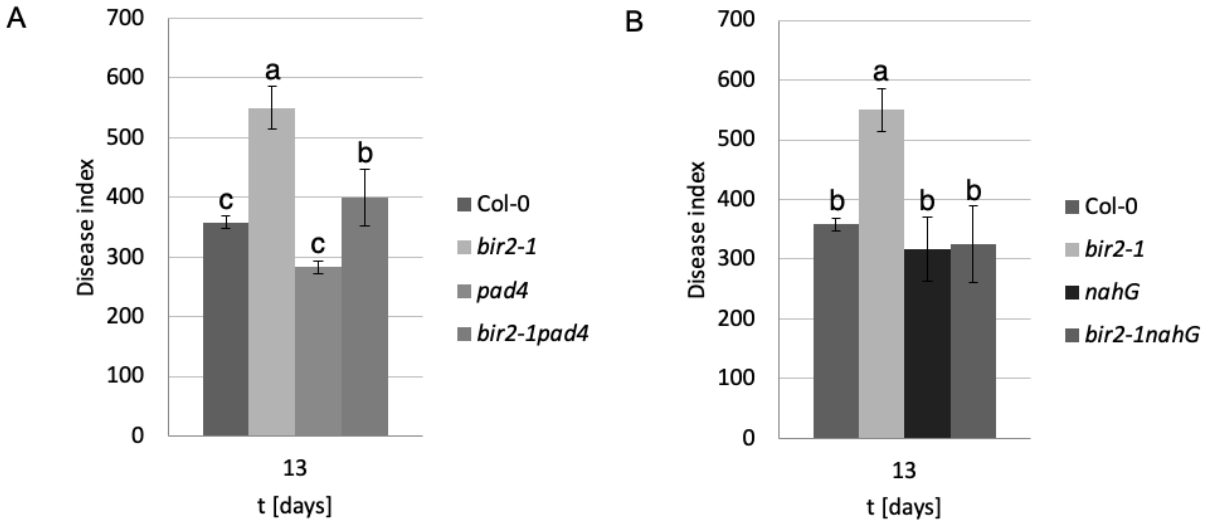

Supplemental Figure 8-1: PAD4 and NahG are necessary for *bir2*-mediated cell death pathway

(A) and **(B)** Disease indices of Alternaria brassicicola infected leaves of the indicated genotypes 13 days after infection shown as mean ± SE (n=12). Different letters indicate significant differences according to one-way ANOVA and Tukey's HSD test ($p<0.05$). The experiments were repeated at least three times with similar results.

8.2 All results of western blotting

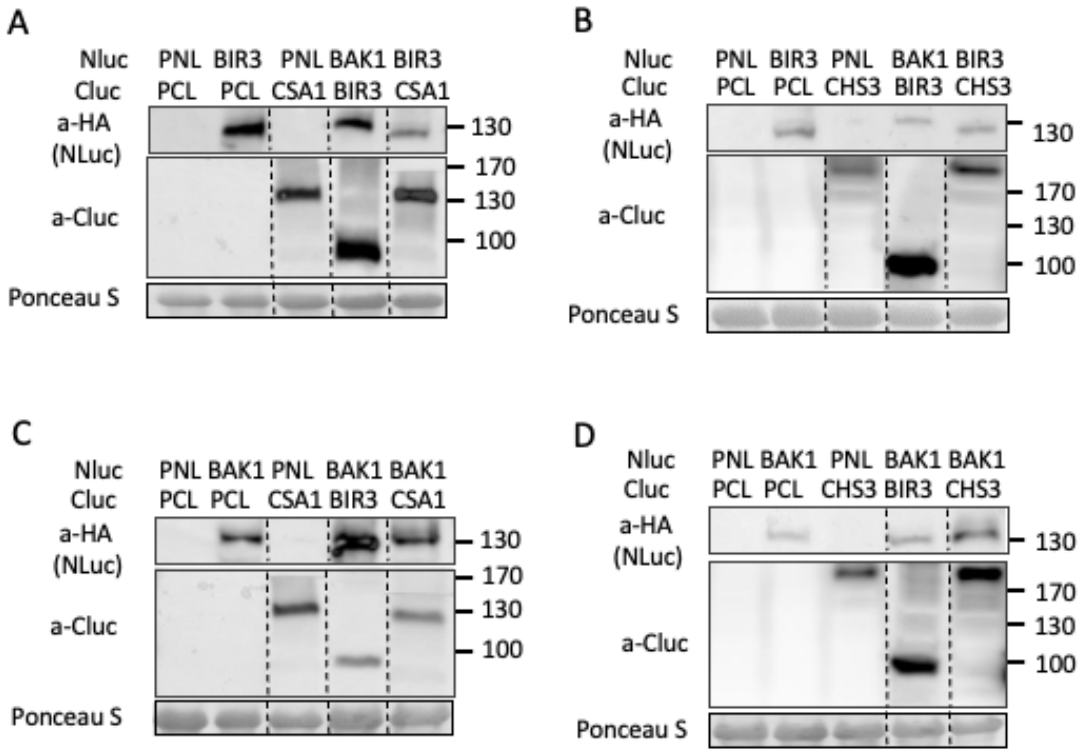

Supplemental Figure 8-2: Expression controls for split-luciferase assays

(A), (B), (C) and (D): Western blots of in *N. benthamiana* expressed fusion proteins as shown in Fig. 3-8, Fig. 3-9 and Fig. 3-13 detected with a-HA (Nluc) and a-luciferase (Cluc) antibodies. Ponceau S staining shows protein loading. Dotted lines indicate cut and rearranged parts of the same blot.

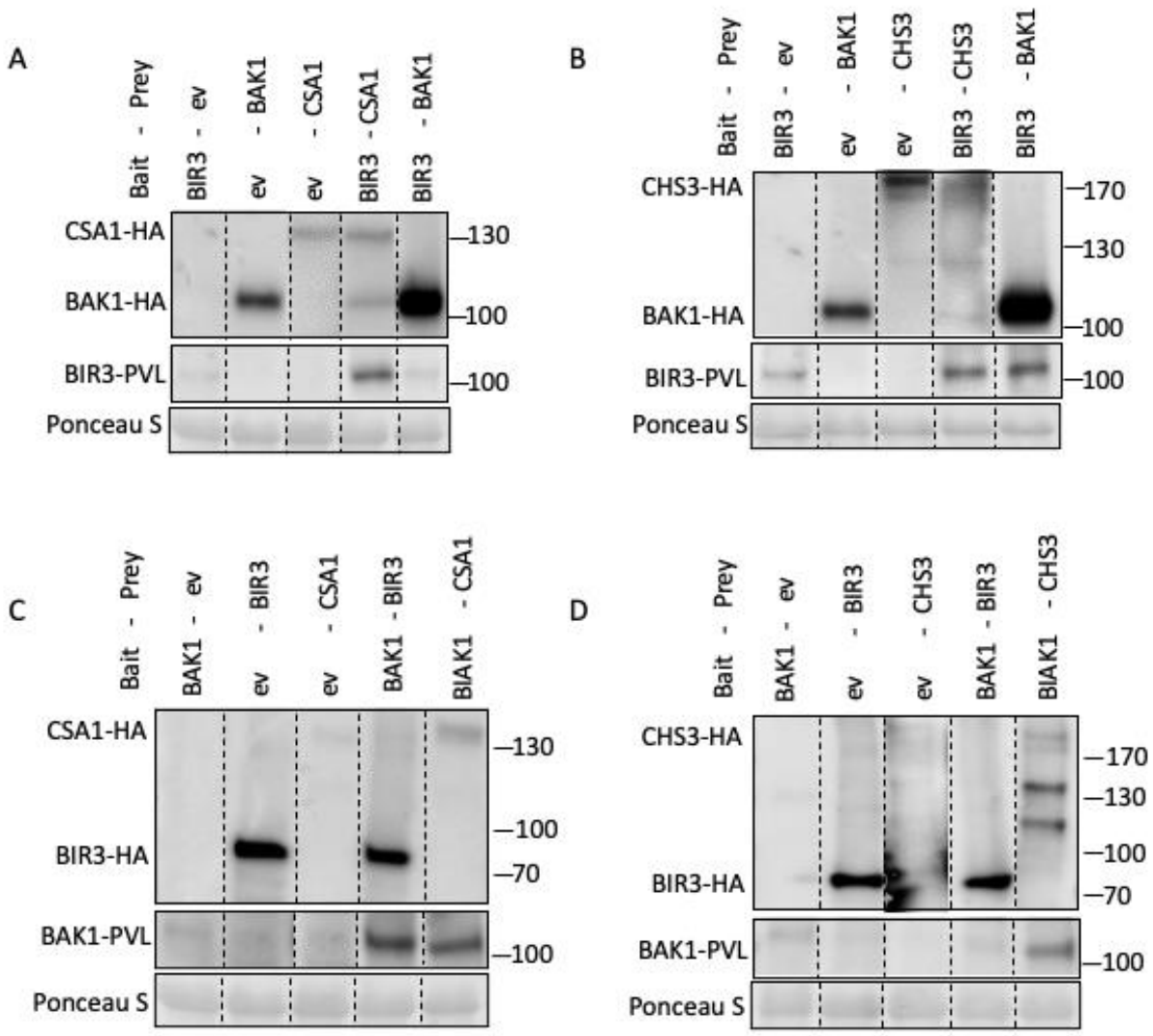

Supplemental Figure 8-3: Expression controls for split-ubiquitin assays

(A), **(B)**, **(C)** and **(D)** Western blots of in yeast expressed fusion proteins as shown in Fig. 3-13, Fig. 3-16 and Fig. 3-17 detected with a-HA (prey) and a-VP16 (bait) antibodies. Ponceau S staining shows protein loading. Dotted lines indicate cut and rearranged parts of the same blot. Note: PVL = proteinA-VP16-LexA domain.

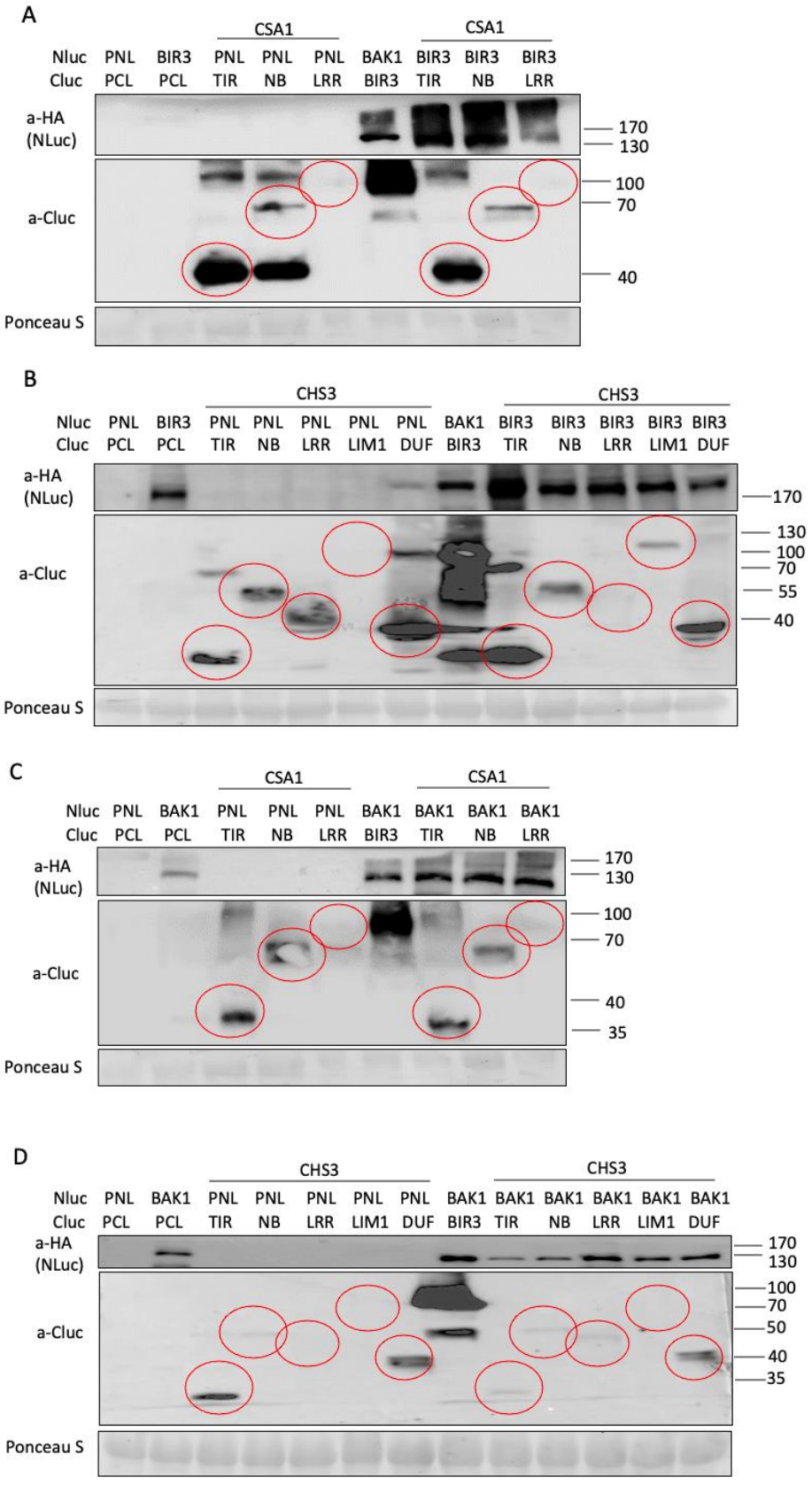
A
CSA1
CSA1
Nluc PNL BIR3 PNL PNL PNL BAK1 BIR3 BIR3 BIR3
Cluc PCL PCL TIR NB LRR BIR3 TIR NB LRR
a-HA (NLuc)
a-Cluc
Ponceau S
170
130
100
70
40
B
CHS3
CHS3
Nluc PNL BIR3 PNL PNL PNL PNL PNL BAK1 BIR3 BIR3 BIR3 BIR3 BIR3
Cluc PCL PCL TIR NB LRR LIM1 DUF BIR3 TIR NB LRR LIM1 DUF
a-HA (NLuc)
a-Cluc
Ponceau S
170
130
100
70
55
40
C
CSA1
CSA1
Nluc PNL BAK1 PNL PNL PNL BAK1 BAK1 BAK1 BAK1
Cluc PCL PCL TIR NB LRR BIR3 TIR NB LRR
a-HA (NLuc)
a-Cluc
Ponceau S
170
130
100
70
40
35
D
CHS3
CHS3
Nluc PNL BAK1 PNL PNL PNL PNL PNL BAK1 BAK1 BAK1 BAK1 BAK1 BAK1
Cluc PCL PCL TIR NB LRR LIM1 DUF BIR3 TIR NB LRR LIM1 DUF
a-HA (NLuc)
a-Cluc
Ponceau S
170
130
100
70
50
40
35

Supplemental Figure 8-4: Expression controls for split-luciferase assays

(A), **(B)**, **(C)** and **(D)** Western blots of in *Nicotiana benthamiana* expressed fusion proteins as shown in Fig. 3-20 and Fig. 3-21 detected with a-HA (Nluc) and a-luciferase (Cluc) antibodies. Ponceau S staining shows protein loading. Some truncated mutants show low expression which have been labelled with red ovals.

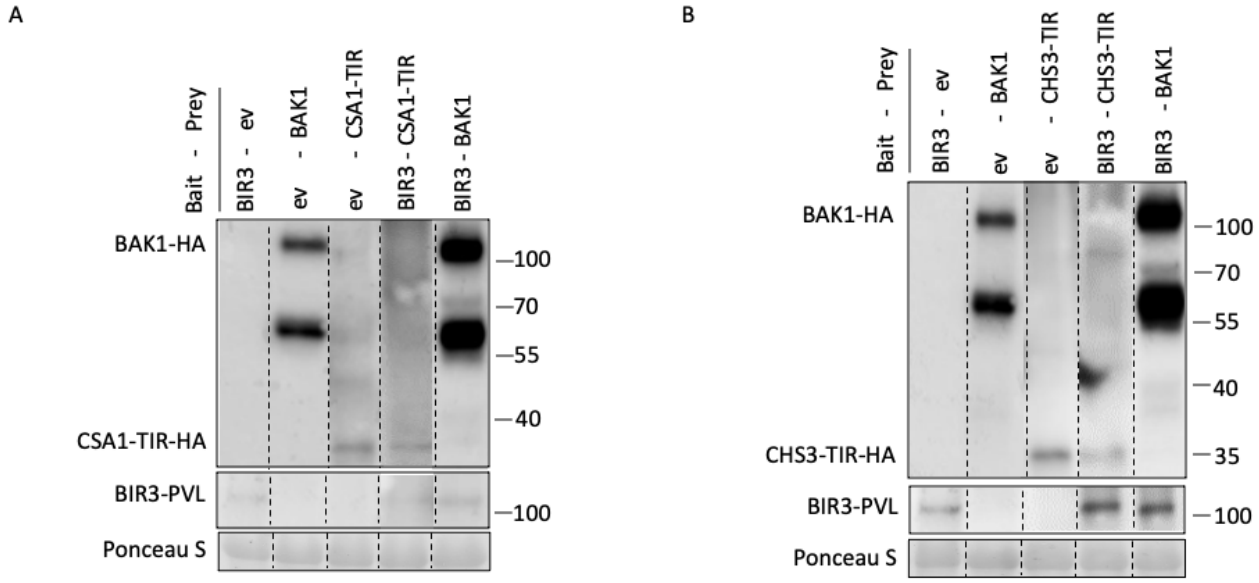

Supplemental Figure 8-5: Expression controls for split-ubiquitin assays

(A) and **(B)** Western blots of in yeast expressed fusion proteins as shown in **A)** and **B)** Fig. 17 detected with a-HA (prey) and a-VP16 (bait) antibodies. Ponceau S staining shows protein loading. Dotted lines indicate cut and rearranged parts of the same blot. Note: PVL = proteinA-VP16-LexA domain.

8.3 Interactors were identified in the IP-MS/MS of CSA1

Table 4: The IP-MS/MS of CSA1 reveales interactome protein of CSA1

Gene name	Protein IDs	Intensity	Q value
At1g15210	ABC transporter G family member 36, ABCG35	$1.57x10^{9}$	0
At1g59870	ABC transporter G family member 36, ABCG36	$1.57x10^{9}$	0
At1g66750	Cyclin-dependent kinase D-2	$4.16x10^{7}$	0
At1g18040	Cyclin-dependent kinase D-3	$4.16x10^{7}$	0
At1g73690	Cyclin-dependent kinase D-1	$4.16x10^{7}$	0
At3g48750	Cyclin-dependent kinase A-1	$4.16x10^{7}$	0

At5g10270	Cyclin-dependent kinase C-1	$4.16x10^{7}$	0
At5g64960	Cyclin-dependent kinase C-2	$4.16x10^{7}$	0
At3g46820	Serine/threonine-protein phosphatase PP1 isozyme 5	$5.81x10^{7}$	0
At5g59160	Serine/threonine-protein phosphatase PP1 isozyme 2	$5.81x10^{7}$	0
At2g29400	Serine/threonine-protein phosphatase PP1 isozyme 1	$5.81x10^{7}$	0
At1g59830	Serine/threonine-protein phosphatase PP2A1	$9.15x10^{7}$	0
At1g10430	Serine/threonine-protein phosphatase PP2A2	$9.15x10^{7}$	0
At4g26720	Serine/threonine-protein phosphatase PP-X isozyme 1	$9.15x10^{7}$	0
At5g55260	Serine/threonine-protein phosphatase PP-X isozyme 2	$9.15x10^{7}$	0
At2g33120	Synaptobrevin-related protein 1, Vesicle-associated membrane protein 722, AtVAMP722	$2.62x10^{8}$	0
At4g26070	Mitogen-activated protein kinase kinase 1, MKK1	$3.81x10^{7}$	0
At4g29810	Mitogen-activated protein kinase kinase 1, MKK2	$3.81x10^{7}$	0
At2g3980	P5CS1, Glutamate 5-kinase	$8.15x10^{7}$	0
At3g55610	P5CS2, Glutamate 5-kinase	$8.15x10^{7}$	0
At1g01560	MPK11, Mitogen-activated protein kinase 11	0	0.0009058
At4g01370	MPK4, Mitogen-activated protein kinase 4	0	0.0009058
At3g09820	Adenosine kinase 1, ADK1	$1.21x10^{7}$	0
At5g03300	Adenosine kinase 2, ADK2	$1.21x10^{7}$	0
At5g63400	Adenylate kinase 4, ADK1	$1.6x10^{7}$	0
At3g51800	ERBB-3 BINDING PROTEIN 1	$1.34x10^{7}$	0.0055732
At4g31390	Protein ACTIVITY OF BC1 COMPLEX KINASE 1	$2.1x10^{7}$	0
At5g08590	Serine/threonine-protein kinase SRK2G	$3.38x10^{6}$	0.0026
At5g63650	Serine/threonine-protein kinase SRK2H	$3.38x10^{6}$	0
At4g11010	NDPK3, Nucleoside diphosphate kinase III	$3.16x10^{8}$	0
At4g23895	Nucleoside diphosphate kinase	$3.16x10^{8}$	0
At4g23900	NDK4, Nucleoside diphosphate kinase IV	$3.16x10^{8}$	0
At5g35170	Adenylate kinase 5, chloroplastic	$3.59x10^{7}$	0
At3g25800	PP2AA2, Serine/threonine-protein phosphatase 2A 65 kDa regulatory subunit A beta isoform	$1.53x10^{8}$	0
At1g71810	Uncharacterized aarF domain-containing protein kinase	$1.66x10^{7}$	0.0025707
At1g31230	AKHSDH1, aspartokinase/homoserine dehydrogenase 1	$2.02x10^{7}$	0
At4g1971	AKHSDH2, aspartokinase/homoserine dehydrogenase 2	$2.02x10^{7}$	0
At2g46090	Sphingoid long-chain bases kinase 2, mitochondrial, LCKB2	$1.4x10^{7}$	0.0009199

At4g35310	Calcium-dependent protein kinase 5, CPK5	$5.52x10^6$	0.0025773
At4g23650	Calcium-dependent protein kinase 3, CPK3	$2.89x10^7$	0
At1g22940	Hydroxymethylpyrimidine kinase, TH1	$1.51x10^7$	0.0017621
At5g64940	Protein ACTIVITY OF BC1 COMPLEX KINASE 8	$3.51x10^7$	0
At3g22960	Plastidial pyruvate kinase 1, PKP1	$5.84x10^7$	0
At1g10760	Alpha-glucan water dikinase 1, GWD1	$6.95x10^7$	0

Some proteins were selected within CSA1-interactome of IP-MS/MS analyses, including gene names and protein IDs. The rule of the choice is only to choose the specific protein after data sorting on values by according to largest to smallest order.

8.4 MS proteins were pacificated by SDS-PAGE short gels in the second-round IP-MS/MS

R06: CSA1_1
R07: CSA1_2
R08: CSA1_3

R09: CHS3_2
R10: CHS3_4
R11: CHS3_5

R12: control_K1
R13: control_K2
R14: control_K3

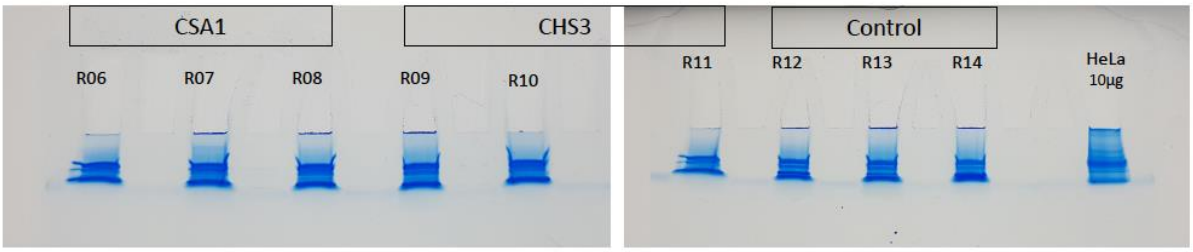

Supplemental Figure 8-6: SDS-PAGE short gel with MS proteins in the second-round IP-MS/MS of CSA1/CHS3

MS protein samples were named shown on above. MS proteins were purificated by SDS-PAGE short gel shown on below. Every MS protein sample were loaded 30ul volume.

8.5 Interactome proteins found in the second-round IP-MS/MS of CSA1/CHS3

Table 5: The second-round IP-MS/MS reveals interactome protein of CSA1/CHS3

Gene name	Protein IDs	CSA1	CHS3
At5g12120	UBA domain-contain, Uncharacterized protein	yes	yes
NSP1; NSP4	Nitrile-specifier protein 1; Nitrile-specifier protein 4	no	yes
At4g39260	Glycine-rich RNA-binding protein 8	yes	yes
At5g16660	Low-density receptor-like protein	no	yes
At5g08540	Ribosomal RNA small subunit methyltransferase	no	yes
At2g44210	Uncharacterized protein	no	yes
At1g11510	Sugar transport protein 1, STP1	no	yes
At3g11930	Ethylene-responsive protein	no	yes
At3g28540	Isoform 2 of AAA-ATPas	yes	no
At3g28510	AAA-ATPase	yes	no
At4g29810	Mitogen-activated protein kinase 2	yes	no
At3g13750	Beta-galactosidase;Beta-galactosidase 1; BGAL1	yes	no
At1g14880	PCR1, Protein PLANT CADMIUM RESISTANCE 1	yes	no
At1g79090	Uncharacterized protein	yes	yes
	TOC159, Translocase of chloroplast 159, chloroplastic	no	yes
At1g01300	Uncharacterized protein	yes	yes
At1g51980	Probable mitochondrial-processing peptidase subunit alpha-2, MPPA2	yes	yes
At3g46820	Serine/threonine-protein phosphatase PP1 isozyme 5	yes	yes
At5g59160	Serine/threonine-protein phosphatase PP1 isozyme 2	yes	yes
At2g29400	Serine/threonine-protein phosphatase PP1 isozyme 1	yes	yes
At5g67500	Mitochondrial outer membrane protein porin 2, VDAC2	yes	yes
At1g29670	GDSL esterase/lipase	yes	yes
At2g19940	N-acetyl-gamma-glutamyl-phosphate reductase	yes	yes
K3M16_80	Glutamine-rich protein	yes	yes
At5g61790	Calnexin homolog 1, CNX1	yes	yes
At5g04140	Ferredoxin-dependent glutamate synthase 1 (GLU1)	yes	yes
At5g42650	Allene oxide synthase, chloroplastic (CYP74A)	yes	yes
At4g02520	Glutathione S-transferase F2	yes	yes
At1g62920	STN7, Serine/threonine-protein kinase, chloroplastic	yes	yes
At5g42070	Mitochondrial import receptor subunit TOM9-2	no	yes
AT1G73690	Cyclin-dependent kinase D-1	yes	yes
At1g66750	Cyclin-dependent kinase D-2	yes	yes

At1g18040	Cyclin-dependent kinase D-3	yes	yes
At4g23900	Nucleoside diphosphate kinase	yes	yes
At4g11010	NDPK3, Nucleoside diphosphate kinase 3	yes	yes
At1g10430	Serine/threonine-protein phosphatase PP2A1	yes	yes
At1g59830	Serine/threonine-protein phosphatase PP2A2	yes	yes
At3g58500	Serine/threonine-protein phosphatase PP2A3	yes	yes
At2g42500	Serine/threonine-protein phosphatase PP2A4	yes	yes
At1g69960	Serine/threonine-protein phosphatase PP2A5	yes	yes
At4g26650	Uncharacterized protein	yes	yes
At4g23895	Nucleoside diphosphate phosphorylation	yes	yes
At4g19360	Cysteine proteinase inhibitor 4, CYS4	no	yes

Some proteins were selected within CSA1-interactome of IP-MS/MS analyses, including gene names and protein IDs. The rule of the choice is only to choose the specific protein after data sorting on values by according to largest to smallest order.

8.6 The same phosphorylation (Ser^{1120}) identified in the second-round IP-MS/MS of CSA1/CHS3

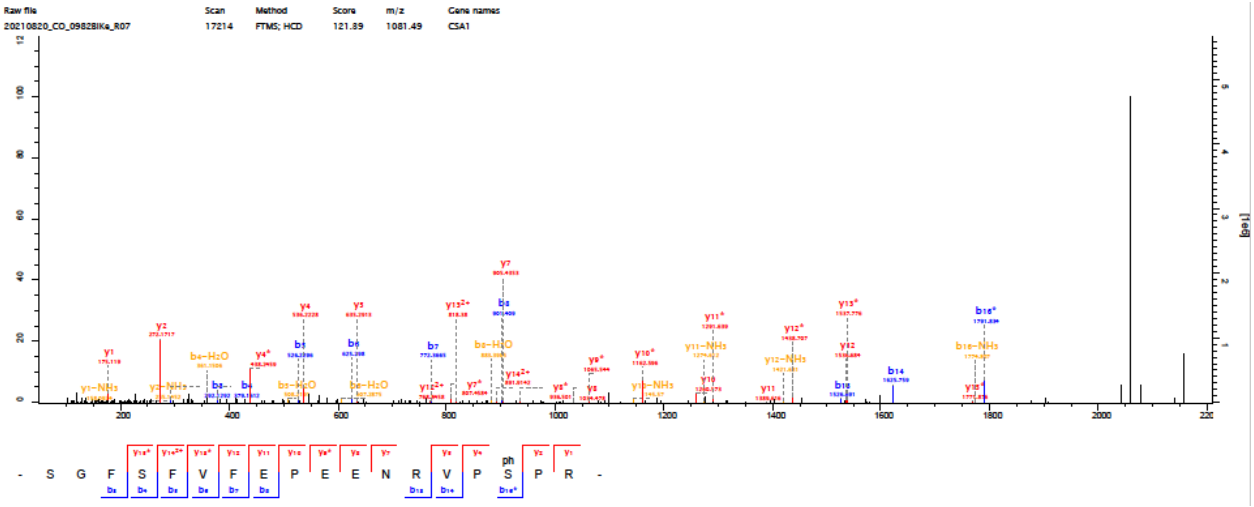

Supplemental Figure 8-7: Spectrum within CSA1-interactome IP-MS/MS analyses

The only phosphorylation site for CSA1 was shown above. Ser^{1120} was marked with phosphorylation.